Interaction between Shallow and Deep Groundwater in Baiyangdian Lake Watershed, North China

中国北部白洋淀湖流域における浅層および深層地下水の交流

A Dissertation Submitted to
the Graduate School of Life and Environmental Sciences,
the University of Tsukuba
in Partial Fulfillment of the Requirements
for the Degree of Doctor in Environmental Studies
(Doctoral Program in Sustainable Environmental Studies)

Jie ZHANG

Abstract

In arid and semi-arid regions, consumption of deep groundwater resources is increasing due to growing water demand for every sector. One fact is that deep groundwater has a longer flow path and residence time than shallow groundwater. So comparing with other water body it will be a more severe environmental problem once deep groundwater was polluted. Improper groundwater exploitation in North China Plain, the one of the most developed industrial areas and the largest agricultural production area in North China, has resulted in serious deep groundwater overdrawing.

Intensive groundwater surveys were conducted in Baiyangdian Lake Watershed (BLW), the northwest part of North China Plain, because BLW is suffering serious water problems due to high economic growth and improper groundwater resource utilization.

The objective of this research is to make clear the characteristics of groundwater flow system in study area, especially focus on the interaction between shallow and deep groundwater by using multi-tracer approach, and quantify the flux exchanges of the interaquifer flows between shallow and deep aquifer. For this purpose, 187 water samples are collected through field surveys since June 2011 to March 2013 for geochemical analysis.

Based on the results of major ions and stable isotopes, an overview of the hydrogeochemistry characteristics in study area can be described as below. The surface water and groundwater collected in mountain area are roughly chemically similar, though the Mg^{2+} concentration is a little different among the samples. In plain area, the groundwater samples of Aquifer 1 show inhomogeneous water type according to the result of trilinear diagram. Groundwater in Aquifer 2 and Aquifer 3 are chemically similar, which have stable concentration in HCO_3 but big variations in cation ions.

In mountain area, the stable isotopic compositions in surface water and groundwater is similar and the trend line slope of these samples is closed to that of Local Meteoric Water Line (LMWL). In plain area, the stable isotopic composition in surface water presents the heaviest value with ranging from -7.60‰ to -4.14‰ for δ^{18}O and -56.35‰ to -40.11‰ for δD, and the slope of these samples is apparently lower than that of LMWL which is caused by isotopic fractionation during water evaporation. The stable isotopic compositions of groundwater samples of Aquifer 1, ranging from -10.09‰ to -4.42‰ for δ^{18}O values and from -72.68‰ to -40.94‰ for δD values, are relatively higher than those in Aquifer 2 and Aquifer 3. Many samples in Aquifer 2 and Aquifer 3 show a mixture together, which indicates that these samples in different aquifers probably originated from the same elevation.

A specific discussion about interaction between shallow and deep groundwater mainly focus on Baoding and Dingzhou area. Geochemical results show that the interaction relationship existing between shallow and deep groundwater can be confirmed in Baoding area. The stable isotopic results show that the groundwater in Aquifer 2 represents light stable isotopic composition and partly mixed with groundwater of Aquifer 1. Similarly, the geochemical results also show a mixture of Aquifer 1 and Aquifer 2 groundwater taken in the vicinity of Baoding city. Furthermore, a cross section figure can help confirm the interaquifer flow processes, especially when comparing it with the previous study. Nevertheless, aforementioned interaction relationship could not be found in other regions within study area.

By using end member mixing analysis, it is clear that for the deep groundwater in Aquifer 2 in the vicinity of Baoding city, the interaquifer flows recharge has become dominated comparing with the lateral flows, and the former one account for about 31% to maximum 81% of deep groundwater recharge. An estimation of interaquifer flows by using Darcy’s Law indicated that interaquifer flows existed in Baoding area will range from $0.1\sim1.19\times10^{8}$ m^{3}/year depending on hydraulic difference between the aquifers and thickness of confining unit.

Keywords: Interaction, deep groundwater, shallow groundwater, interaquifer flows,
major ions, stable isotopes, EMMA, Baiyangdian Lake Watershed

Table of Contents

List of Tables

List of Figures

Chapter 1: Introduction

I. Research motivations associated with groundwater resources usage

Groundwater is the major water source in arid and semi-arid region and thus plays a strategically important role in society and economic development. However, groundwater problem nowadays has become a global environmental problem due to over-exploitation and other improper use of groundwater in last two decades (Wada *et al*, 2010; Mays, 2013). For sustainable groundwater resource management, a lot of related researches have been conducted and are focusing on, for example, groundwater flow regime, contaminant transfer and remediation and long term monitoring of groundwater table change (e.g., Su *et al*., 2013; Lalehzari *et al*., 2013; Guba *et al*., 2015; Esquivel *et al*., 2015).

On the other hand, it has been recognized that deep groundwater has better properties than shallow groundwater, such as steady and sufficient yield and better water quality. As a result, deep groundwater consumption has grown rapidly throughout the world in recent years, especially in arid and semi-arid regions where deep groundwater has become the main water resource for social and economic sectors (Plummer, 1994; Seiler and Lindner, 1995; UNESCO, 2009 and 2012). Therefore, for the society and economic sustainable development, it will be very important and necessary to pay close attention to deep groundwater today.

II. Review of related previous studies

1. Definition of shallow groundwater and deep groundwater

Shallow groundwater and deep groundwater, as the name implies, is the groundwater buried in different depth. However, in fact there is no determined depth defining what depth is shallow groundwater and deep groundwater. The depth will be very different in different researches, for example, the depth of shallow groundwater can range from less than 10 m to more than 100 m (Qian *et al*., 2006; Dhar *et al*. 2008;), while the depth of deep groundwater can up to several hundreds of meters (Ahmed *et al*., 2011; Ryu *et al*., 2012).

Even so, some methods are now usually to be used in defining shallow groundwater and deep groundwater. Some researches consider the groundwater in unsaturated aquifer as the shallow groundwater, and corresponding to this the groundwater flowing in the confined unit known as the confined groundwater is thought to be deep groundwater (Misra and Mishra, 2006; Taylor and Stefan, 2009). Tritium-Null-Fläche line (TNF) line is another useful method in defining shallow and deep groundwater (Seiler and Lindner, 1995). The depth at which tritium concentration become unmeasurable is called “tritium zero limit” (TNF), and the groundwater flowing above this line is called shallow groundwater, and that flowing below this line is called deep groundwater usually with ages exceeding 50 years to several thousand years.

2. Characteristics of deep groundwater

Figure 1 shows the main characteristics of deep groundwater comparing with shallow groundwater (Seiler and Lindner, 1995). It has been recognized that deep groundwater has better properties than shallow groundwater, such as steady and sufficient yield and better water quality. As a result, deep groundwater consumption has grown rapidly throughout the world in recent years, especially in arid and semi-arid regions where deep groundwater has become the main water resource for social and economic sectors (Plummer, 1994; Seiler and Lindner, 1995; UNESCO, 2009, 2012). Seiler and Lindner (1995) explained that deep groundwater has a longer flow path and residence time compared with shallow groundwater, because it is buried in deeper confined aquifers. This also suggests that once deep groundwater is contaminated, it creates a more severe environmental problem because it is more difficult to restore the water stored in deeper aquifers.

Aquifer-scale interaction estimates are essential for groundwater resource management (Scanlon and Cook, 2002). However, limited research concerning the interaquifer recharge between shallow and deep aquifers exists. Seiler and Lindner (1995), and Wang (1995) emphasized that this recharge may occur even if there is aquitard or aquiclude existing between the shallow and deep aquifers. Carucci *et al.* (2012) reported that the ratio of interaquifer recharge in the Tivoli Plain (Central Italy) is about 48~62% of the total recharge in the area.

Problems will occur if shallow groundwater, which is polluted and not suitable for drinking, recharges deep groundwater (Wang, 1995). What is worse is when these two

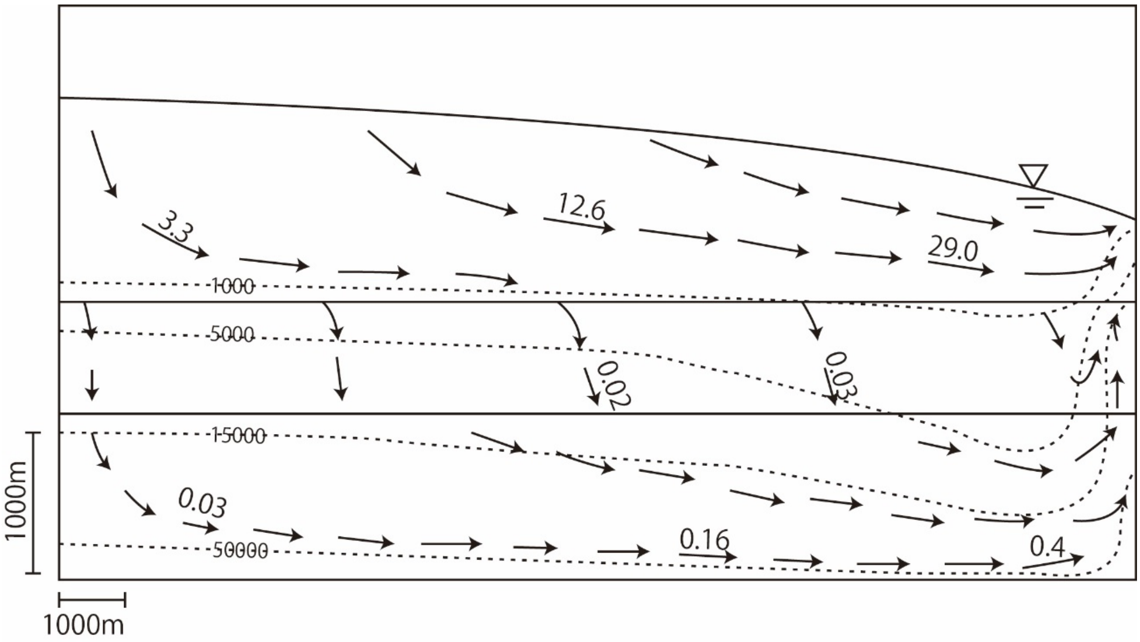

Figure 1: The distribution of flow velocities (m/day, arrows) and water ages (years, dotted lines) in groundwater flow system (Basing on Seiler and Lindner, 1995)

conditions co-exist, i.e., shallow groundwater pollution forces people to extract groundwater from a deep aquifer, and, consequently, the shallow groundwater table rises above the deep groundwater head, which enhances the recharge between different aquifers. Some researchers have reported cases of intrusion of shallow groundwater into deep groundwater due to an overexploitation of the deep groundwater in, for example, China, Thailand and India, although strong evidence (i.e., stable isotopes analysis) were not supplied in these studies (Guo and Shen, 1995; Onodera *et al.*, 2009; Saha *et al.*, 2011. Figure 2).

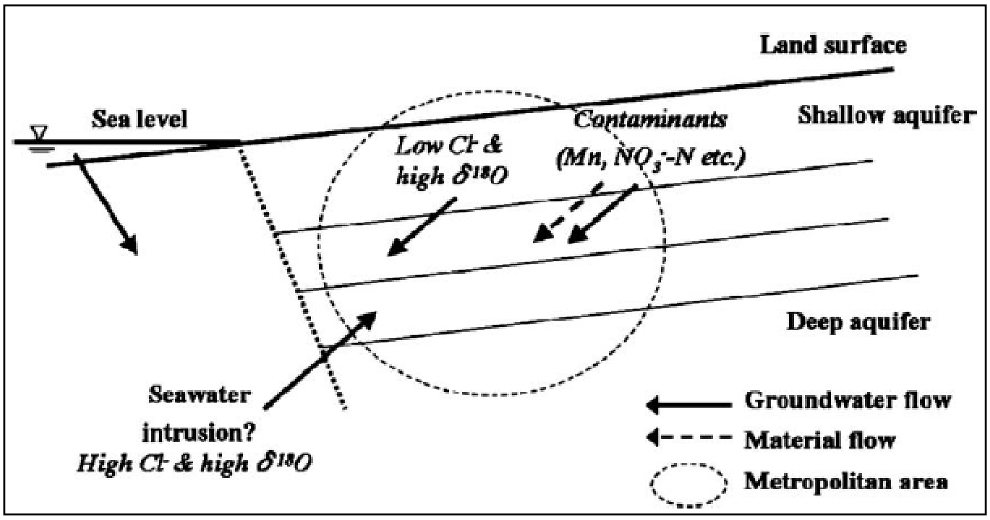

(a) Intrusion of shallow groundwater and seawater into deep groundwater in Bangkok (Onodera *et al*., 2009)

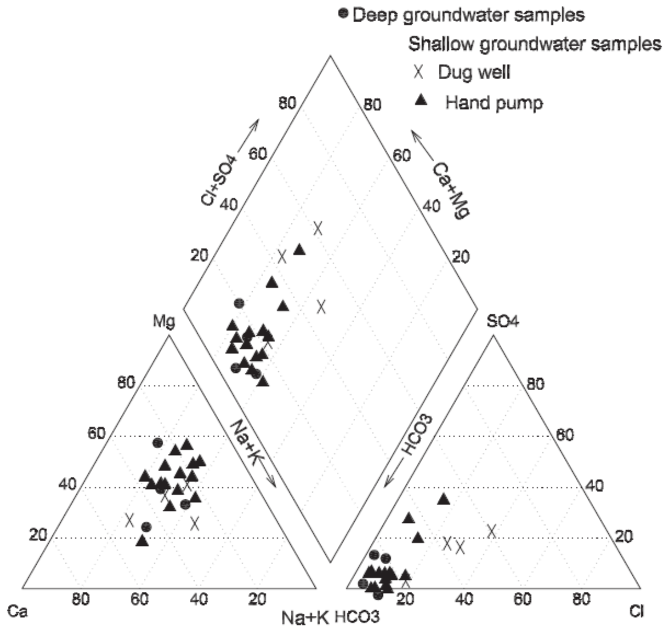

(b) Interaquifer processes in Ganga Plain, India (Saha *et al*., 2011)

Figure 2: Previous studies which reported the cases of intrusion from shallow groundwater into deep groundwater

3. Groundwater usage status in North China Plain

The North China Plain (NCP) is well-known as one of the most developed industrial areas and one of the largest agricultural production areas in China (Sun *et al.*, 2009; Zhang *et al.*, 2014). A lot of researches are focusing here because intensive and improper groundwater development in this area has caused many problems. Fang *et al.* (2010) and Shu *et al.* (2012) proposed some methods for improving water use efficiency by using a hydrological model and assessing spatial and temporal availability of water resources in the NCP. Other more researches concerned hydrochemical groundwater characteristics and processes in the NCP (e.g., Hu *et al.*, 2005; Wang *et al.*, 2008; Yuan *et al.*, 2011; Xing *et al.*, 2013), as serious pollution problems in groundwater, especially in the shallow aquifer are mentioned frequently.

Intensive and improper groundwater development in this area resulted in over use of groundwater resources. Figure 3 shows the historical evolution of water-table of shallow aquifer along transect of NCP (Foster *et al.*, 2003), which indicates that shallow groundwater table greatly depressed since 1960s, especially under some large cities like Handan, Shijiazhuang and Baoding. Forster *et al*. (2004) also reported that serious groundwater level depression occurred in both shallow aquifer and deep aquifer in NCP (Figure 4). A degree assessment of deep groundwater exploitation in NCP showed that the deep groundwater in most part of this area is under an over-exploitation situation (Figure 5; Shi *et al.*, 2009). Due to the over-exploitation of deep groundwater, it has been confirmed that groundwater depression cones have formed under many major cities of NCP (Chen *et al*., 2009; Nakayama, 2011; Zhang and Li, 2014).

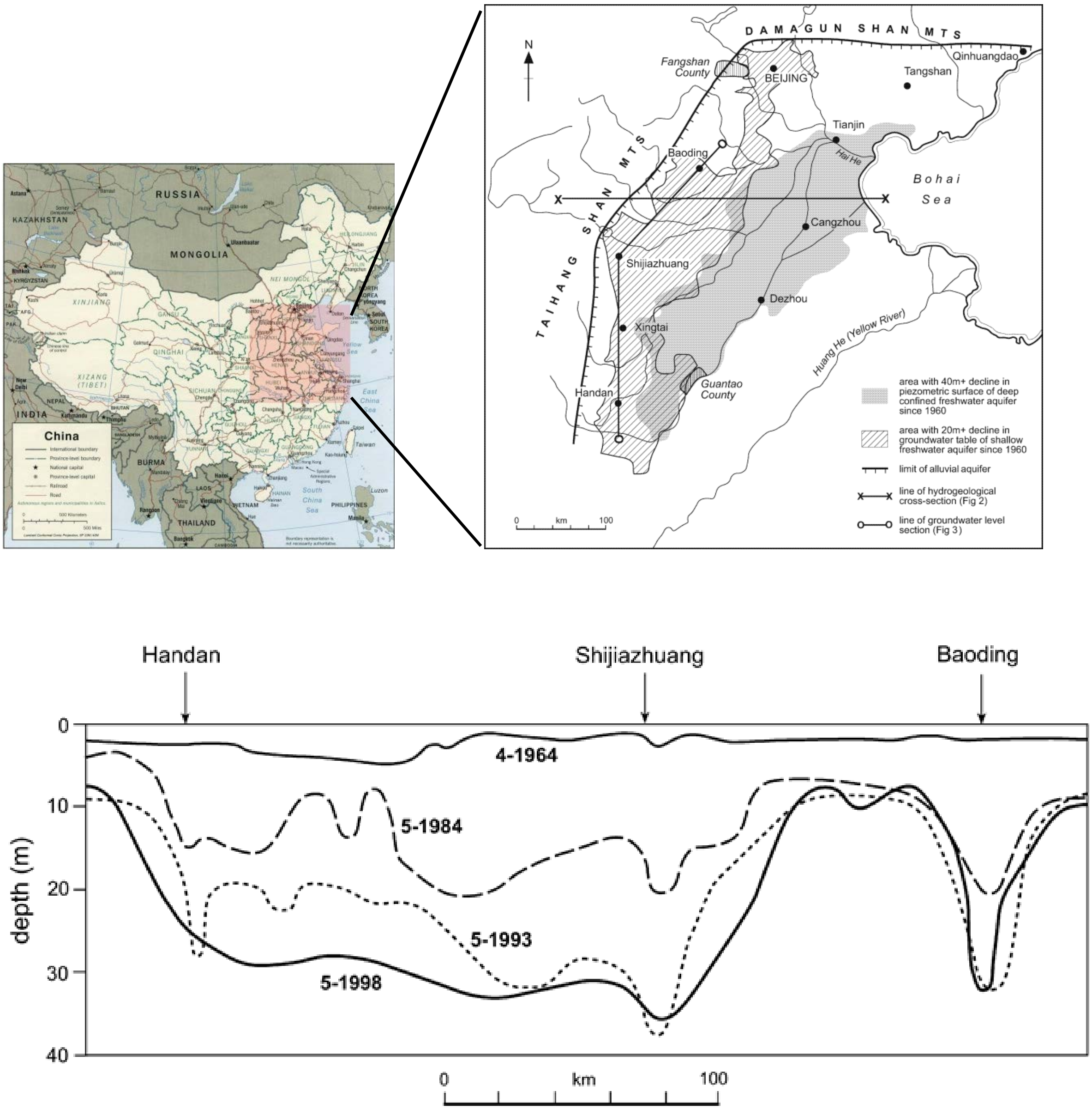

Figure 3: Historical evolution of water-table of shallow aquifer along transect of North China Plain (Foster *et al*., 2003)

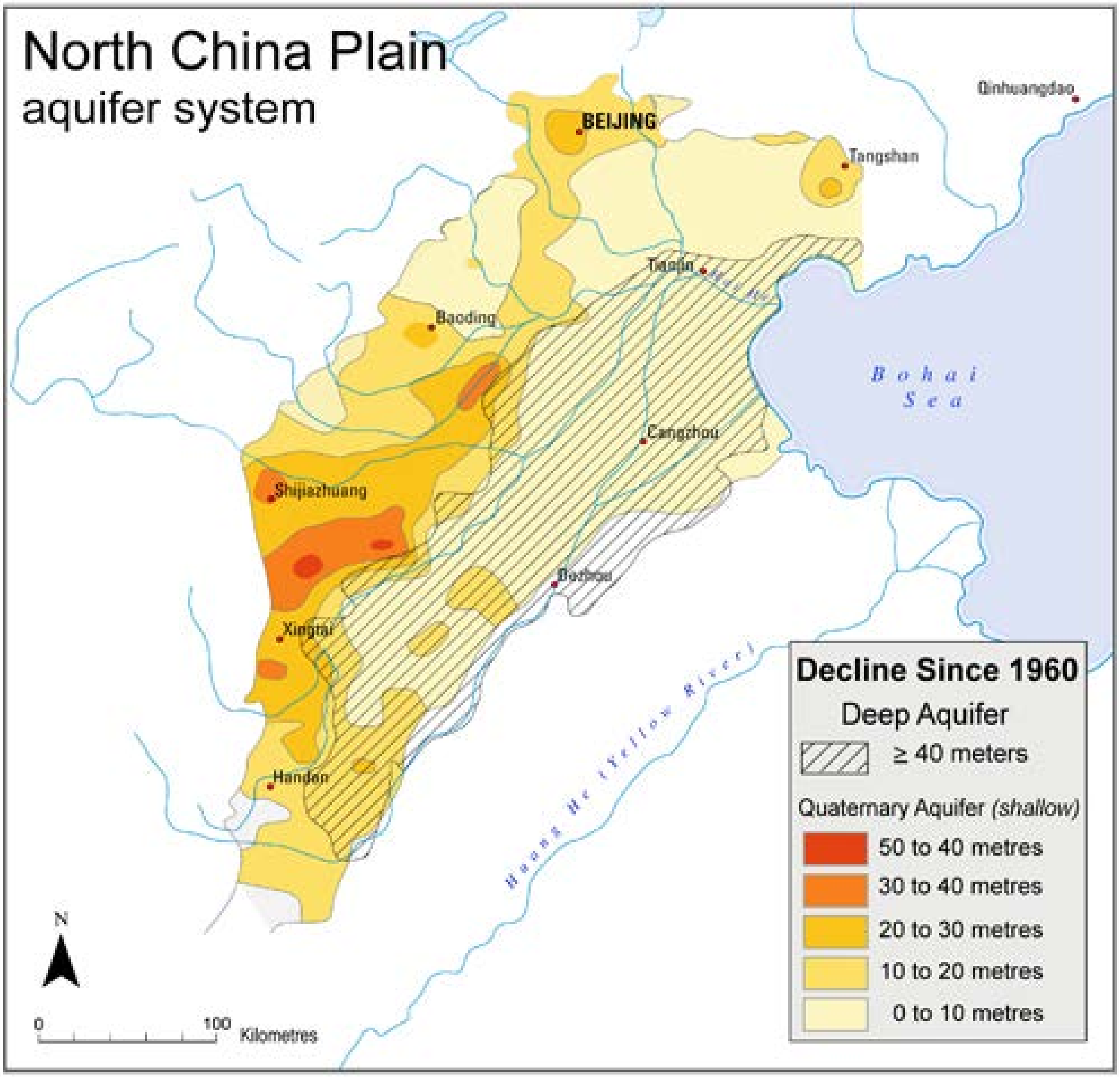

Figure 4: Decreased water table in both the shallow quaternary aquifer and the confined deep aquifer (Foster and Garduño, 2004)

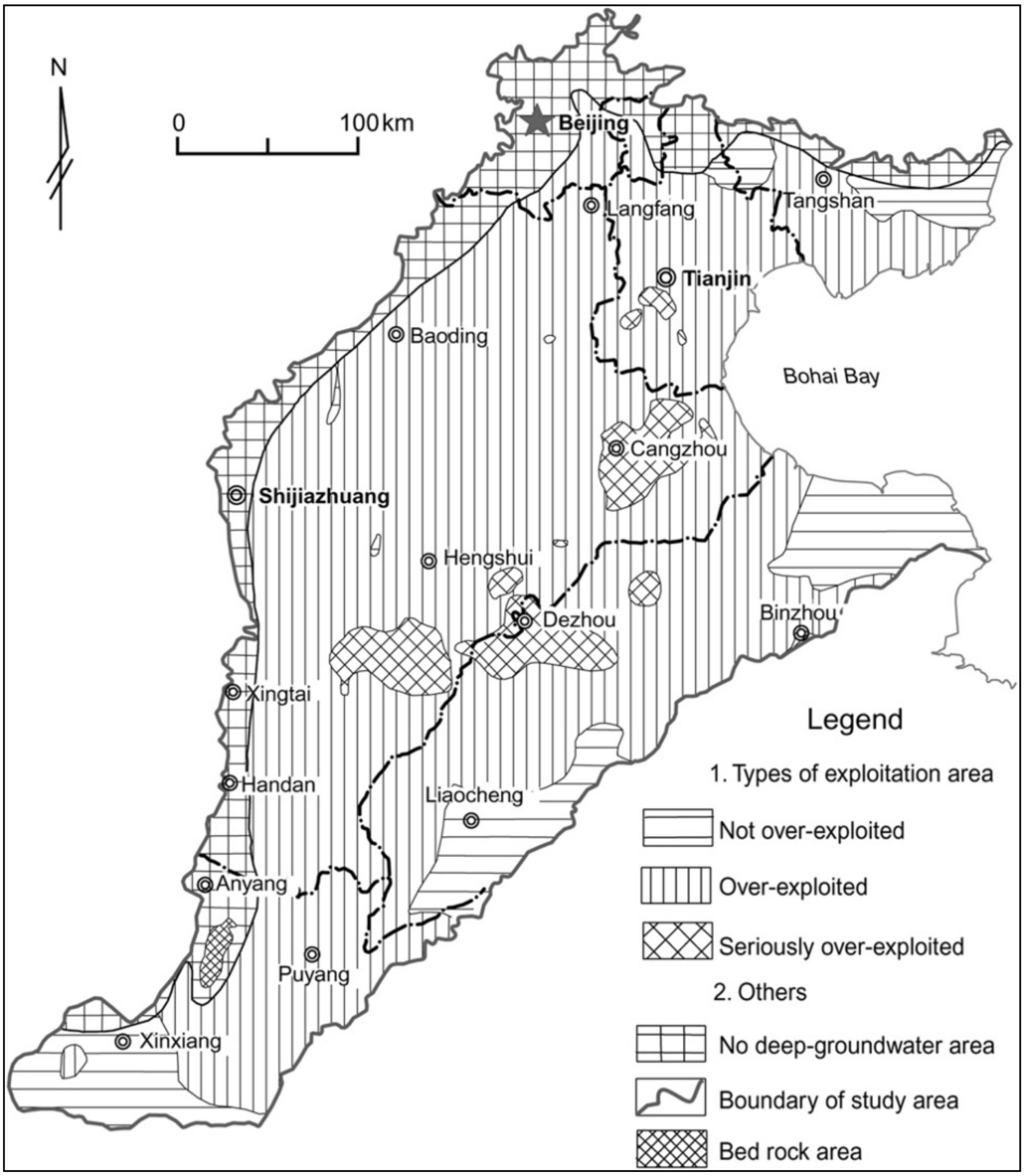

Figure 5: Assessment of deep groundwater over-exploitation in North China Plain (Shi *et al*., 2011)

In this situation, the interaquifer flows recharge from shallow to deep aquifer may occur with high possibility. In fact, by using numerical simulation model, Cao (2013) has reported that lateral flow to the deep aquifer in NCP is now limited and interaquifer flows from shallow aquifer has become dominated as recharge water sources (Figure 6). Due to over-exploitation of deep groundwater, the direction of interaquifer flows changed from shallow aquifer to deep aquifer (Figure 7).

4. Summary

The related previous studies have made clear the characteristics of deep groundwater, and the possibility of the interaquifer flow between shallow and deep groundwater. However, there are very few researches which reported such kind of interaction relationship, especially in arid and semi-arid areas. Previous studies about the North China Plain revealed that the deep groundwater resources have been excessively exploited in an unsustainable way. The numerical simulation suggested that interaquifer flows have become the dominated recharge sources in NCP. However, there is no geochemical evidences which can support this result.

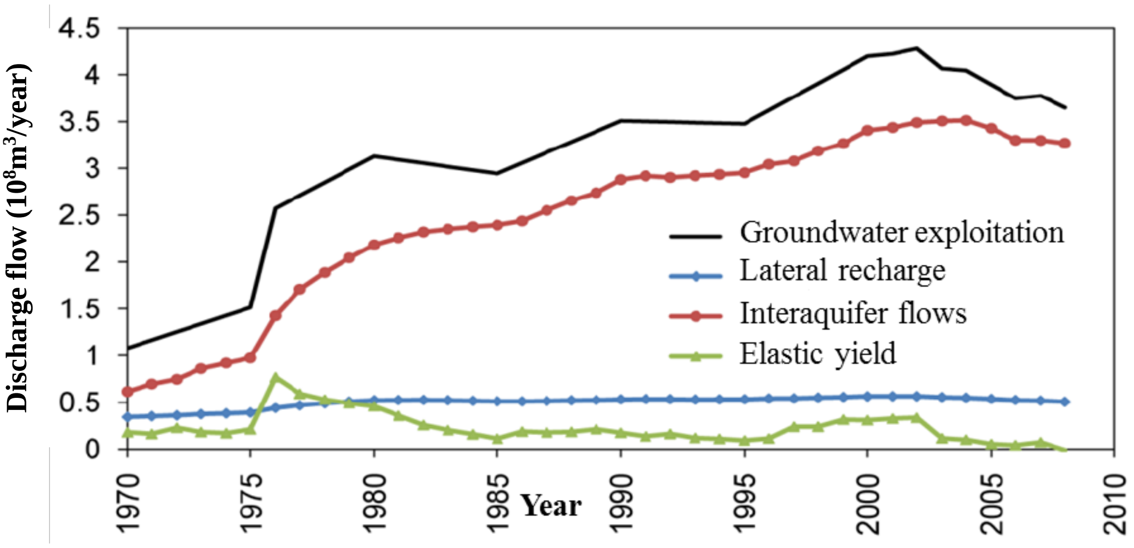

Figure 6: Simulation results of discharge flow of different recharge sources by using *Zonebudget tools* (Cao, 2013)

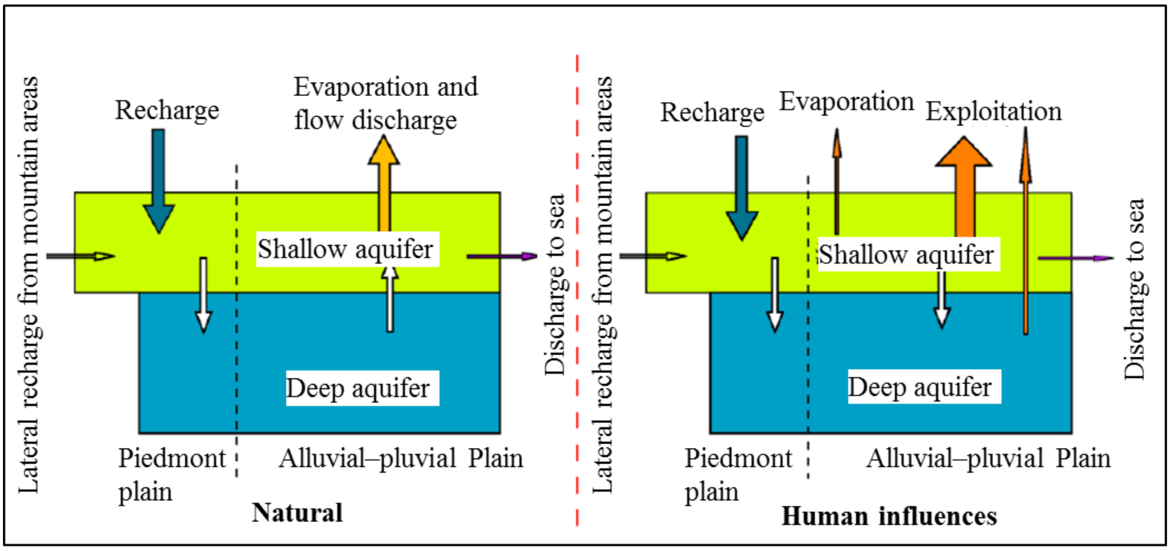

Figure 7: An image of groundwater flow path change in natural and exploited condition in North China Plain (Cao, 2013)

III. Research objective

Groundwater isotopes combined with chemistry can produce a more reliable conceptual model of a groundwater flow system (e.g., Tsujimura *et al.*, 2007; Chkirbene *et al.*, 2009). Specifically, due to the efficiency and economy, stable isotopes combined with major ions are prior to be used in clarifying the primary hydrogeological situation for one objective area (Kohfahl *et al*., 2008; Harker *et al*., 2015). In this study, the authors investigate the possibility and characteristics of the interaction between shallow and deep groundwater in the study area by using major ions and stable isotopes, and furthermore quantify the flux exchanges of the interaquifer flows with a view to sustainable groundwater resource management.

Chapter 2: Study area and methodology

I. Introduction to the study area

1. Location and topography

The Baiyangdian Lake Watershed (BLW) covers an area of about 36,000 km^2, ranging in latitude and longitude between 38.16-40.07°N and 113.66-116.12°E respectively (Figure 8), and has an urban population of over 12 million (Juana *et al*., 2010). Located in the northwest part of the NCP, the BLW is a typical alluvial fan where Baoding city, the largest city in this area with a population of over 8 million, is located in. Baiyangdian (BYD) Lake, the largest fresh lake of the NCP with area of 366 km^2 is located in southeast part of BLW (Figure 8).

The elevation inclines towards the northwest, from the southeast plains to the Taihang mountainous area, with elevation ranging from around 5.5~6.0 m at the bottom of Baiyangdian Lake to 2,088 m. The mountainous areas (above 100 m a.s.l.) occupy approximately 53% of this watershed (Long *et al*., 2010; Figure 9). In the mountain area there are 4 large reservoirs, namely Wangkuai, Xidayang, Longmen and Angezhuang reservoir, lies in the upstream of Zhulong river, Tanghe river, Cao river and Yishui river respectively (Yang and Yang, 2014). Due to the influences of these dam projects, the downstream part of rivers has become dried up for more than 20 years.

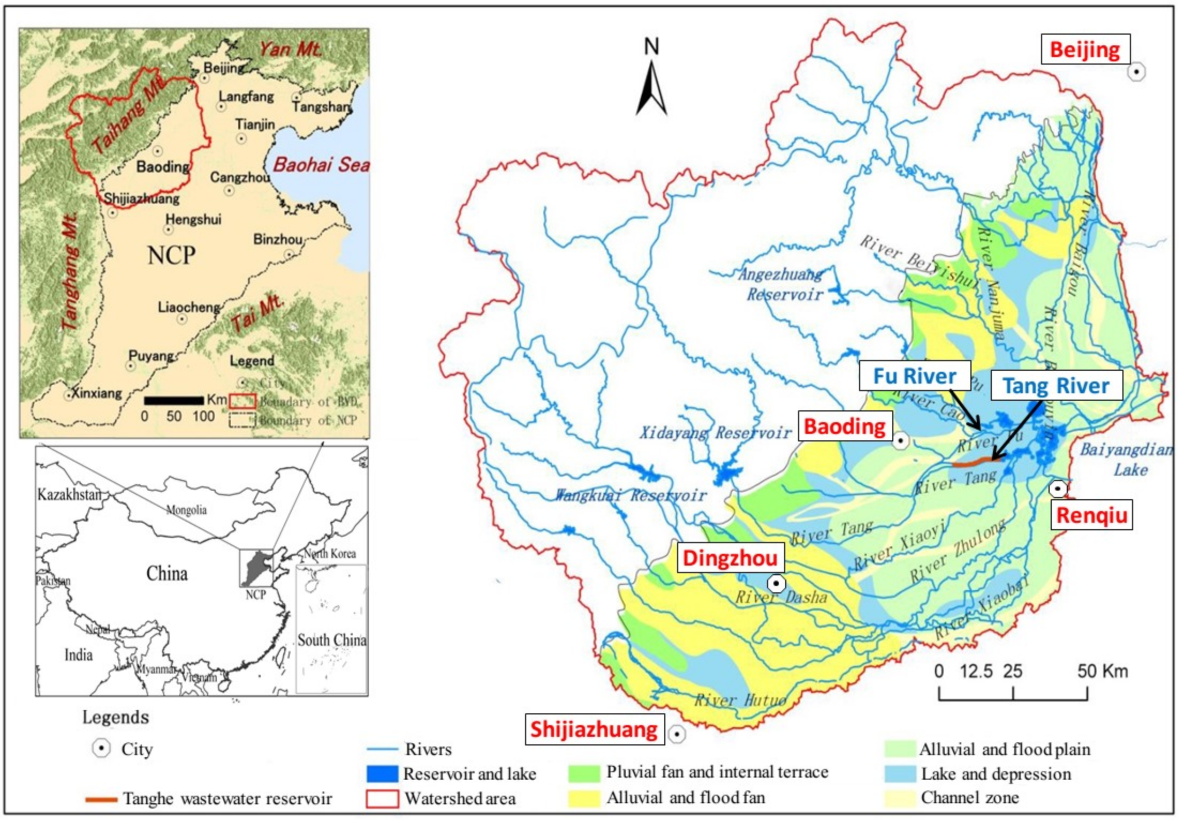

Figure 8: Location and major geological formation of study area

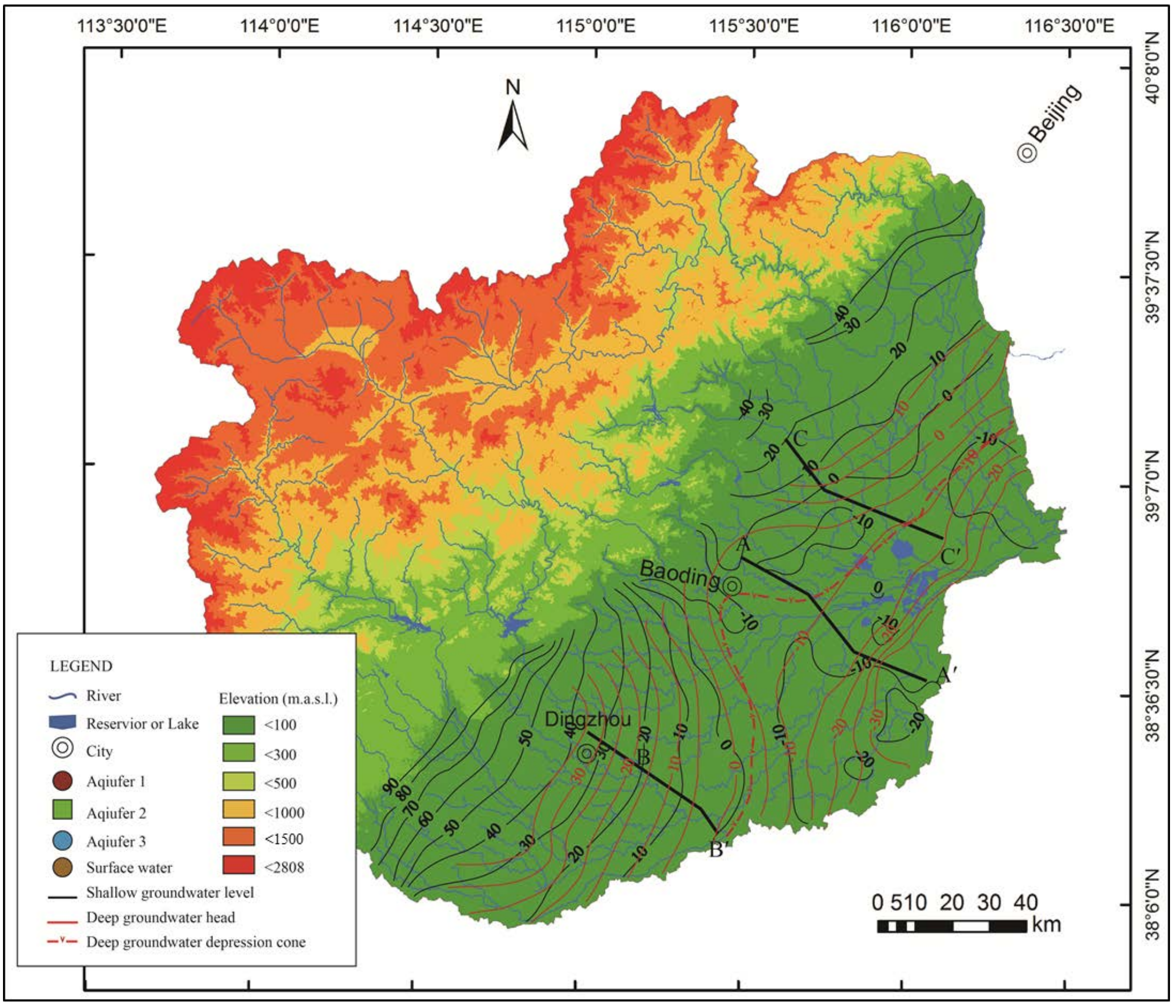

Figure 9: Topography and groundwater level information of study area

2. Climate characteristics

The study area has a continental climate, which is predominantly influenced by continental monsoon winds, with distinct seasonality. The average temperature in the coldest month of January is –11°C compared to 27°C in the hottest month of July. Average annual temperature, precipitation, and lake evaporation are 12°C, 581 mm, and 1,581 mm, respectively. Around 60~75% of precipitation falls in the summer months of July to August (Li and Zheng, 2001; Yang and Tian, 2009).

3. Land use and land cover

According to the land use statistics results of the study area, farmlands were mainly found in the plain accounting for 49.8%, 44.5% and 48% of the total watershed in 1980, 1995 and 2000, respectively. In addition to farmlands, there are also urban area, rural residence area and surface water body in the fan area (Figure 10; Long *et al.*, 2010; Wang *et al.*, 2014). Long-term utilization of fertilizer and manure, and the leakage of animal waste from the rural resident region are the major sources of NO_3^- contamination in surface water and groundwater in some big cities (Wang *et al.*, 2013; Wang *et al.*, 2014). The polluted rivers and wastewater irrigation also contributes greatly to NO_3^- contamination of groundwater in area between Baoding city and BYD Lake.

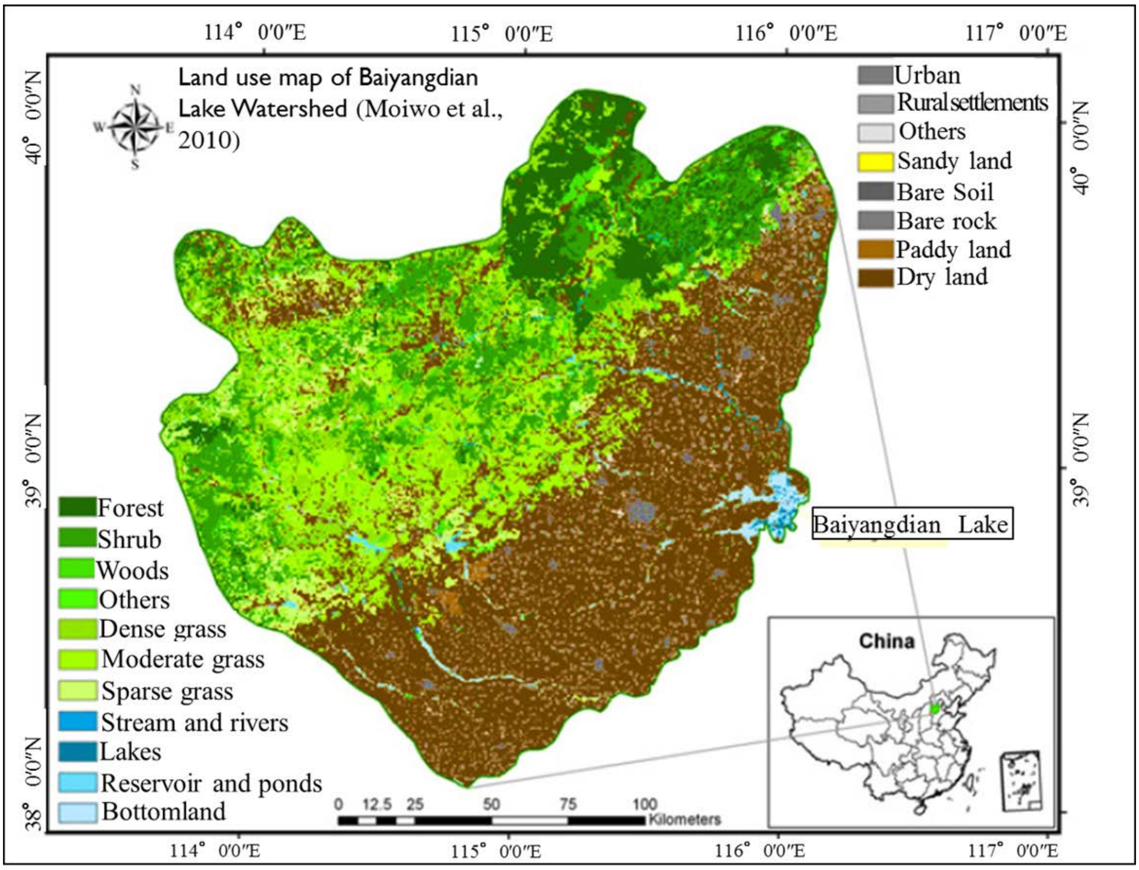

Figure 10: Land use information of Baiyangdian Lake Watershed

4. Geological settings

The Hebei Plain Basin, where Baiyangdian Lake Watershed is located in, is the biggest Cenozoic rifted basin in eastern China (Chen, 1987). It is adjacent to Taihang Mountain piedmont fault zone in west, to Liaodong and Jiaodong in East, to southern North China Basin through Xinxiang-Lankao fault zone in south, and Yanshan Mountain upwarping zone through Beijing-Penglai fault zone and Ninghe-Changli fault zone in North. There are five depression zones, which are Beijing, Jizhong, Huanghua, Bozhong (part), Linqing, and four upwarping zones, which are Daxing, Cangxian, Chengning, Hengshui-Xingtai, within Hebei Plain Basin. The mountain area in BLW belongs to Taihang Mountain upwarping zone, and the plain area belongs to Jizhong depression zone.

The Jizhong depression zone is an unremitting depression zone formed since the Eocene epoch, and the bedrock here belongs to blind arch structure, the axis of which is approximately along Gu’an-Gaoyang-Dacheng line, with north-north-east direction.

5. Hydrogeological settings

Hydrogeological conditions are represented in profile along three transect lines, A-A′ line and B-B′ line, C-C′ line in plain areas (Figure 11; see cross-section line in Figure 9). The thickness of the Quaternary system is about 200~600m, and become thin from west to east direction (Chen, 1987). The hydrogeological settings information along A-A′ line shows that the unconsolidated sediments of Quaternary Q4 constitute the main stratigraphy of the plain area, and these sediments mainly include sand, clay or silt clay, and silt. According to the features of the stratigraphy, it can be divided into four aquifer groups. However, due to thin thickness of the first unconfined aquifer and strong hydraulic connection, the 1st and 2nd aquifer is usually considered as one aquifer group, the shallow aquifer, and the aquifers below it is considered as deep groundwater system (Chen, 2004; Zhang *et al*., 2006; Wang *et al*., 2014). Basing on this, along the profile line A~A' in the vicinity of Baoding, the first aquifer group (Aquifer 1) includes aquifers of Holocene Qh4 and upper Pleistocene Qp3 with depth of 60~120 m. The second aquifer group (Aquifer 2) is the Middle Pleistocene Qp2 aquifer with depth of 120~360 m along line A~A'. The third aquifer group (Aquifer 3) with depth of deeper than 360 m is the lower Pleistocene Qp1 aquifer.

Because the deep aquifer is a semi-enclosed system, the recharge source usually cannot be from precipitation infiltration or surface water recharge, but mainly from vertical interaquifer flows and lateral flows with slow flow velocity. On the other hand, the shallow groundwater gets the recharge from precipitation or surface water, irrigation water, lateral water in piedmont zone, and drain the water by artificial exploitation and evaporation, lateral flows (Zhang *et al*., 2005).

6. Piezometric behavior

Regional shallow and deep groundwater levels have been compiled by Zhang and Fei (2009; Figure 9). The main flow direction of both shallow and deep groundwater is roughly from north and south side of plain area towards Baiyangdian Lake. Especially, in the southeast area of Baoding, the deep groundwater hydraulic head begins to fall below the shallow groundwater level, and then formed a deep groundwater depression cone region.

(a)

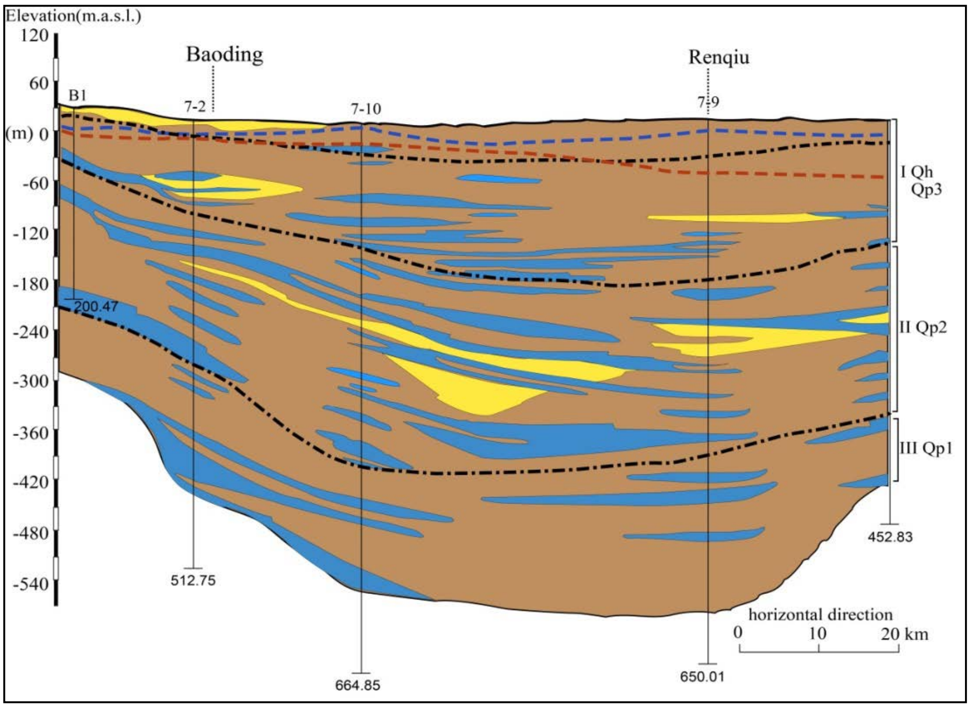
Elevation(m.a.s.l.)
120
60
(m) 0
-60
-120
-180
-240
-300
-360
-420
-480
-540
Baoding
Renqiu
B1
7-2
7-10
7-9
200.47
512.75
664.85
650.01
452.83
I Qh
Qp3
II Qp2
III Qp1
horizontal direction
0
10
20 km

(b)

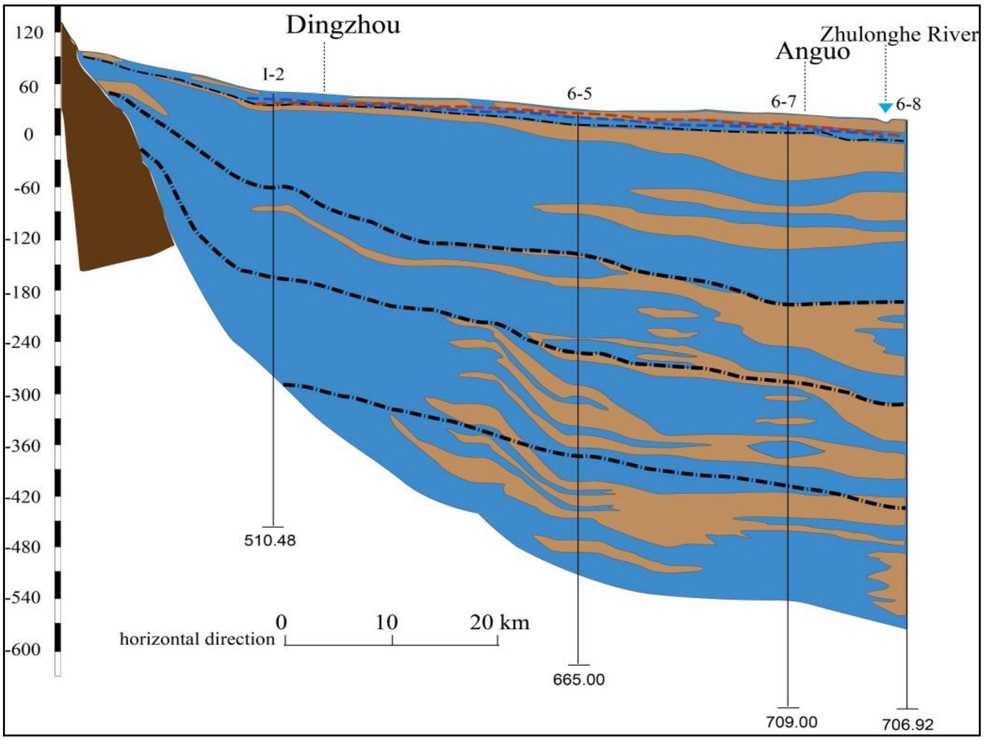
120
60
0
-60
-120
-180
-240
-300
-360
-420
-480
-540
-600
Dingzhou
Anguo
Zhulonghe River
I-2
6-5
6-7
6-8
510.48
665.00
709.00
706.92
horizontal direction
0
10
20 km

(c)

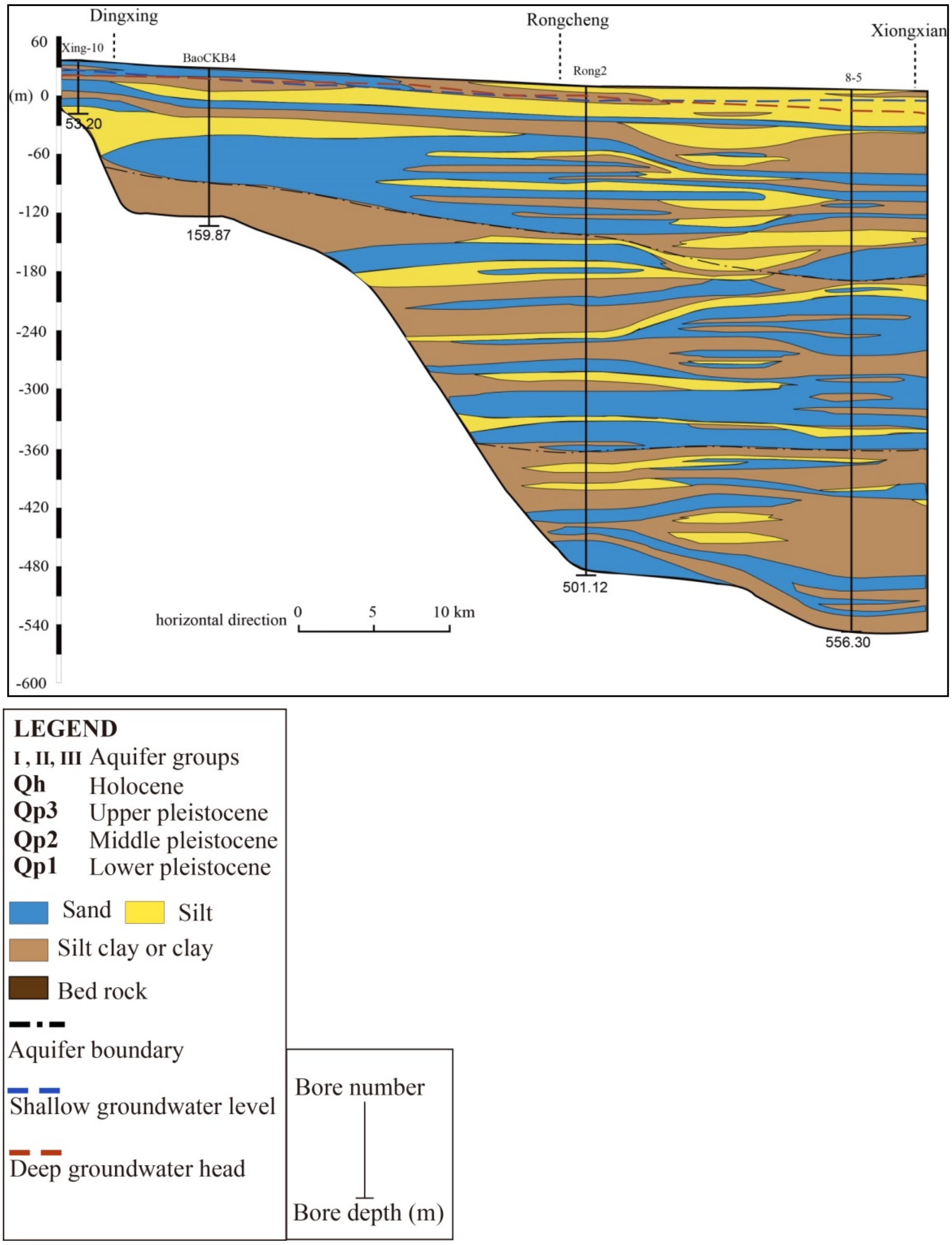

Figure 11: Profile of hydrogeological setting along (a) A-A′, (b) B-B′ and (c) C-C′ (see cross section location in Figure 9)

7. Water use problems

The development of groundwater in the BYD lake watershed began from 1950's with a quantity of 1.78×10^8 m^3/a. The amount increased to 27.08×10^8 m^3/a in 1980's. With the dry-up of rivers and over pumping, the BYD Lake has dried for several times (Liu *et al*. 2007). The hydrologic conditions have changed a lot including the decline of the inflow of the lake etc. (Figure 12; Zhuang *et al*., 2011). The groundwater level decreased continuously at the ratios of 0.51 m/a from 1974 to 2000, and 0.99 m/a from 2000～2007, respectively (Zhao *et al*., 2005; Liu *et al*., 2007; Zhang *et al*., 2007; Yang and Tian 2009; Lu *et al*. 2010). As well as the water shortage problems, water pollution is also serious (Ma *et al*., 1995; Zhang *et al*., 1997). Of 8 inflow rivers for the BYD Lake, only the Fu River is a perennial river which accepts the sewage from Baoding city without primary treatment (Zhang *et al*., 1999; Li *et al*., 2006;). Tang River has been completely dried in recent years. Paralleling to the Tang River, the Tanghe wastewater reservoir (TWR), an artificial channel with length about 15 km, was constructed in 1970's to store the industrial effluents from Baoding City. Sluice gate was set in the east end of it to prevent the effluents from flowing into the lake. Thus, the Fu River and TWR have become line sources to influence the regional groundwater on both quality and quantity.

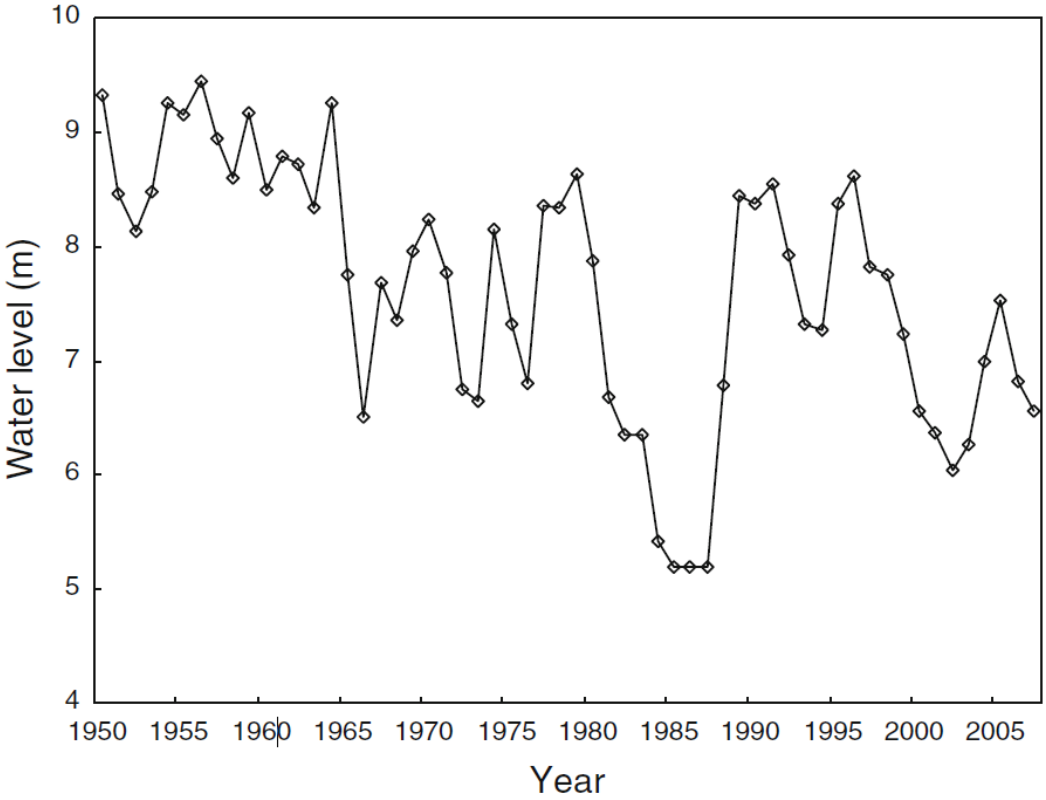

Figure 12: Annual mean water level in Baiyangdian Lake between 1950 and 2007 (Zhuang *et al*., 2011)

II. Field survey actives

1. Water samples information

The water samples information is shown in Appendix. For the objective of this research, four field work activities were conducted since June 2011 to March 2013 in the study area. In total, 187 water samples are collected from groundwater and surface water, which are located in mountain area (MA) and plain area (PA) (Figure 13). Because only one groundwater aquifer exists in mountain area, so the focus of this research, namely the interaction relationship between shallow and deep aquifer can only be found in the plain area. Therefore, discussion of this research will be held mainly for the results of plain area. However, for understanding the geochemical difference between mountain area and plain area, the situation of mountain area will also be included in results part.

The samples taken in PA are mainly located around two cities. One is Baoding city, the biggest city in the Baiyangdian Lake Watershed, and the other is Dingzhou city, which is county-level city in south BLW. The groundwater samples taken in plain area were divided into 3 groups (Aquifer1, Aquifer2 and Aquifer 3) according to the aquifer they belong to (see aquifer classification in *Chapter II section 1 sub-section 5 Hydrogeological settings*). Based on the information from local villagers, for accessing safe water resources, the government helped to drill the deep well. So it is assumed that these deep wells have good enough structure and quality to prevent the leakage from shallow aquifer to deep aquifer.

A special area, named surface water region is defined in the vicinity of Baoding city (Figure 13). That is because two artificial rivers flow through here. One river is called Fu River, which receives sanitary sewage without primary treatment from Baoding city, and the other river is Tang River, which is used as an industrial sewage reservoir (Dai *et al*., 2011). Both of these two surface waters bring great influences to the qualities of the water body in this area (Zhao *et al*., 2012). The influences of these two rivers to groundwater will be discussed in the result part. Furthermore, due to dam projects in the upstream of Baoding and Dingzhou city, downstream part of these natural rivers have become dried up for many years, which consequently exacerbated the influences of these two artificial rivers to groundwater body.

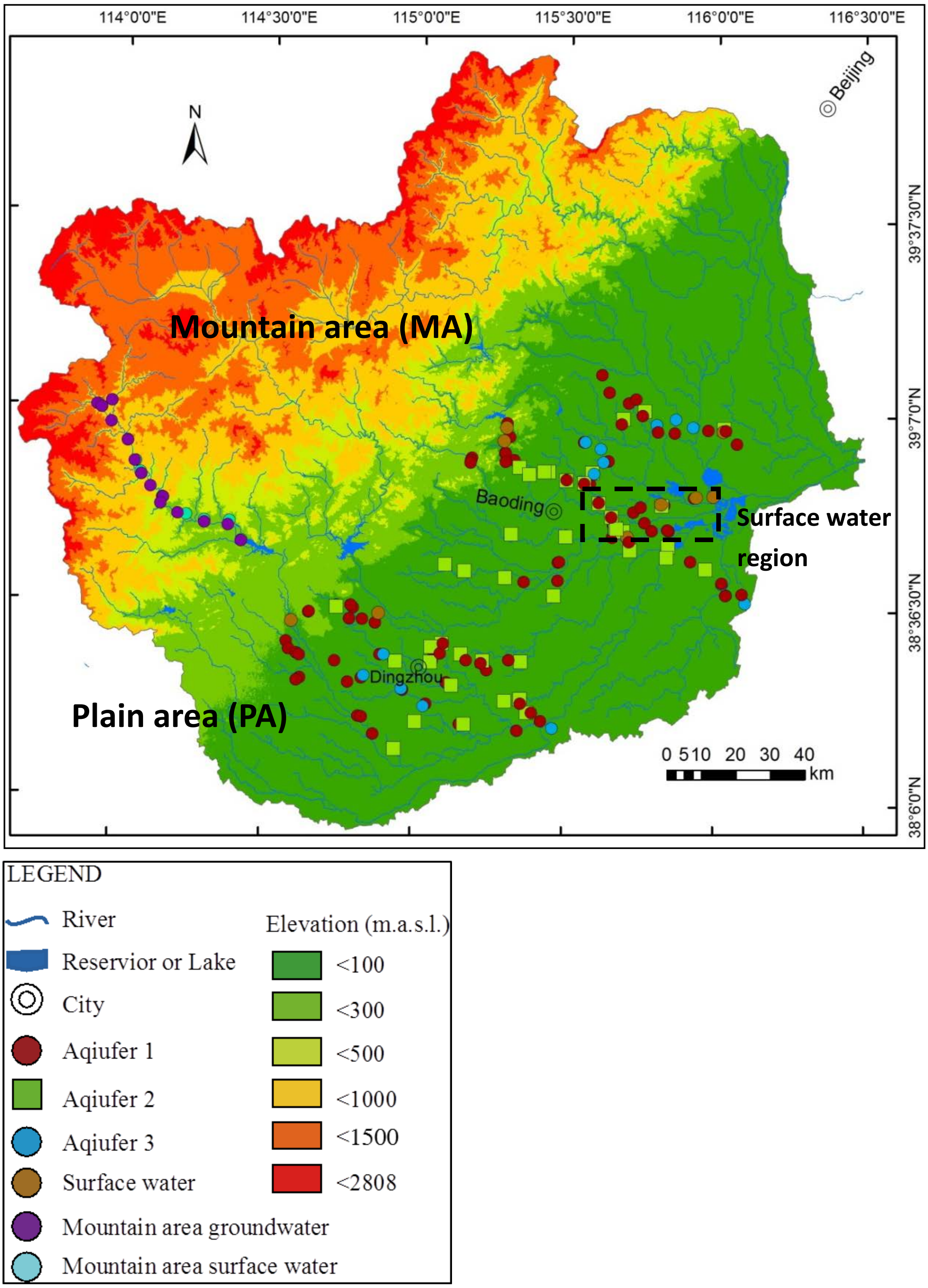

Figure 13: Sampling locations in study area

2. Field measurement and analysis methods

Temperature (Nikkyo Technos Co. Ltd., Petten Kocher), Electrical Conductivity (EC; HORIBA Ltd., Twin Cond B173) and pH value (HORIBA Ltd., Twin PH Meter B121) of water samples were measured in situ. The well depth information was recorded in situ by groundwater level meter or asking local villagers (in case of deeper than 50 m). The locations of each sampling point was determined by a portable GPS meter (GARMIN Ltd., GPSMAP 76S). Each sample was filled and sealed in a 100ml polyethylene bottle and brought back for chemical and isotopic compositions analysis in the laboratory of University of Tsukuba, Japan. The chemical composition was characterized by an ion chromatography analyzer (Shimazu Co. Ltd., HIC-SP/VP Super) for major anions (Cl^-, NO_3^-, SO_4^{2-}) and an inductively coupled plasma atomic emission spectrometer (PerkinElmer Inc., Optima 7300DV) for major cations (K^+, Na^+, Ca^{2+} and Mg^{2+}). Bicarbonate (HCO_3^-) concentration was measured by the titration method with sulfuric acid as soon as when took the samples back to the laboratory. The stable isotopes of $\delta^{18}O$ and δD were measured with a mass spectrometer (Finnigan Inc., MAT 252). The $\delta^{18}O$ and δD values are reported as per mill (‰) deviations from the international standard V-SMOW (Vienna Standard Mean Ocean Water). The analytical errors were 0.1‰ for $\delta^{18}O$ and 1‰ for δD, respectively.

III. Data analysis and interpretation

Water samples information were collected on field and analyzed in laboratory. However, the analysis results can become easy to understand and interpret only after reprocessing. Below are main reprocessing methods and some necessary theories used in this research.

1. Chemical results analysis and interpretation

More than 99% of the dissolved solids in natural groundwater are composed of less than a dozen constituents. The bulk of these consist only seven ions - Cl^-, SO_4^{2-}, K^+, Na^+, Ca^{2+}, Mg^{2+} and HCO_3^- - and other dissolved SiO_2. Traditional chemical analysis of water samples reports these contents, so they can be used to provide information both on the aquifer materials and the suitability of water for human use (Mazor, 2003). The major ions results (Cl^-, NO_3^-, SO_4^{2-}, K^+, Na^+, Ca^{2+}, Mg^{2+}, HCO_3^-) of the water samples were analyzed and interpreted by using Trilinear diagram and Hexa diagram.

Trilinear diagram, also called by Piper diagram (Piper, 1953), consists of two triangles and one rhombus. The triangle in left bottom represents the mill equivalent percentage of cations (K^+, Na^+, Ca^{2+}, Mg^{2+}), and the one in right bottom is the mill equivalent percentage of anions (Cl^-, NO_3^-, SO_4^{2-} , HCO_3^-). The relative content of cations and anions for each water sample will be marked in the corresponding location within two triangles, and the intersection of two lines from these two locations in rhombus will be the relative ions contents for one water sample. The different size of circle marks means different mineralization degree. Water samples distribution in different areas in the rhombus represents different chemical characteristics.

Hexa diagram, also called by Stiff diagram (Hem, 1985) are the most familiar application of profile plots in water resources. In a Hexa diagram, the mill equivalents of major water-quality constituents are plotted for each sample, with the cations profile plotted to the left of the center line, and anion profile to the right. Comparison between several samples based on multiple water-quality constituents is then easily done by comparing shapes of the Hexa diagrams.

2. Stable isotopes

Stable isotopes of oxygen (^{16}O, ^{18}O) and hydrogen (^{1}H, ^{2}H) are by far the most frequently used isotopes in water studies. Their applicability was pointed out more than 30 years ago (Dansgaard, 1964), and their application in hydrological studies has increased gradually since that time and currently are some of the most commonly and most useful parameters in many watershed studies.

Generally, a given isotope of an element (e.g.,^{16}O of oxygen) is overwhelmingly abundant compared to other isotopes of that same element. Natural changes in the relation between dominant and rare isotopes due to fractionation are often too small to be measured accurately. Therefore, isotopic abundances are reported as positive or negative deviation away from a standard. This convention, yielding the δ values, was established in the following general equation (Gat, 1980):

$$\delta(‰) = \frac{R_{sample} - \quad R_{stndard}}{R_{standard}} \times 1000$$

(Equation 1)

where R is the isotope ratio given by the relation between the number of atoms for two isotopes, e.g. $^{18}O/^{16}O$, $^{2}H/^{1}H$.

The ^{18}O and D (D=deuterium, namely ^{2}H) isotopes are integrated parts of the water molecule and are therefore well-suited for hydrological tracing studies. The ^{18}O and D contents are normally expressed as $\delta^{18}O$ and δD, related to the standard SMOW (Standard Mean Ocean Water; Craig, 1961). The fractionation effects for D are similar to those for ^{18}O, although the fractionation is larger for D, giving a proportionally larger variation in the δ-value of this isotope than for δ^{18}O. In precipitation or a certain water body (e.g., a groundwater aquifer), the relationship between these two isotopes is linear, given by the so-called meteoric water line for precipitation or water line for other water body (Craig, 1961):

$$\delta \mathrm{D} = a\delta^{18}\mathrm{O} + b \quad (‰)$$

(Equation 2)

where a and b are typical constants for a specific area.

Stable isotopic compositions in groundwater is hardly affected by water- rock/soil ion exchange under normal temperature, and also hardly affected by evaporation as long as under certain depth which is usually not too deep (McCarthy *et al*., 1992; Gat, 1996). Therefore, the stable isotopic variations existing in groundwater might be the consequence of the concentration variations from the input such as precipitation and surface water (Kendall and Mcdonnell, 1998). Based on the δ values in different water body and precipitation within a watershed, it is possible to build groundwater flow regime.

3. End member mixing analysis

End member mixing analysis (EMMA) is a commonly applied method to identify and quantify the dominant runoff producing sources of water (Ali *et al*., 2010; Yang and Hur, 2014). It employs tracers like isotopes and dissolved ions to determine the dimensionality of the hydrologic system. The application of this mixing model are basing on the assumptions as below (Hooper *et al*., 1990):

(1) Tracers are conservative (no chemical reactions);

(2) All components have significantly different concentrations for at least on tracer;

(3) Tracer concentrations in all components are temporally constant or their variations are known;

(4) Tracer concentrations in all components are spatially constant or treated as different components;

(5) Unmeasured components have same tracer concentrations or don't contribute significantly.

4. Darcy's law

Darcy's law was firstly proposed by Darcy (1856) that for saturated conditions the flow rate through a porous medium is proportional to the hydraulic gradient. Later studies have verified that this relation is also valid for unsaturated flow and interaquifer flows (Berndtsson *et al*., 1987; Dettinger 1989; Lerner, 1990; Hamed *et al*., 1998). Darcy's law can be written as:

$$Q = K \cdot A \cdot \frac{\mathrm{d}\Phi}{\mathrm{d}x}$$

(Equation 3)

where Q = discharge (m^3/s), K = hydraulic conductivity (m/s), A=cross section area (m^2), $d\Phi/dx$ = total potential gradient (hydraulic gradient) (m/m).

Specifically, the hydraulic conductivity K varies with the water content of the soil. The variation depends upon the pore size distribution of the soil. The hydraulic conductivity of a given soil increase rapidly with increasing water content, mainly due to the increasing radius of the water-filled pores, and reaches its maximum when the soil is saturated.

Chapter 3: An overview of the hydrogeochemistry characteristics in Baiyangdian Lake Watershed revealed by all water samples

I. Trilinear diagrams results of all water samples

Trilinear diagrams result of all water samples are shown in Figure 14 (a) for these taken in mountain area and in (b) for these taken in plain area. It is clear that surface water and groundwater collected in mountain area are chemically similar, though the Mg^{2+} concentration is somehow a little varied. This might be induced by water-rock reaction during surface water recharging to groundwater or groundwater flowing through the pathway (Shikazono, 2001).

The situation is much more complicated in the samples taken in plain area. The chemical compositions of surface water are quite different from groundwater and shows an abnormal water type. This is because surface water is mainly from artificial rivers used as sewage water reservoirs (see surface water region introduction in Chapter 2). The groundwater samples of Aquifer 1 show inhomogeneous water type and so distribute relatively widely in trilinear diagram. This is in part because the influences of surface water which is recharging to shallow aquifer, and also might because the shallow groundwater buried condition is naturally inhomogeneous within watershed. Groundwater of Aquifer 2 and Aquifer 3 are chemically similar, which show stable concentration in HCO_3 and variations in cations.

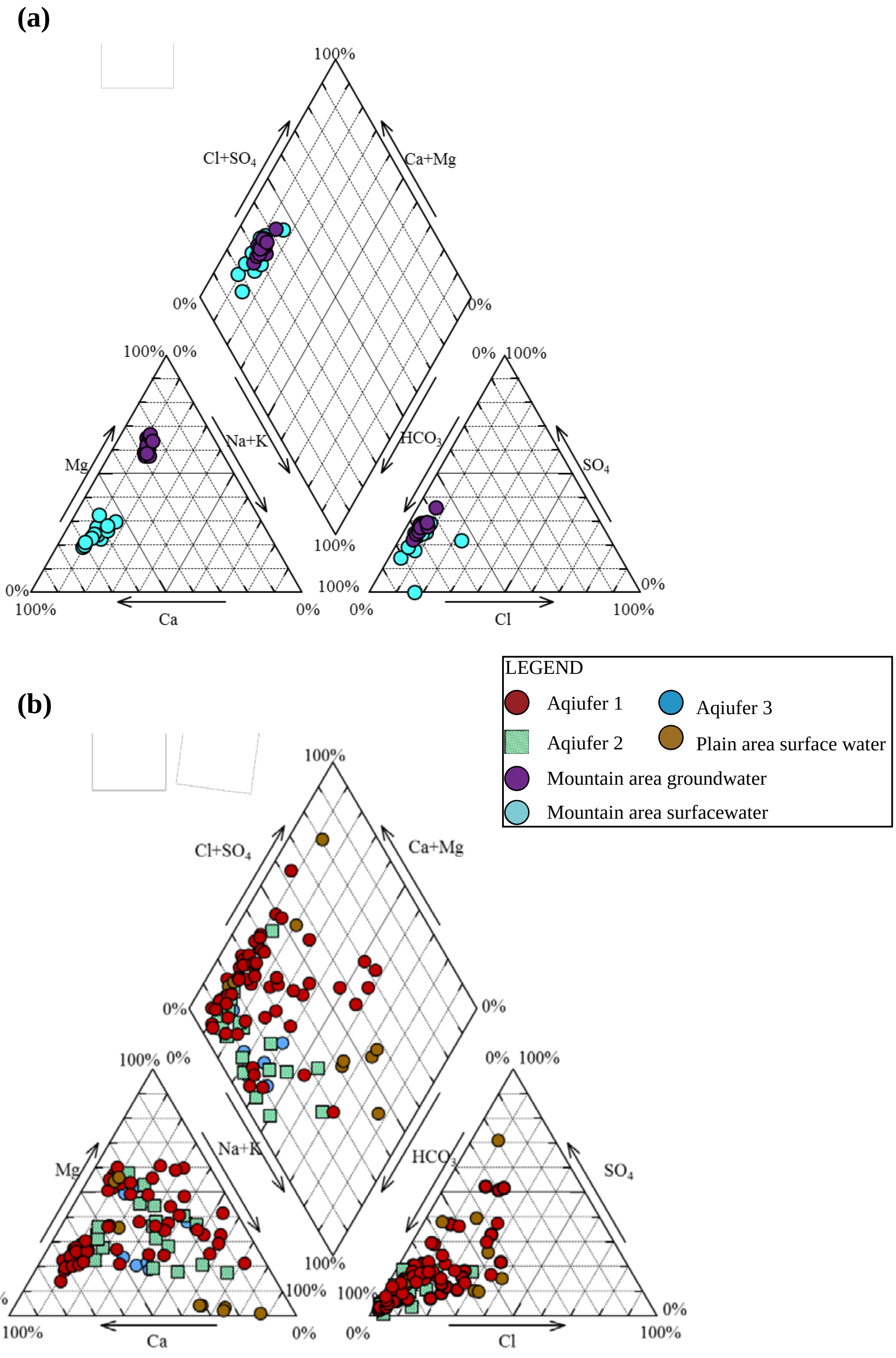

Figure 14: Trilinear diagrams results for (a) all samples in mountain area and (b) all samples in plain area

II. Stable isotopic compositions of all water samples

Figure 15 shows the relationship between δD and δ^{18}O values of surface water and groundwater in mountain area (1) and plain area (2) with a local meteoric water line ($\delta D = 8.2\delta^{18}O + 9.4$; LMWL; precipitation in Shijiazhuang; WMO/IAEA, 2003), which is quite close to the global meteoric water line ($\delta D = 8\delta^{18}O + 10$; GMWL; Craig, 1961). The δD and δ^{18}O values of LMWL were plotted by using the weighted mean year values with large variation ranging from -11.13‰ to -6.50‰ for δ^{18}O values and from -81.20‰ to -39.73‰ for δD values.

In mountain area, the stable isotopic compositions in surface water and groundwater show little dissimilarities with value ranging from -9.75‰ to -6.65‰ for δ^{18}O and -70.35‰ to -51.37‰ for δD, and the slope of these samples is closed to that of LMWL. This suggests that there are strong hydraulic connections between surface water and groundwater in mountain area and precipitation is recharging to both surface water and groundwater. Furthermore, altitude effect is can be found in mountain area groundwater, with a decrease rata of 0.3 ‰/100m (Figure 16). According to Clark and Fritz (1997), the depletion varies from -0.15‰ and -0.5‰ per 100m in altitude in precipitation. Therefore, such kind of decrease rate can prove again that the precipitation is directly recharging groundwater in this area.

In plain area, the stable isotopic composition in surface water presents heaviest value with value ranging from -7.60‰ to -4.14‰ for δ^{18}O and -56.35‰ to -40.11‰ for δD, and the slope of these samples is distinctively lower than that of LMWL. This kind of enrichment is caused by isotopic fractionation during water evaporation (Stewart, 1975; Ozawa and Nagahara, 2001). In this area, the stable isotopic compositions of groundwater samples of Aquifer 1, ranging from -10.09‰ to -4.42‰ for δ^{18}O values and from -72.68‰ to -40.94‰ for δD values, are relatively higher than those in Aquifer 2 and Aquifer 3. Although the same samples of Aquifer 1 are away from LMWL, there are still a set number of Aquifer 1 samples closed to it. Specifically, these, which are away from LMWL, are almost from surface water region. This suggests that part of the samples from Aquifer 1 is significantly influenced by surface water, and rest parts of these samples are recharged directly by precipitation without intensive evaporation processes. The groundwater samples in Aquifer 2 and Aquifer 3 present stable isotopic compositions with ranging from -11.22‰ to -8.15‰ for δ^{18}O values and from -83.91‰ to -61.35‰ for δD values, and ranging from-10.98‰ to -8.72‰ for δ^{18}O values and from -81.28‰ to -64.79‰ for δD values, respectively. Several samples in Aquifer 2 and Aquifer 3 are mixing together (Figure 15), which indicates that these samples in different aquifers probably originated at the same elevation. There are some other samples in Aquifer 2 are more closed to the samples in Aquier1, which perhaps implies an interaction (interaquifer flows processes) between these two aquifers, and this will be discussed in detail later.

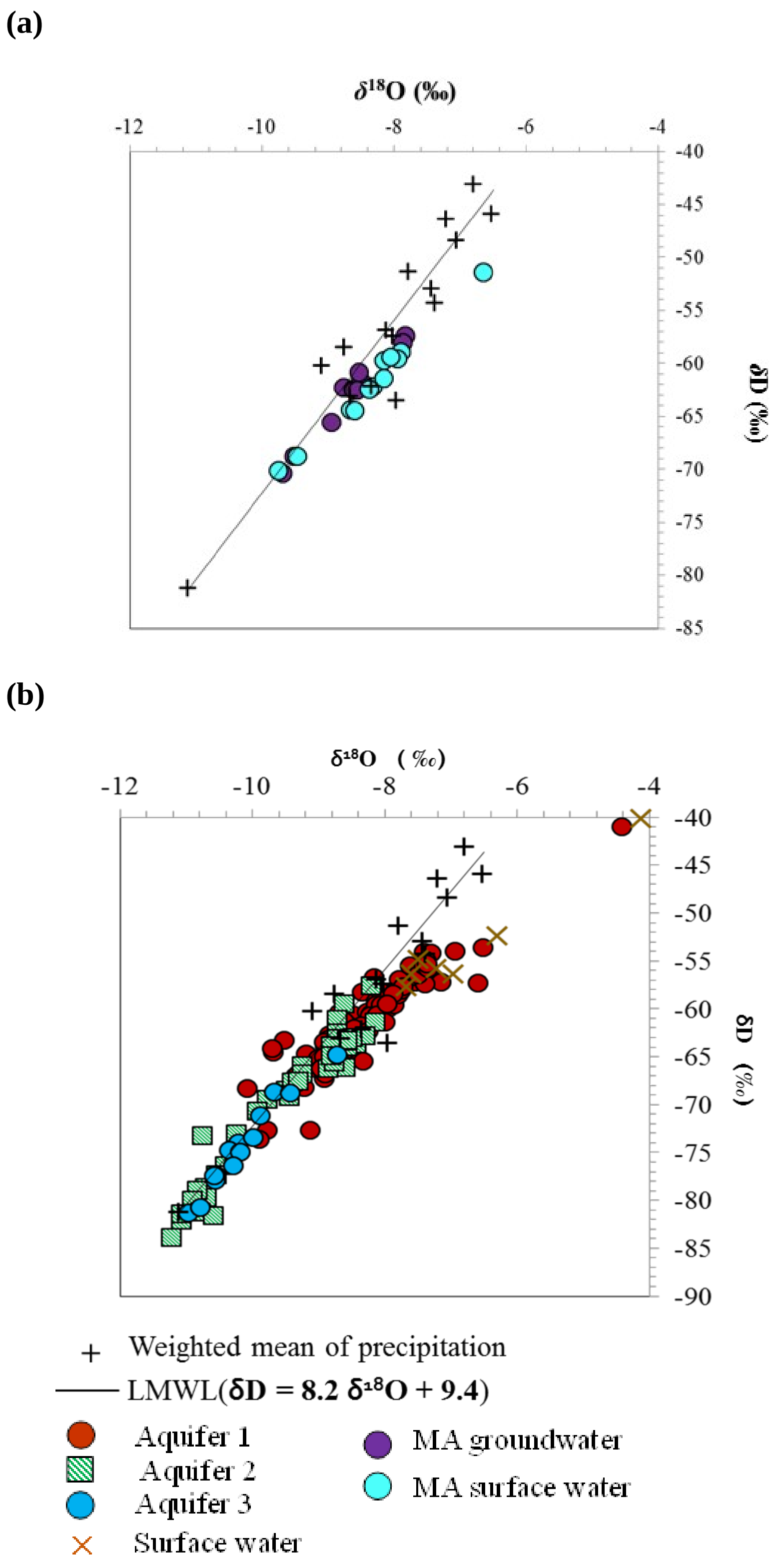

Figure 15: Relationship between δD and δ^{18}O values of surface water and groundwater for (a) all samples in mountain area and (b) all samples in plain area

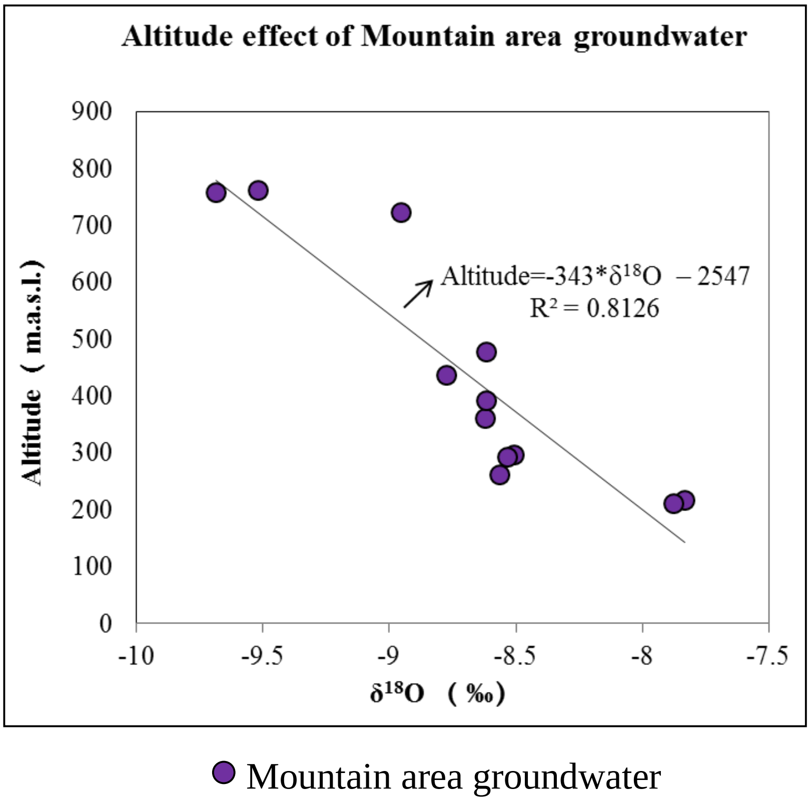

Figure 16: Stable isotopes altitude effect in mountain area groundwater

III. Spatial distribution of electrical conductivity value of all water samples

Based on the electrical conductivity (EC) results, all water samples were divided into 4 classes and then spatially distributed in Figure 17. Relatively high EC value mainly come from surface water and groundwater of Aquifer 1, especially from these taken in surface water region in the vicinity of Baoding city. The highest EC value of surface water in this region was up to more than 5000μS/cm, and corresponding to it, EC value of some Aquifer 1 groundwater in this region were up to more than 2000μS/cm in several locations. This indicates the great influences of surface water to shallow groundwater in this region. A research focusing the heavy metal situation in groundwater in NCP reported that heavy metal pollution in local groundwater is more serious in the suburban parts of cities, and the pollution tends to spread from cities to villages (Li *et al.*, 2015). Because most of groundwater samples in this research were taken from suburban or village area, the heavy metals perhaps contributed on the high EC value.

In contrast, EC value of the water samples taken in mountain area are usually less than 1000μS/cm and these taken in Aquifer 2 and Aquifer 3 in plain area is mostly less than 500μS/cm. This is because without excessive human impacts, water body can keep the characteristics of the natural water quality. However, because the water in mountain area is more exposed to outside environment than that in deep aquifers (Aqufier2 and Aquifer3), so the EC value of mountain area samples will be a little higher than that of deep aquifer samples, because the former can get other recharge sources more easily.

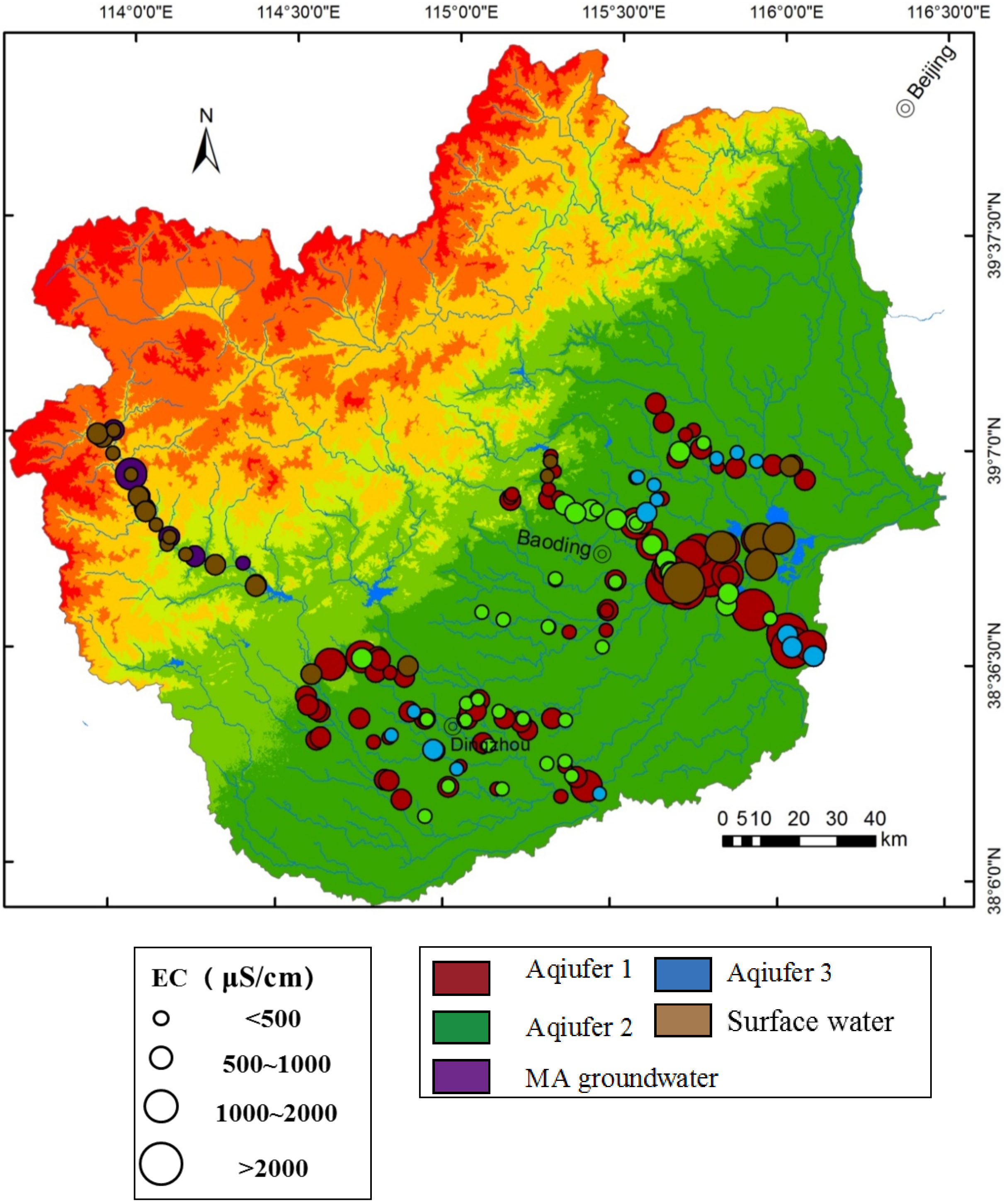

Figure 17: Spatial distribution of electrical conductivity value of all water samples

IV. Spatial distribution of δ^{18}O value of all water samples

Figure 18 exhibits a spatial distribution of δ^{18}O of all water samples in research area. Similar to the EC value distribution, the water samples with relatively heavy δ^{18}O are mainly from surface water and shallow groundwater no matter it is in mountain area or plain area. This is because the heavy stable isotope in surface water can be enriched during evaporation processes, and then infiltrate into shallow aquifer as a recharge source.

The water samples of Aquifer 2 and Aquifer 3 in plain area represent relatively light stable isotopic compositions. This is because deep groundwater is usually recharged not locally but in mountain area with high altitude by precipitation infiltration. Due to altitude effects, the precipitation falling on there is usually with light stable isotope contents (Liu *et al.*, 2014). However, some samples of Aquier2 also show high value closed to that in Aquifer 1, which might imply some influences from shallow aquifer.

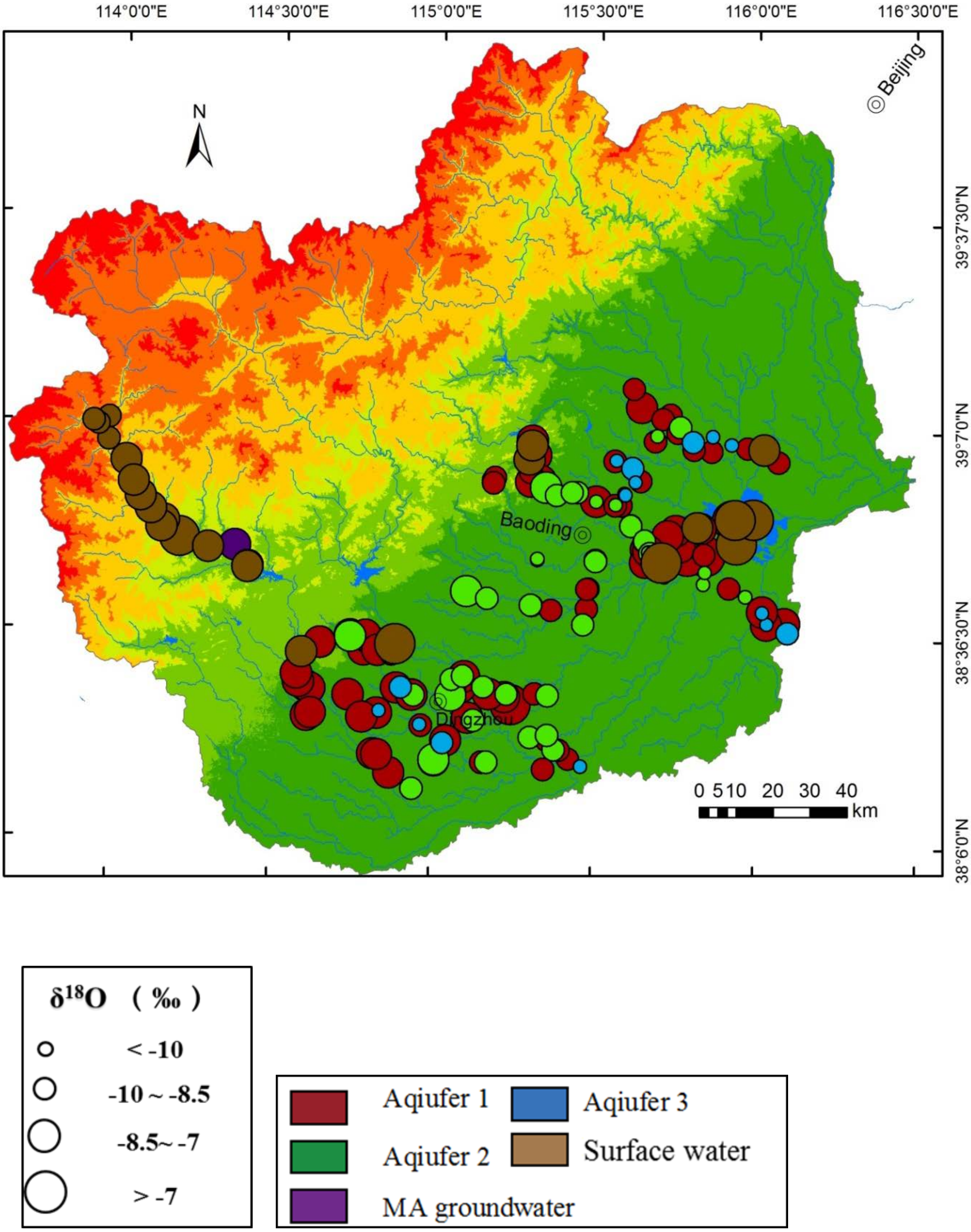

Figure 18: Spatial distribution of δ^{18}O value of all water samples

V. Spatial distribution of Hexa diagram of all water samples.

Figure 19 shows the spatial distribution of Hexa diagram of all the water samples in research area. The chemical composition of water samples in mountain area and those in Aquifer 1 in Dingzhou area and north of Baoding city can be characterized as Ca-HCO_3 type with the exception of a few samples with a slight increase of sodium concentration (e.g., DZ42 and DZ44). Many samples with high nitrate concentration were also found in upstream region of this area, which is probably caused by fertilizer use in agriculture (Owens *et al.*, 1992). The situation of chemical composition in Baoding area is much more different. Affected by surface water, the groundwater samples of Aquifer 1 in surface water region cannot be characterized by a uniform type. However, other samples in Aquifer 1, far away from surface water region, can be characterized by Mg-HCO_3 water type. The chemical composition of groundwater of Aquifer 2 and Aquifer 3 in Baoding area varied from Ca·Mg-HCO_3 to Na-HCO_3 roughly along northwest-southeast direction, which implies a Na-Ca · Mg exchange reaction in this area. The geochemical characteristics of groundwater of Aquifer 2 and Aquifer 3 in Baoding area is also different from those of Aquifer 2 and Aquifer 3 in Dingzhou area, and the latter one show less Mg contents. This might be caused by different geological setting conditions in these two areas.

(a)

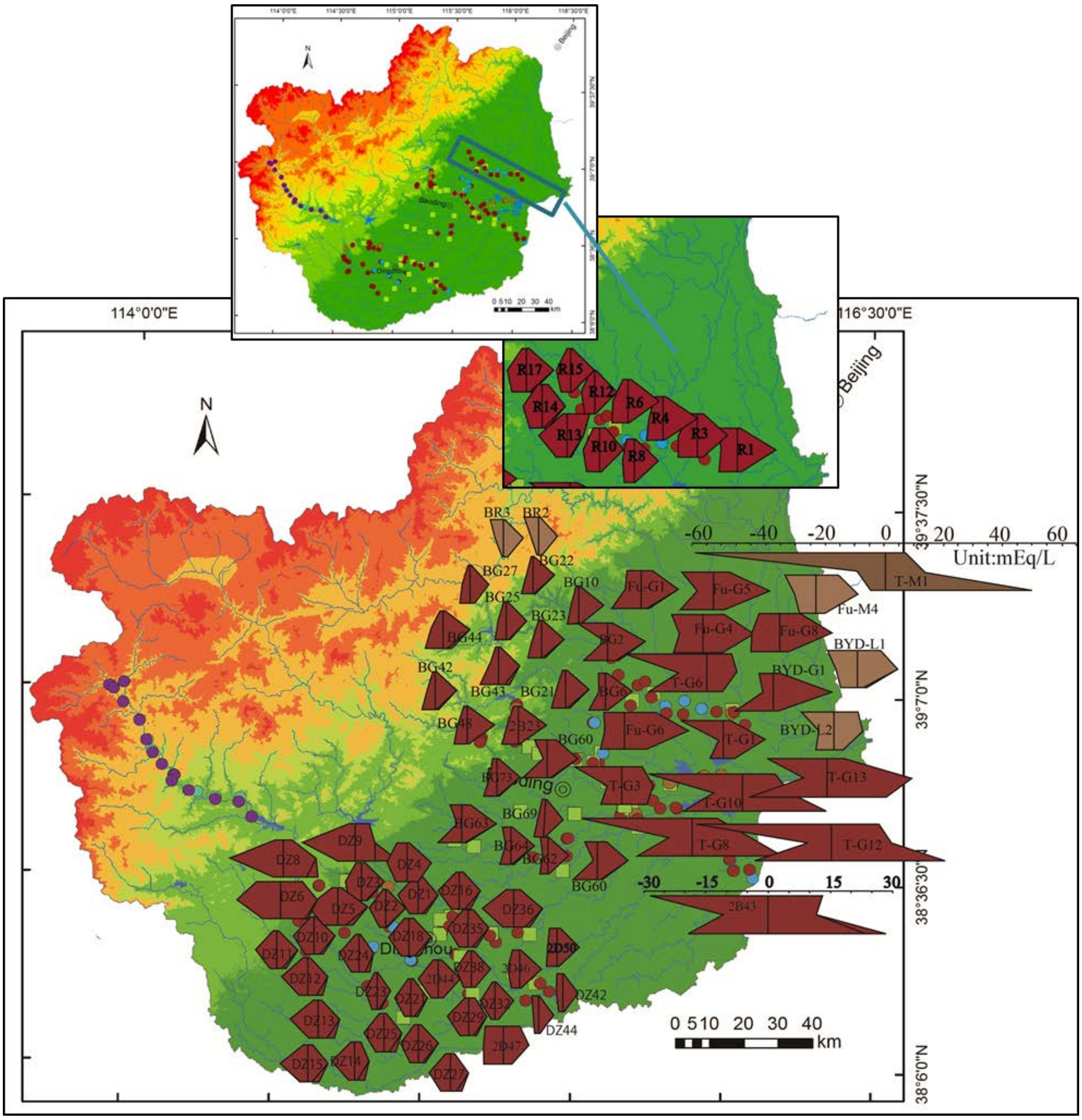
114°0'0"E
114°30'0"E
115°0'0"E
115°30'0"E
116°0'0"E
116°30'0"E
Beijing
Baoding
Dingzhou
0 5 10 20 30 40
km
N
R17
R15
R12
R14
R6
R4
R13
R3
R10
R8
R1
39°37'30"N
39°7'0"N
38°36'30"N
38°6'0"N
-60 -40 -20 0 20 40 60
Unit:mEq/L
T-M1
Fu-M4
BYD-L1
BYD-G1
BYD-L2
BR3
BR2
BG27
BG22
BG25
BG10
Fu-G1
Fu-G5
BG23
Fu-G4
Fu-G8
BG44
BG2
BG42
BG43
BG21
BG6
T-G6
BG48
2B23
BG60
Fu-G6
T-G1
BG73
T-G3
T-G10
T-G13
BG63
BG69
BG64
BG62
T-G8
T-G12
BG60
-30 -15 0 15 30
2B43
DZ8
DZ9
DZ3
DZ4
DZ6
DZ5
DZ2
DZ1
DZ16
DZ36
DZ18
DZ35
DZ10
DZ50
DZ11
DZ24
DZ12
2D44
DZ38
2D46
DZ23
DZ21
DZ32
DZ42
DZ13
DZ25
DZ26
DZ29
DZ44
DZ15
DZ14
2D47
DZ27
0 510 20 30 40
km

(b)

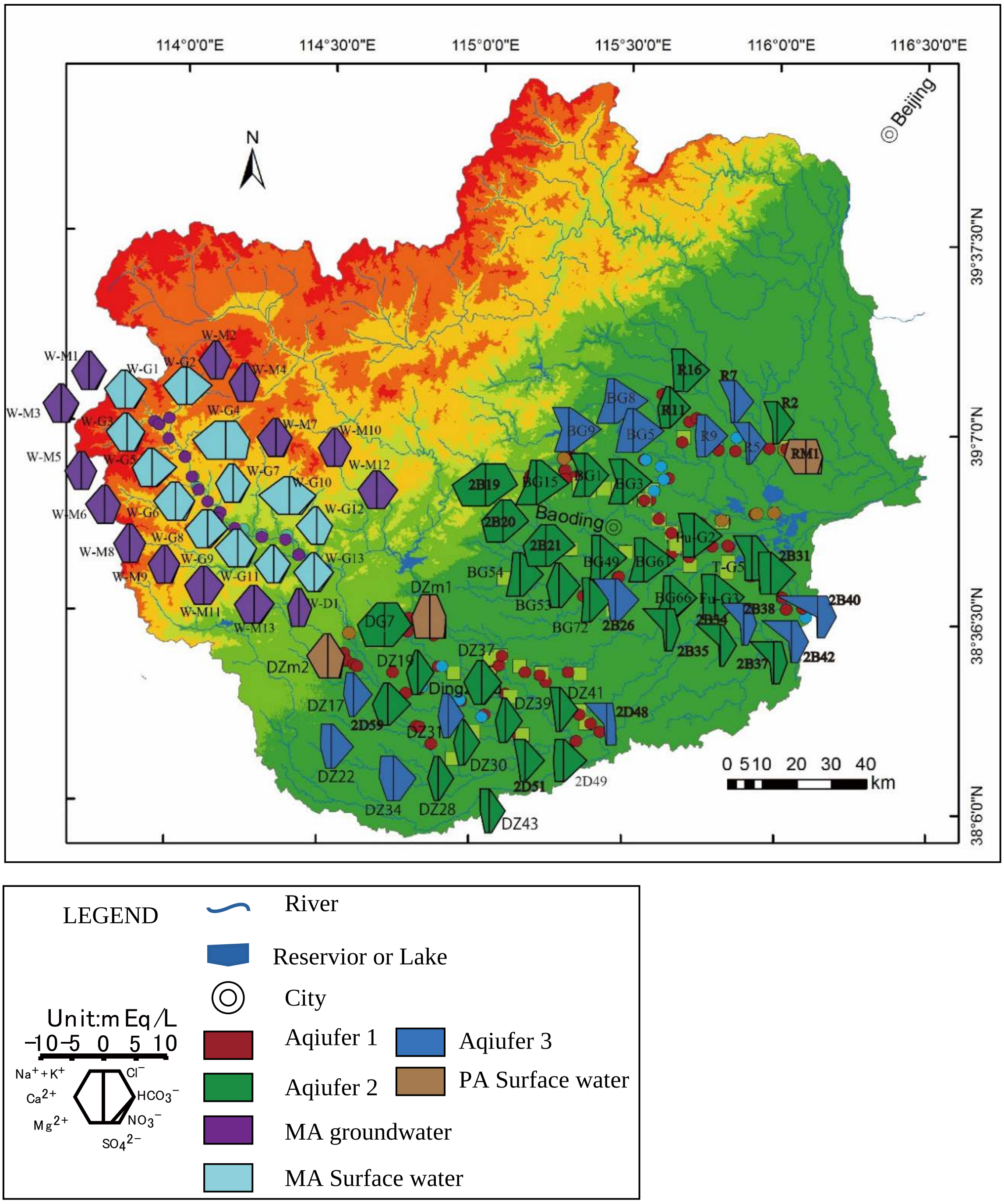

Figure 19: Spatial distribution of hexa-diagram of (a) Aquifer 1 and surface water samples in plain area and (b) all the rest water samples

Chapter 4: Specific analysis on hydrochemical processes associated with the interaction between shallow and deep groundwater in Baoding and Dingzhou area

I. Introduction

As the biggest city in BLW, there are over 8 million people living in Baoding city, which account for three quarters of whole watershed population. Besides, the center position in economics and industries exacerbated groundwater resources pressure here, and actually a deep groundwater depression cone formed in the vicinity of this city has proved this fact, which should be the result of intensive groundwater exploitation behaviors (Li *et al.*, 2014). On the other hand, as the representative of secondary cities in BLW, Dingzhou city is located in southwest of Baoding with a distance of about 70km. There are only 0.4 million people here, and the industries is also little. Therefore, the specific analysis of the water samples distributed around these two cities can represent the hydrochemical processes situation in plain area, and it is also possible to find the differences between these two locations which represent two different groundwater exploitation statuses.

II. Hydrochemical processes revealed by stable isotope

Figure 20 shows the relationship between δD and δ^{18}O values of surface water and groundwater in Baoding area (a) and Dingzhou area (b) with a local meteoric water line ($\delta D = 8.2\delta^{18}O + 9.4$; LMWL; precipitation in Shijiazhuang; WMO/IAEA, 2003), which is quite close to the global meteoric water line ($\delta D = 8\delta^{18}O + 10$; GMWL; Craig, 1961).

1. Baoding area

In Baoding area, the stable isotopic composition in surface water presents heaviest value with ranging from -7.60‰ to -4.14‰ for δ^{18}O and -56.35‰ to -40.11‰ for δD, and the slope of these samples is apparently lower than that of LMWL. This kind of enrichment is caused by isotopic fractionation during water evaporation (Craig *et al.*, 1963). In this area, the stable isotopic compositions of groundwater samples in Aquifer 1, ranging from -10.09‰ to -4.42‰ for δ^{18}O values and from -72.68‰ to -40.94‰ for δD values, are relatively higher than those in Aquifer 2 and Aquifer 3. Although the slope of water line of the Aquifer 1 samples ($\delta D = 4.9\delta^{18}O - 20.0$) is lower than that of LMWL, there are a set number of Aquifer 1 samples closed to the LMWL. Specifically, these, which are away from LMWL, are almost from surface water region. This suggests that groundwater samples of Aquifer 1 taken in surface water region are signally affected and recharged by surface water, and rest parts of Aquifer 1 samples are recharged directly by precipitation without intensive evaporation processes.

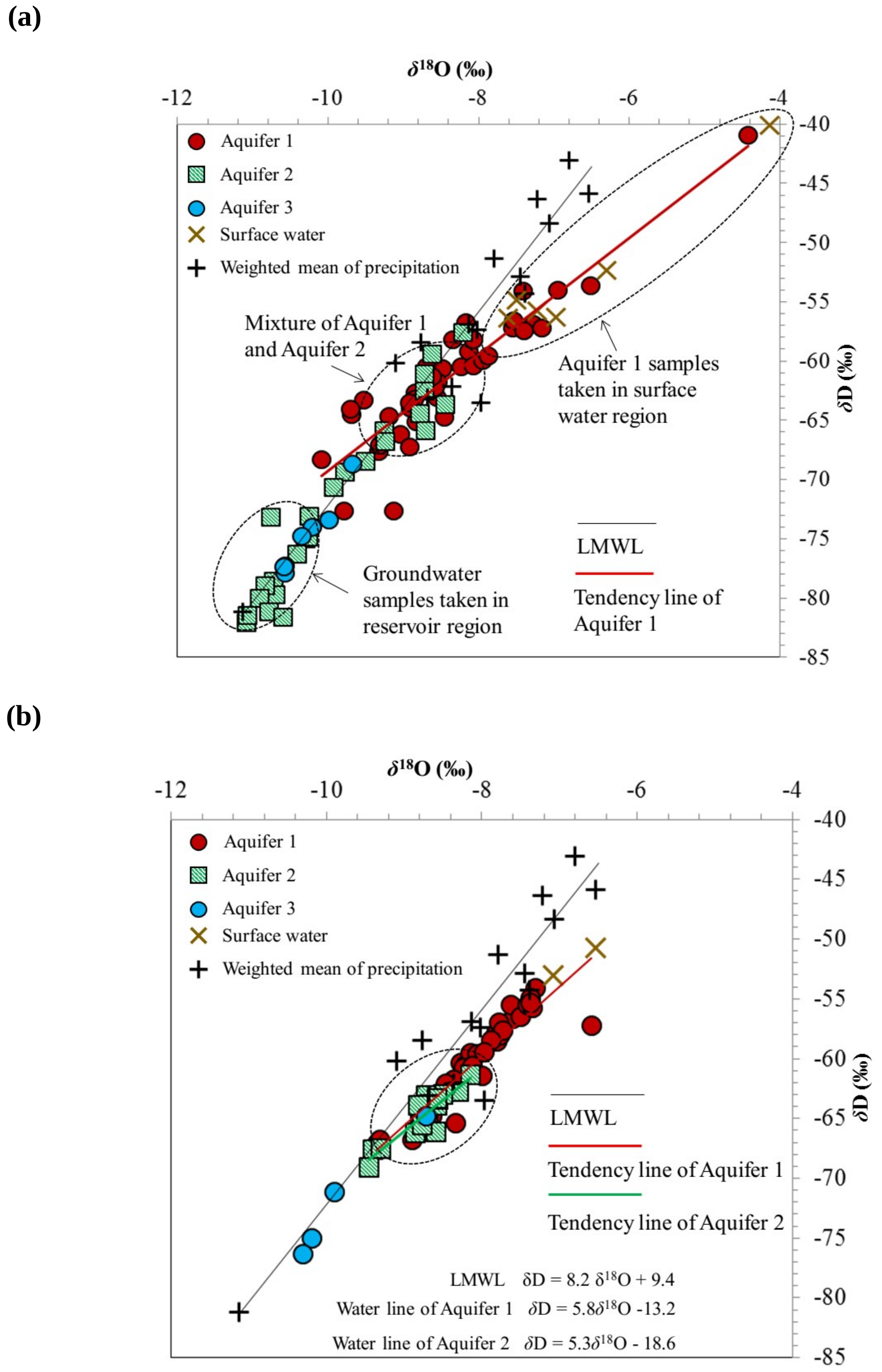

Figure 20: Relationship between and δ^{18}O and δD values of surface water and groundwater in (a) Baoding area and (b) Dingzhou area (LMWL δD = 8.2 δ^{18}O + 9.4; Water line of Aquifer 1 δD = 4.9δ^{18}O – 20.0)

The groundwater samples in Aquifer 2 and Aquifer 3 present light stable isotopic compositions with ranging from -11.08‰ to -8.20‰ for δ^{18}O values and from -82.12‰ to -57.61‰ for δD values, and ranging from-10.59‰ to -9.68‰ for δ^{18}O values and from -77.93‰ to -68.74‰ for δD values, respectively. In Baoding area, for the groundwater samples of Aquifer 2 taken outside of surface water region, part of these samples are mixing with the samples of Aquifer 1, and part of them show relatively low isotopic values which is closed to samples of Aquifer 3. This might be a strong evidence that can prove an interaction processes (interaquifer flows recharge) existing between shallow and deep aquifer. Generally speaking, groundwater in deep aquifer usually represents lower stable isotopic compositions (Mook, 2005). Due to this, Aquifer 2 samples mixing with these of Aquifer1 is probably induced by an interaquifer flows recharge process from shallow aquifer to deep aquifer. Such kind of interaquifer flows from shallow aquifer to deep aquifer is mainly resulted from hydraulic difference between shallow aquifer and deep aquifer induced by groundwater over-exploitation. However, this kind of interaquifer flows recharge process cannot be concluded inside surface water region, because samples of Aquifer 2 taken in this region are much different from these of Aquifer 1 in stable isotopic compositions (Figure 20).

A small part of groundwater samples has also been collected in north of Baoding city (Figure 21), but no strong connection relationship can be found among these samples.

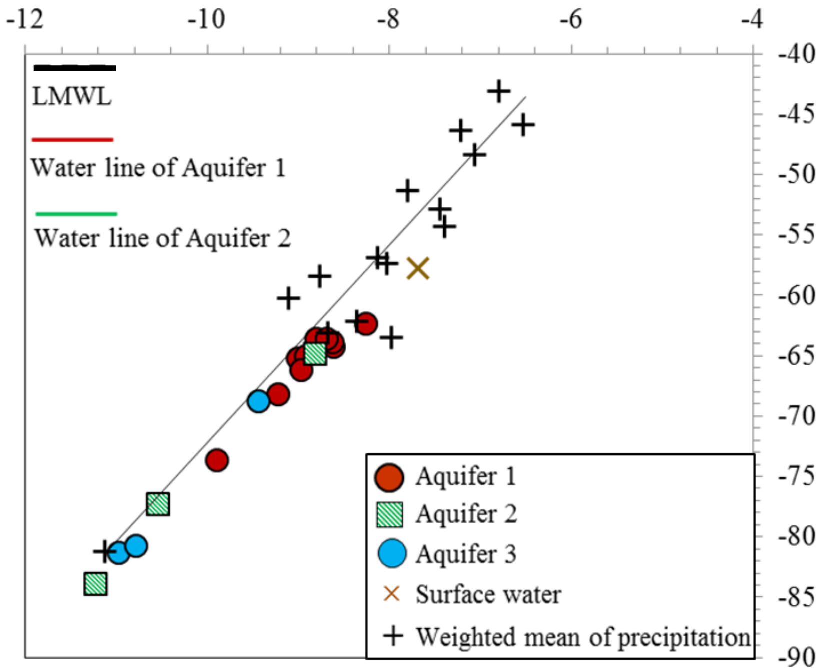

Figure 21: Relationship between δD and δ^{18}O values of surface water and groundwater in North of Baoding city

2. Dingzhou area

Similar to Baoding area, the surface water samples in Dingzhou area represent the heavy value of stable isotopic composition in this area, which also reflect the isotopic fractionation during water evaporation (Figure 21). The Aquifer 1 samples in this area shows a relatively high variation of stable isotopic compositions, ranging from -9.36‰ to -6.59‰ for δ^{18}O values and from -67.09‰ to -54.15‰ for δD values. The water tendency line of these samples ($\delta D = 5.8\delta^{18}O-13.2$) shows a lower slope than that of LMWL, and these samples are not closed to the LMWL except one sample (DZ41). This suggests that groundwater in Aquifer 1 in Dingzhou area probably originates not from present-day precipitation but from some water body which experienced strong evaporation processes.

Such kind of evaporation enrichment also can be found in samples of Aquifer 2 in this area. The groundwater samples in Aquifer 2 of Dingzhou area, with the values ranging from -9.45‰ to -8.15‰ for δ^{18}O and from -69.13‰ to -61.35‰ for δD, are chiefly mixing with these of Aquifer 1 and far away LMWL except one sample (DZ43). This departure to LMWL is also the result of isotopic fractionation which causes the isotopes enrichment before recharging groundwater bodies. Similarly, the isotopic composition mixture of Aquifer 1 and Aquifer 2 here might imply another interaquifer flow processes between shallow and deep aquifers like what exists in Baoding area. Nevertheless, the major ions showed a contrary result and we will discuss it in next chemical composition part. The groundwater samples of Aquifer 3 in Dingzhou area represent the lightest stable isotopic composition values in this area, and they well distributed along the LMWL except one sample (DZ31). This indicates that the groundwater in Aquifer 3 is recharged by precipitation infiltration at a relative high altitude.

3. Recharge altitude of deep groundwater

Some simulation results have reported that, in North China Plain because the deep aquifer is a semi-enclosed system, the recharge water is not from precipitation infiltration or surface water, but mainly from vertical interaquifer flows and lateral flows from piedmont area or mountain area with different altitude (Wang *et al*., 2008; Cheng *et al*., 2014). Therefore, it can be assumed that in BLW the similar situation also exists.

Figure 22 shows that the stable isotopic composition of Aquifer 2 groundwater samples in Dingzhou area has the same value range with the samples taken in south mountain area. Therefore, there is a high possibility that the deep aquifer in Dingzhou area is receiving the recharge water from this mountain area. On the other hand, the groundwater samples in mountain area wells showed the altitude effect with a decrease rata of 0.3 ‰/100m (see in Chapter 3), so the isotopic composition spatial distribution for deep groundwater in Dingzhou area also should exhibit some kind of features if they are being recharged by water source from mountain. Table 1 and Figure 23 presents a possible recharge altitude for Aquifer 2 samples in Dingzhou basing a decrease rate of 0.3 ‰/100m. The possible recharge altitude range from 252m to 698m, whereas the recharge altitude will be up to more than 1100m for these samples in Aquifer 3 due to the lighter isotopic compositions. Specifically, the spatial distribution shows that recharge altitude increases from the area closed to piedmont towards downstream area, which exhibits like a common groundwater flow path system. Figure 24 further confirms this result, because the δ^{18}O value also shows correlation ship with altitude in Dingzhou area in certain degree. Although some previous researches reported that many concealed fault zones exist in piedmont area in BLW, the results in Dingzhou area indicate that the concealed fault might not exist here or is not giving noted influences to local groundwater flow system.

However, the isotopic compositions of groundwater samples present quite different results in Baoding area. The result shows that the isotopes of groundwater in Aquifer 3 here varied in a wider value range which cannot be covered by the data from groundwater in mountain area. These facts indicate that the recharge area for these deep groundwater in Baoding area should be some other different areas with higher altitude.

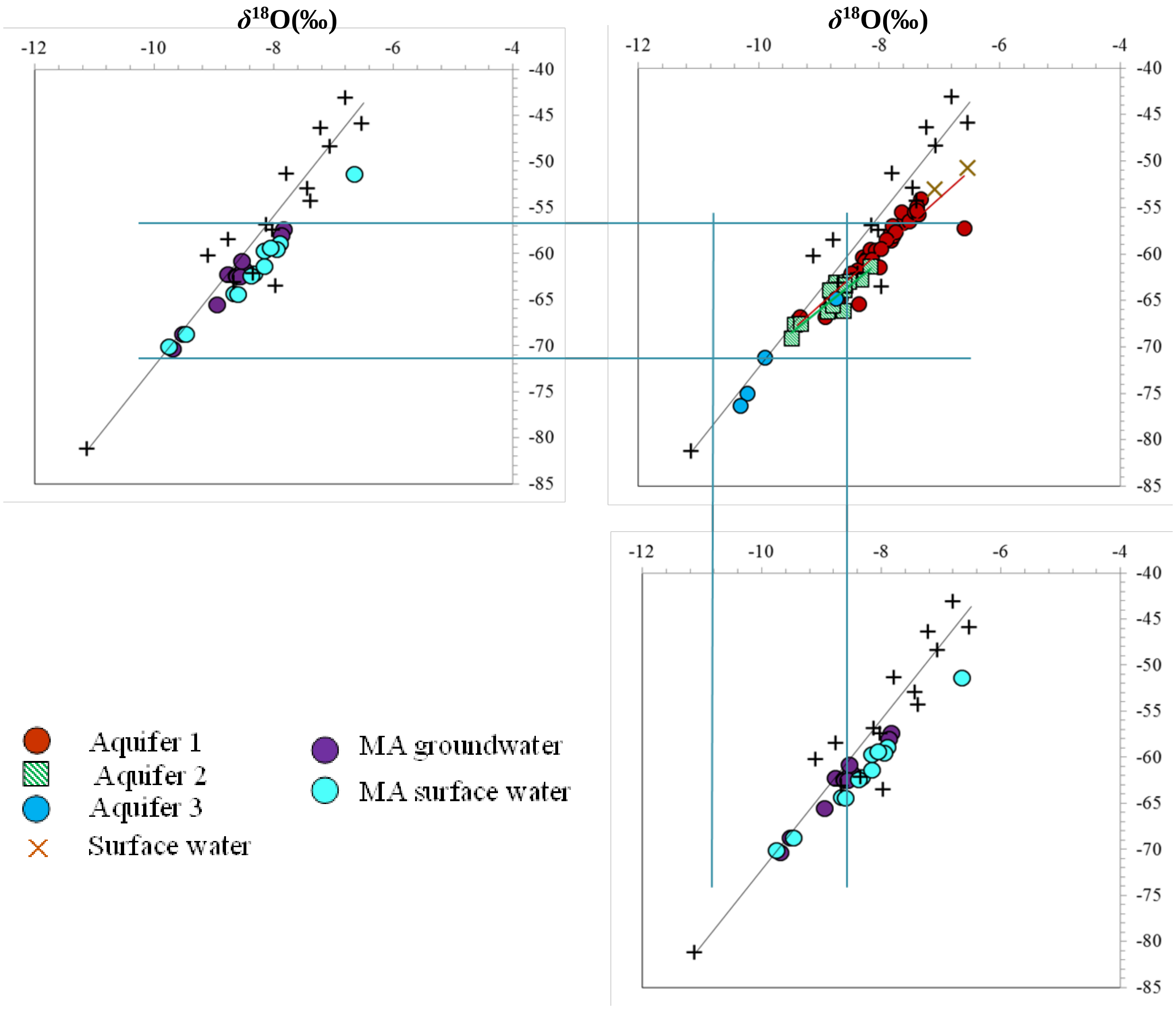

Figure 22: Comparison of stable isotopic compositions between water samples of mountain area and those of Dingzhou area

Table 1: Estimated recharged elevation of groundwater in Aqufier2 in Dingzhou area

well ID	DG7	DG19	DG28	DG30	DG37	DG39	DG41	DG43	2D49	2D51	2D53	2D55	2D56	2D58	2D59
well elevation(m a.s.l.)	89	54	46	47	53	43	35	38	33	31	31	40	45	50	49
δ^{18}O(‰)	-8.15	-8.57	-8.57	-8.30	-8.50	-8.72	-8.59	-9.40	-8.79	-9.45	-9.30	-8.58	-8.82	-8.86	-8.76
recharge elevation(m a.s.l.)	252	396	394	304	370	447	404	680	470	697	647	398	481	494	462

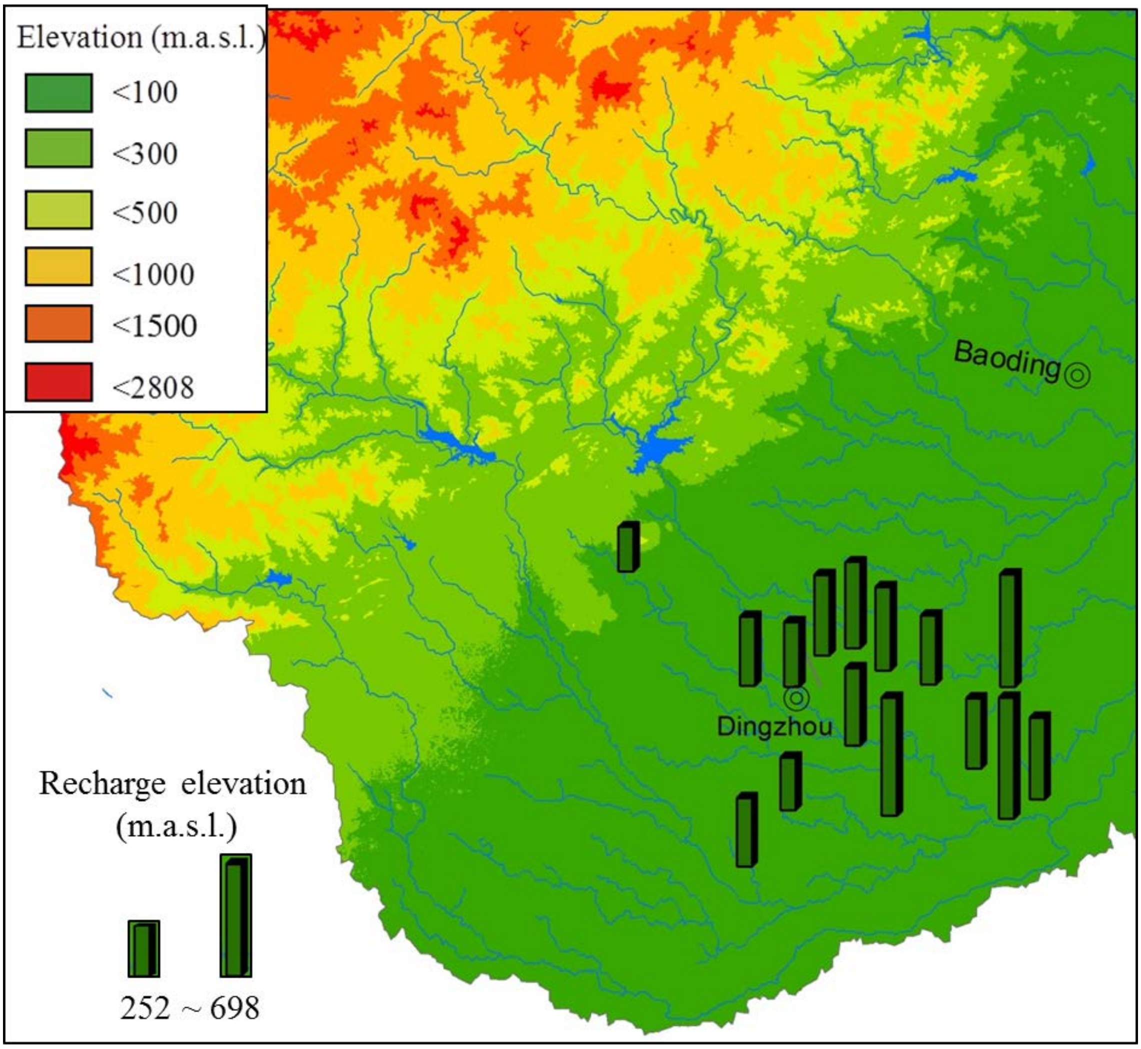

Figure 23: Estimated recharge elevation for Aquifer 2 groundwater samples in Dingzhou area

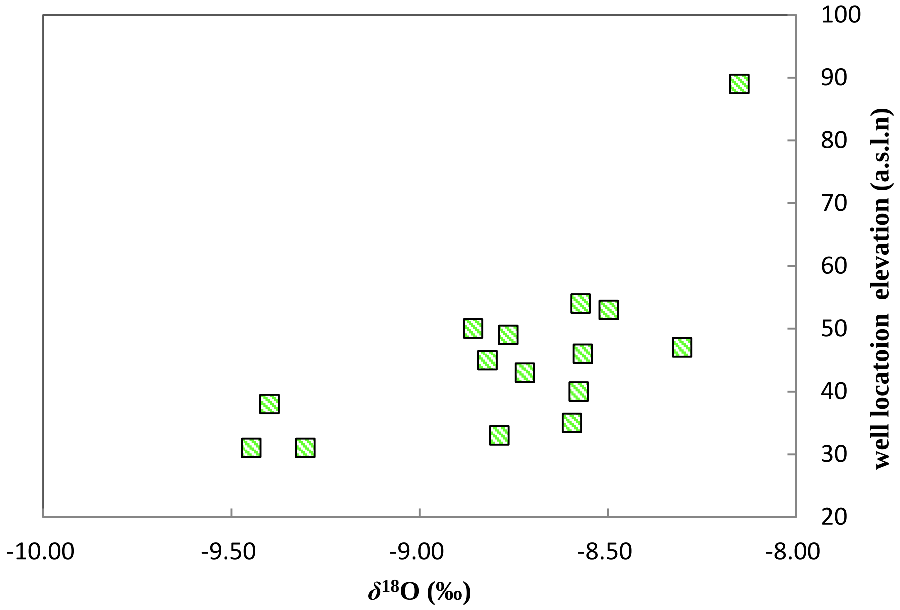

Figure 24: The relationship between stable isotope and well elevation for groundwater samples of Aquifer 2 in Dingzhou area

III. Hydrochemical processes revealed by major ions

1. Baoding area

A trilinear diagram is shown in Figure 25 for the water samples of Baoding area. Corresponding to the results of stable isotopic compositions, groundwater in Aquifer 1 of Baoding area taken from surface water region is chemically different from other groundwater in this area. However, these samples did not either coincide to the surface water, although these samples are quite closed to surface water in stable isotopic compositions (Figure 20). This might suggest that these samples are being affected by both surface water and precipitation. However, due to the same reason, no strong connection relationship can be found among the samples taken in the north of Baoding city (Figure 26)

On the other hand, rest part of Aquifer 1 groundwater, main taken outside of surface water region, is well mixing with groundwater from Aquifer 2, which can further confirm the possibility of interaquifer flow recharge process existing from shallow aquifer to deep aquifer in Baoding area.

Another two types of water are also defined in this area. One is called upstream type, which are from the groundwater samples taken in the upstream of Baoding city, existing in both Aquifer 1 and Aquifer 2. These water can be characterized by relative high and stable Ca·Mg concentration and variation in HCO_3 concentration. The other water type is High-Na water, as the name suggests, it refers to the groundwater with high sodium concentration. For this phenomenon, it can be explained by geochemical evolution process (Wang, 1995; Ma *et al*., 2011; Diaw *et al*., 2012). As the Figure 27 suggests, at the very beginning, the geochemical elements (e.g., Ca, Mg and Na) distributed very uniformly within a watershed. However, due to the differences of dissolving capacity, sodium can dissolve into water easily than other cations. After long period leaching, most of sodium in the upstream of a watershed has flowed to downstream regions and accumulate there. On the other hand, cations like calcium and magnesium remain in upstream. Due to this, if without human activity influences, the fresh groundwater firstly formed in upstream region in a watershed can mainly dissolve cations like Ca and Mg, but when groundwater moves to the downstream region where high Na accumulated. An exchange reaction can happen between Na and Ca · Mg. In this research, high Na groundwater samples are mainly taken in the downstream region of Baoding city, and are mainly from deep groundwater (Aquifer 3), so it is reasonable to explain these results by using this theory.

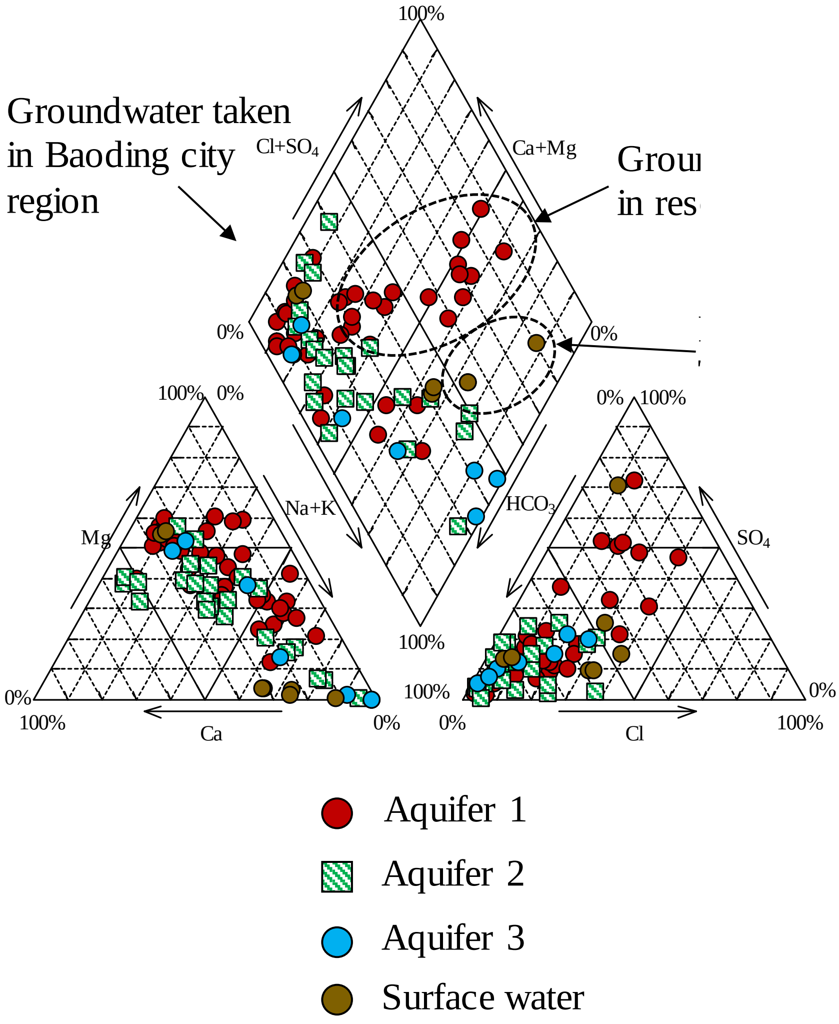

Figure 25: Trilinear diagram of the water samples in Baoding area

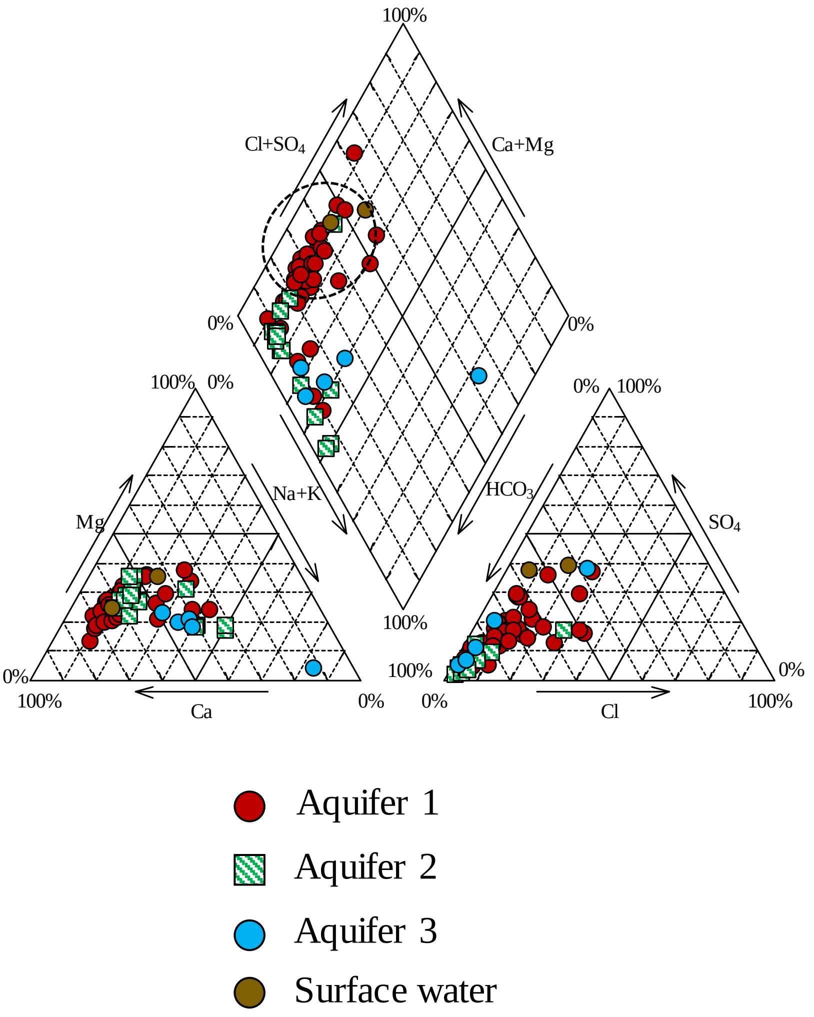

Figure 26: Trilinear diagram for the water samples in the north of Baoding city

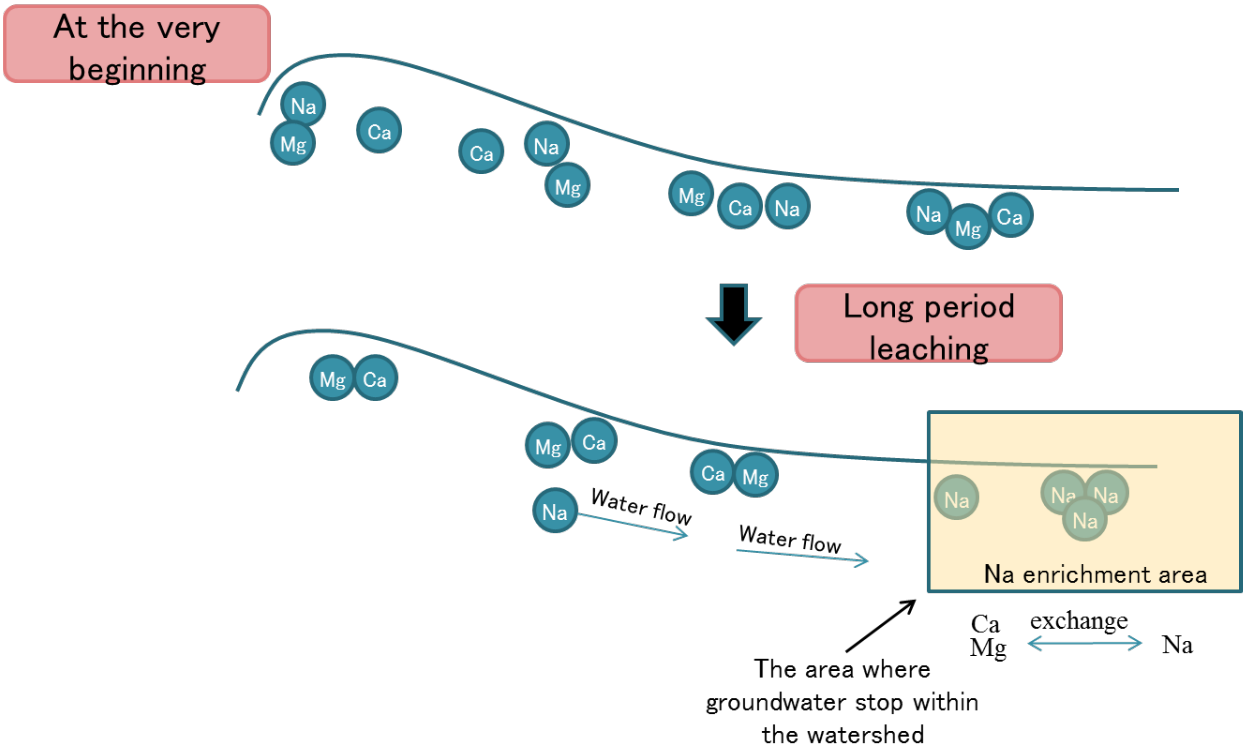

Figure 27: An explanation on high Na area in Baoding area (Basing on the theory by Wang *et al*., 1995)

2. Dingzhou area

Figure 28 shows a trilinear diagram for the water samples taken in Dingzhou area. It is clear that the groundwater samples of Aquifer 2 are not chemically similar to these of Aquifer 1, which shows a contrary result to stable isotopic compositions (Figure 20). As mentioned previously, a possible interaction relationship might exist between shallow and deep aquifer in Dingzhou area because of mixing of stable isotopic compositions in this area. Therefore, the chemical composition should be also closed each other if this process truly existed. However, the chemical results showed a contrary result, because few Aquifer 1 and Aquifer 2samples are mixing in the trilinear diagram. Basing on this fact, the interaquifer flows perhaps are not existing or at least not dominant in Dingzhou area.

One groundwater type exist in this area, which can be characterized by high and stable Ca·Mg concentration and variation in HCO_3 concentration. In fact, such kind of water type also exists in Baoding area, where they are called upstream type. However, the difference is that in Dingzhou area this water type is mainly from groundwater in Aquifer 1, whereas, in Baoding area this water type exists in both Aquifer 1 and Aquifer 2 in upstream area. These two water types are mainly located in the regions where human activities influences are relatively smaller, so this Ca·Mg- HCO_3 water type can be thought to widely represent a natural water type in BLW. However, the sodium concentration will increase with different degree when these water move to the downstream regions due to ions exchange reactions which has been talked about in last section.

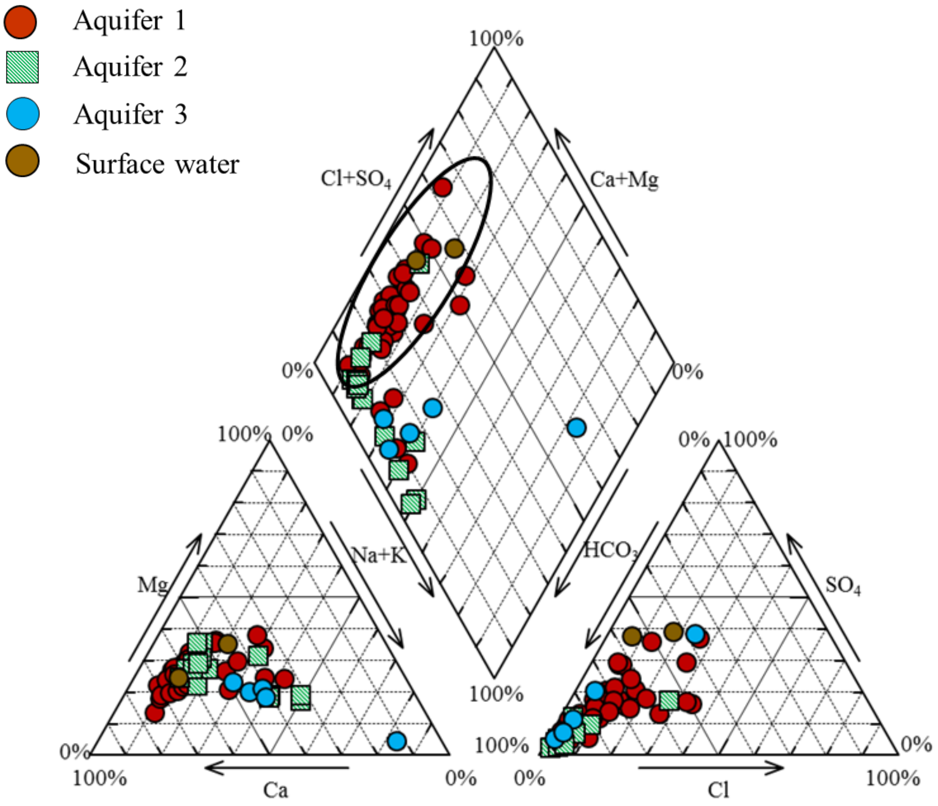

Figure 28: Trilinear diagram of the water samples in Dingzhou area

IV. Profile features combining geochemistry results and hydrogeological settings

For the purpose of better understand the hydrogeological processes in plain area, a profile distribution of Hexa diagram and δ^{18}O value is shown in Figure 29 for Baoding area and in Figure 31 for Dingzhou area.

In Baoding area, corresponding to the results of chemistry and stable isotopic compositions, the profile distribution of stable isotopes confirmed the possibility of interaction relationship existing between shallow and deep aquifer once again. A previous study conducted by Zhang (2009; Figure 30) shows a δ^{18}O value distribution along the same profile line by using the observed results measured before 2005. Comparing to the results of this previous study, in the vicinity of Baoding area, the stable isotope compositions in groundwater of Aquifer 2 have increased distinctly. As the equal hydraulic head in Figure 29 shows, due to the great hydraulic difference between shallow and deep aquifer existing in this area, the groundwater flows not only from upstream to downstream known as the lateral flows, but also from shallow aquifer to deep aquifer known as the interaquifer flows. It is just because part of shallow groundwater began recharging to deep aquifer with such kind of interaquifer flows, it made the stable composition change in deep aquifer. The place where we can clearly find the isotopic compositions increased is well located in the southeast of Baoding, where a deep groundwater depression cone exists. Due to the great potential difference between shallow and deep groundwater here, the interaquifer flows recharge can be found more dominated here than in other places.

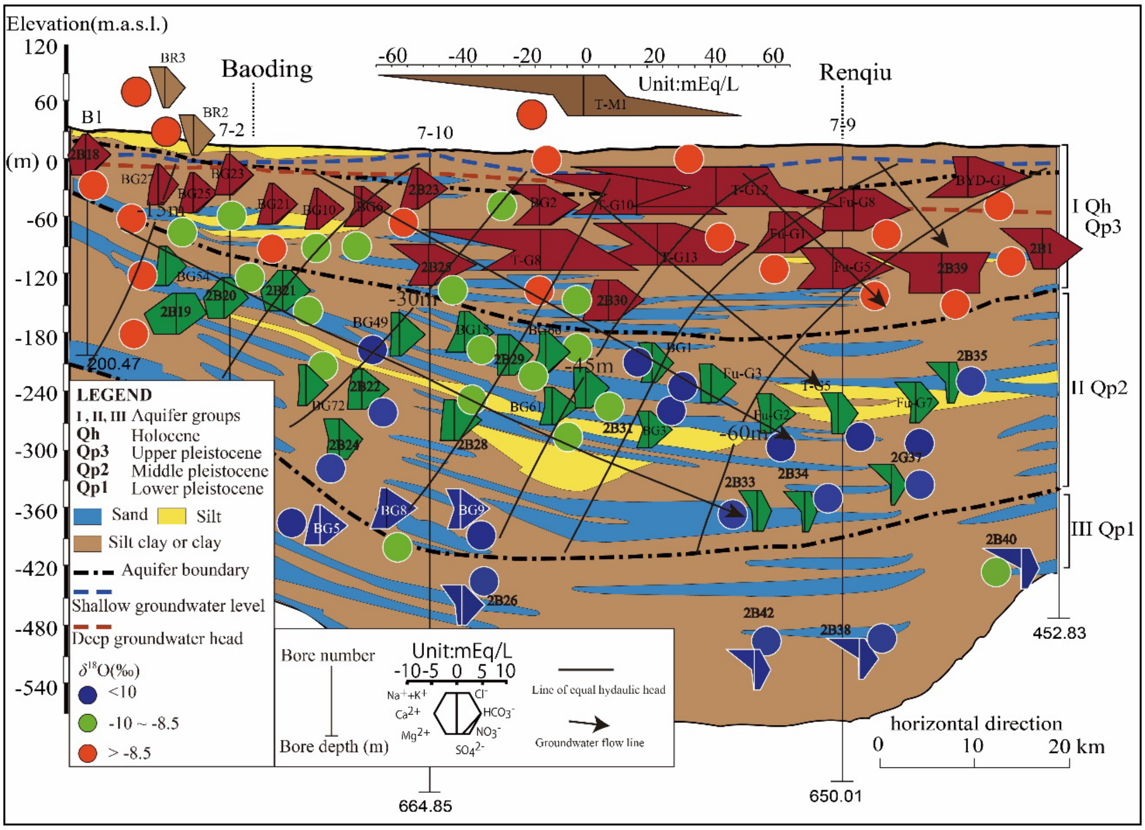

Figure 29: Profile distribution of Hexa Diagram and δ^{18}O value in Baoding area (Line of equal-hydraulic head was compiled basing on geological investigation by Zhang *et al*. (2009))

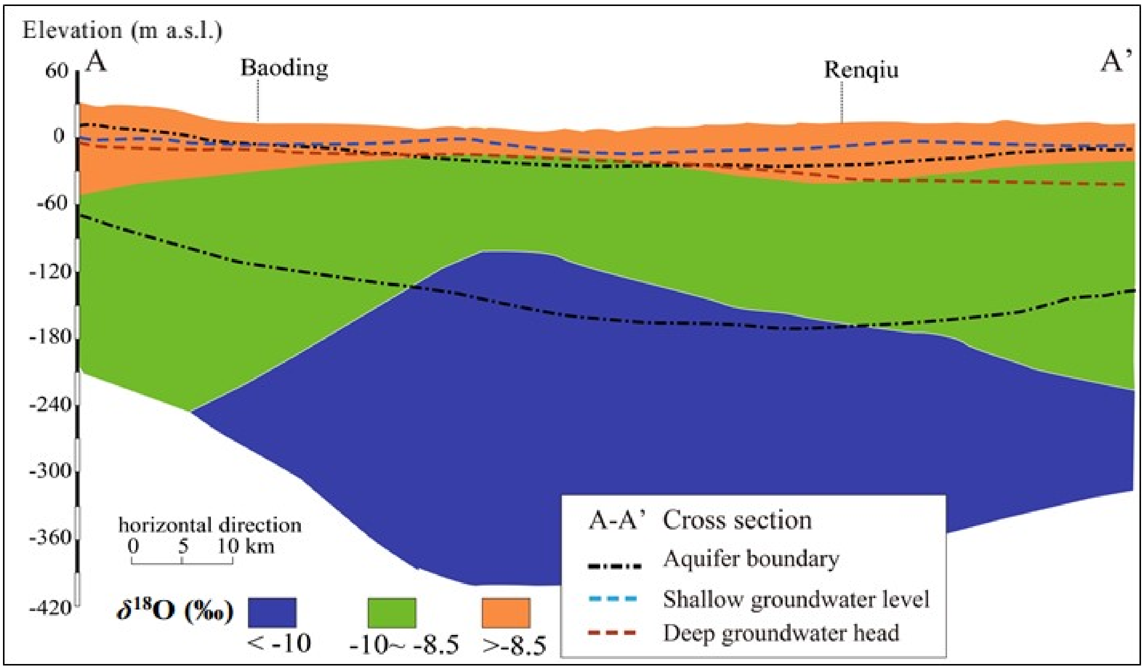

Figure 30: Profile distribution of δ^{18}O value in Baoding area revealed by previous studies (Zhang *et al*., 2009)

As to the situation in Dingzhou area (Figure 31), the contrary results of isotopic compositions and major ions have indicated that the similar interaquifer flows recharge processes cannot exist or at least not dominated in this area. The profile futures along the transect line in this area also confirmed this view. In Dingzhou area, the isotopic compositions of groundwater samples distribute relatively strictly in accordance with the aquifers. With the increase of well depth, the δ^{18}O value decrease accordingly. No interaquifer processes can be observed here. Besides, because the potential difference of deep groundwater head and shallow groundwater level is not big enough, the groundwater flow direction here is roughly consistent with topographic conditions.

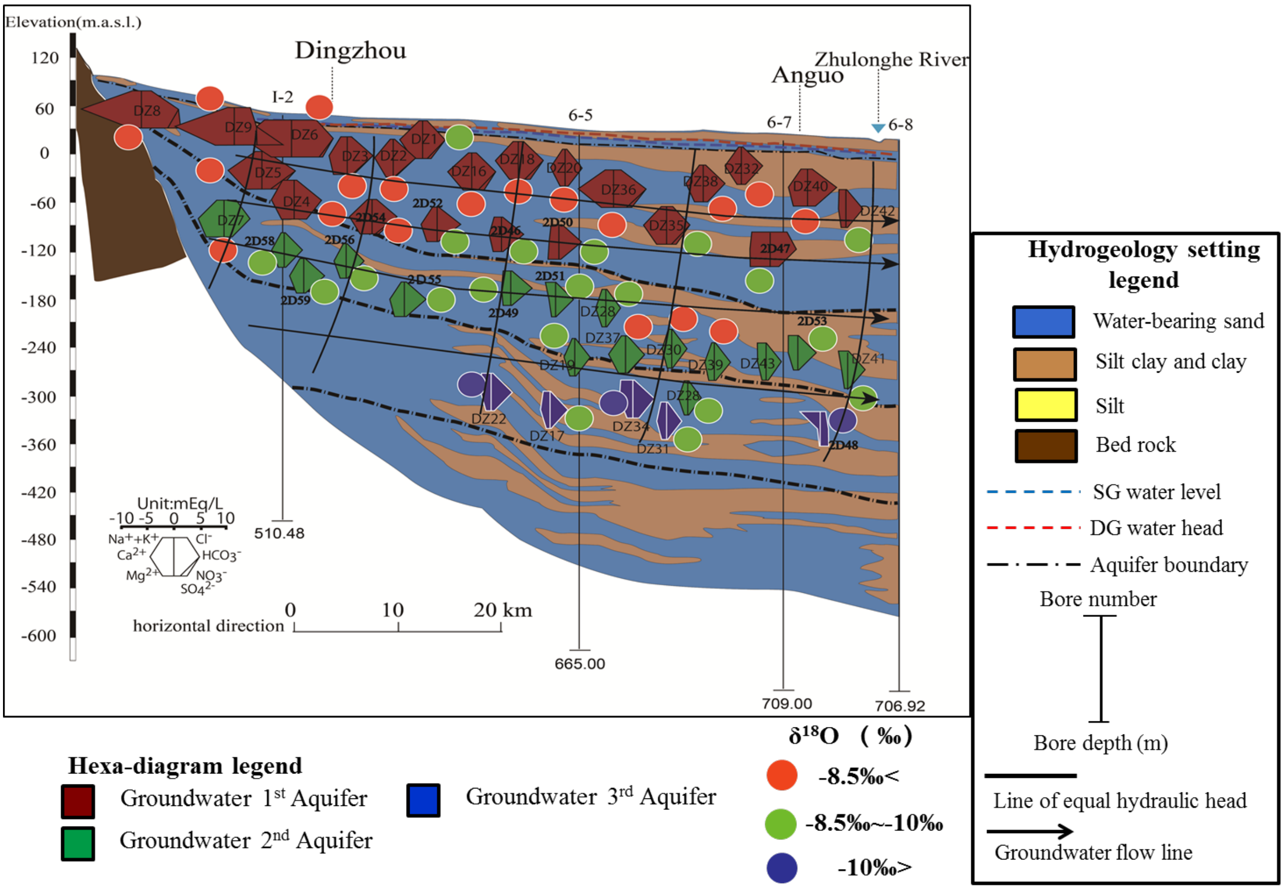

Figure 31: Profile distribution of Hexa Diagram and *δ*^{18}O value in Dingzhou area (Line of equal-hydraulic head was compiled basing on geological investigation by Zhang *et al*. (2009))

V. Summary

From the viewpoint of stable isotope and geochemical composition results, the interacted relationship existing between shallow and deep groundwater (specifically speaking, the interaquifer flows recharge processes from shallow aquifer to deep aquifer) can be concluded in non-surface water region in Baoding area. The stable isotopic results show that the groundwater in Aquifer 2 of this region can be divided into two parts (Figure 20). One part presents light stable isotopic composition and is closed to those in Aquifer 3, and the other part is mixing groundwater in Aquifer 1 showing relatively heavy isotopic composition. Although the groundwater in both Aquifer 1 and Aquifer 2 of this region distributed along LMWL, the variation of the values suggest that they originated from the precipitation infiltration at different altitude (Gat, 1980; Clark and Fritz, 1997), and then transfer to different aquifers. Therefore, such kind of divergence in the same aquifer can be explained by an extra interaquifer flows recharge from shallow aquifer to deep aquifer. Not only the stable isotopic compositions, but the geochemical results also show a mixing of Aquifer 1 groundwater with Aquifer 2 groundwater in the non-surface water region of Baoding area (Figure 25). Furthermore, the profile distribution of Hexa diagram and δ^{18}O value along the transection line for water samples can confirm this process comparing to the previous study by Zhang *et al*. (2009).

Nevertheless, aforementioned interacted relationship existing between shallow and deep groundwater was not found in other areas, namely the surface water region in Baoding area and whole Dingzhou area. In the surface water region in Baoding area, there is no doubt that surface water gives remarkable influences to the groundwater in the Aquifer 1 basing on the results of stable isotopic and geochemical compositions. However, the groundwater in this aquifer didn’t transfer these influences downward. Because neither isotopic results (Figure 20) nor geochemical results (Figure 25) show that groundwater in Aquifer 2 is similar and closed to these in Aquifer 1. The situation is a little different in Dingzhou area, where the stable isotopic composition and geochemical composition showed totally contrary results (Figure 20 and Figure 28). The former shows that groundwater in Aquifer 2 is mixing with these in Aquifer 1, which implies an interacted relationship between them, whereas, the latter one indicates that the groundwater in Aquifer 2 is quit chemically dissimilar to these in Aquifer 1. Therefore, the interaquifer flows from shallow aquifer to deep aquifer do not exist or at least not dominate here.

The stable isotopes data reveal that the groundwater of Aquifer 2 in Dingzhou area is recharged in mountain area where we took the samples in this research. The recharge altitude ranges from 252m~698m for the groundwater in Aquifer2, whereas the groundwater in Aquifer 3 is recharged in higher altitude up to about 1144m. However, the results suggest that the deep groundwater in Baoding area may be recharged in other mountain areas with wider altitude range.

Two water types have been defined in the plain area. One is characterized by Ca·Mg-HCO_3 water type and the other can be characterized by Na- HCO_3, both of which represent the natural water type in research area. Ca·Mg- HCO_3 water type can mainly be found in the upstream of Baoding area and Aquifer 1 in Dingzhou area, where there is small human activities influences, and Na- HCO_3 water type, formed during ion exchange processes, are mainly exist in deep aquifer in downstream regions.

Chapter 5: Quantification of the interaction between shallow groundwater and deep groundwater in Baoding area

I. Contribution ratio of groundwater recharge source by using end member mixing analysis

1. End member mixing analysis model and the selection of end members and tracers

Through the results of stable isotopes and major ions, and a comparison with previous studies, it has been confirmed that there is an interaquifer flows recharge process exists and dominates in the vicinity of Baoding city, which cause the isotopic compositions abnormally increase for the groundwater in Aquifer 2. For this reason, it is possible to use end member mixing analysis (EMMA) to quantify contribution ratio of recharge sources for these samples if meeting certain some conditions (see in Chapter 2). Because it has been clear that these samples with abnormal isotopic compositions are recharged by two sources, one is lateral flows from upstream in the same aquifer and the other is interaquifer flow from upper shallow aquifer, it is suitable to use one-tracer two-member EMMA model for calculation. The model can be as below:

$$\begin{cases} Q_1 + Q_2 = 1 \\ C_1Q_1 + C_2Q_2 = C_t \end{cases}$$

(Equation 4)

where Q_1 and Q_2 is the contribution ratio of recharge source from interaquifer flows and lateral flows respectively, C_1 and C_2 is the tracer concentration of end member 1 and end member 2 in interaquifer flows and lateral flows respectively, C_t is the tracer concentration of the water being recharged.

As to the selection of end members, the end member 1 (C_1) should of course be selected from theses samples in Aquifer 1 and located in upstream, including 2B23, 2B25, 2B27, 2B30, BG62, BG63, BG64 and BG69. End member 2 (C_2) should be from the samples in Aquifer 2 which are also located in upstream with relatively light isotopic compositions, including BG49, 2BG22 and 2BG24. As the output after mixing, C_t values of these samples which are abnormally high will be calculated, including BG15, 2BG29, 2BG28, BG66, BG61 and 2BG31 (Figure 32).

As for the selection of tracers, the conventional way is by using multivariate statistics analysis (usually the principal component analysis) to find some possible useful tracers, and then determine the best tracers by drawing scatter diagrams (Barthold *et al.*, 2011). However, in this research only one tracer is needed for EMMA model and it has been clear the most distinct variation in these samples is the δ^{18}O composition, so the δ^{18}O value will be the best model tracer. In fact, the scatter diagram result (Figure 33) shows that two end member groups and output samples well distributed in this diagram by using δ^{18}O value. Basing on this result, 2B23 was selected as the end member 1, BG49 was selected as the end member 2 and δ^{18}O was used as tracer in EMMA model.

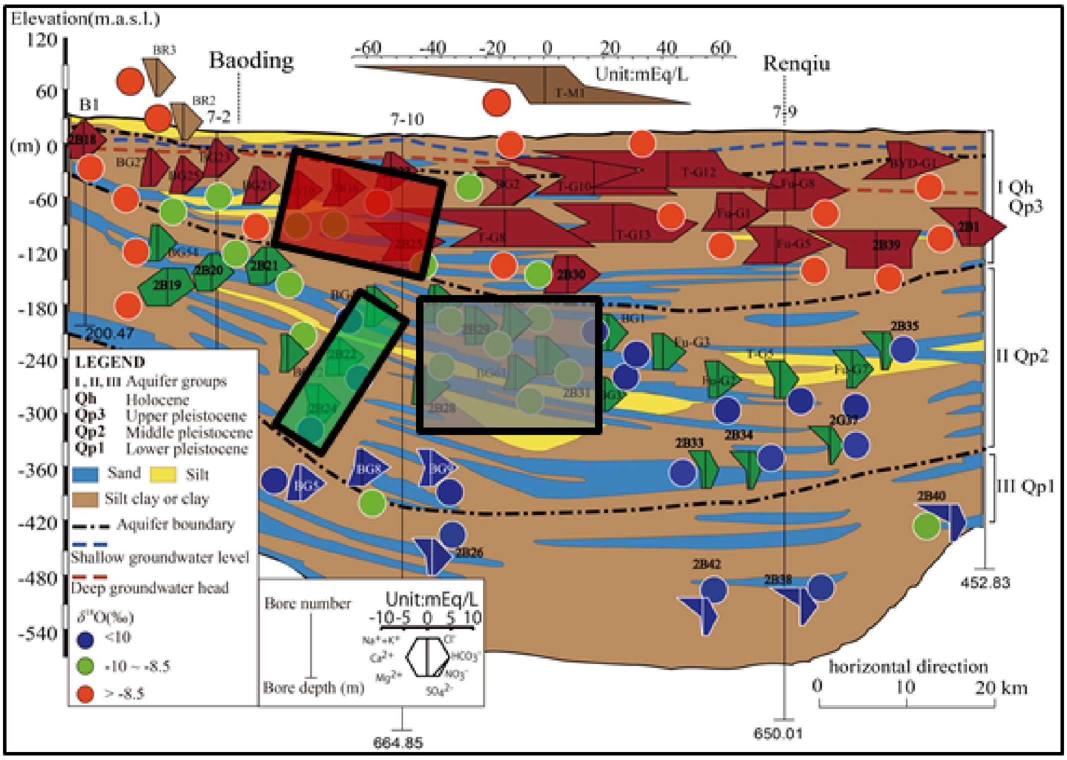

C_1 group: 2B23 2B25 2B27 2B30 BG62 BG63 BG64 BG69

C_2 group: BG49 2BG22 2BG24

C_t group: BG15 2BG29 2BG28 BG66 BG61 2BG31

Figure 32: Selection of end members for one tracer two members EMMA model

]

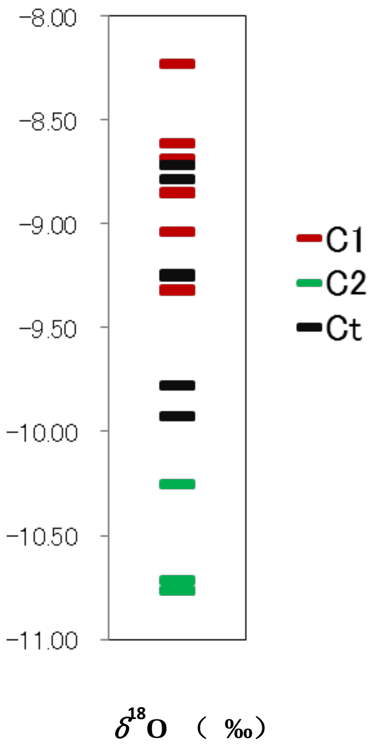

Figure 33: The scatter diagram of two end member groups (C_1 and C_2) and output samples (C_t) by using $\delta^{18}O$ value

2. Contribution ratio of groundwater recharge source

Results of contribution ratio for lateral flows and interaquifer flows recharging to some groundwater samples in Aquifer 2 is shown in Figure 34. Through the results, it is clear that more than half of the samples are mainly recharged by interaquifer flows, the contribution ratio of interaquifer flows ranges from 60% to 81%. Only in two samples (2B29 and 2B31) the lateral flows contribute more than half with the ratio of 61% and 67% respectively. In spite of it, interaquifer flows still contribute about one third in this two samples. Therefore, it is not hard to conclude that interaquifer flow has been dominated in recharge system in this special area. This result also has been reported by Cao (2013), who concluded this result by using numerical simulation methods.

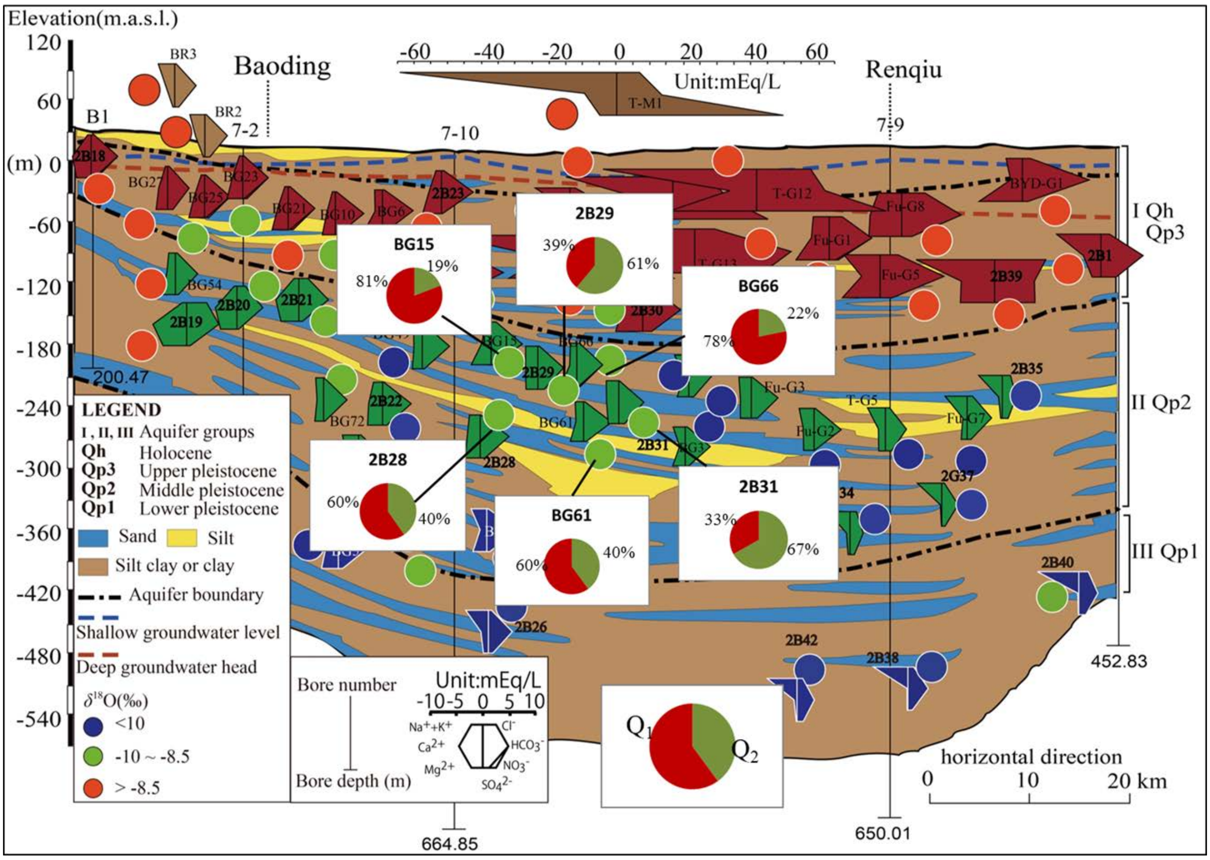

Figure 34: Results of end member mixing analysis in the vicinity of Baoding area (Q_1 and Q_2 is the recharge percentage from Aquifer 1 and Aquifer 2 respectively)

II. An estimation of interaquifer flows by using Darcy’s Law

1. A minor transformation in Darcy’ Law

Interaquifer flows are the flows to and from other aquifers, which can be important parts of the water balance of an aquifer, and must be taken into account when modeling water and solute fluxes **(**Saether and Caritat, 1996). As what have been discussed in Chapter 2, interaquifer flows can also be governed and described by Darcy’s Law with a minor transformation as below, and the signification of each parameter is show in Figure 35.

$$Q = \ K' \cdot A \cdot \frac{\mathrm{dh}}{\mathrm{b}}$$

(Equation 5)

where Q = discharge (m^3/s), K' = hydraulic conductivity (m/s), A=cross section area (m^2), dh/b = total potential gradient (hydraulic gradient) (m/m).

Basing on this formation, it is easy to find that the interaquifer flows will be highest where (1) Vertical hydraulic conductivity K' is highest; (2) Confining unit (*b*) is thinnest; and (3) potential difference between two aquifers (*dh*) is greatest.

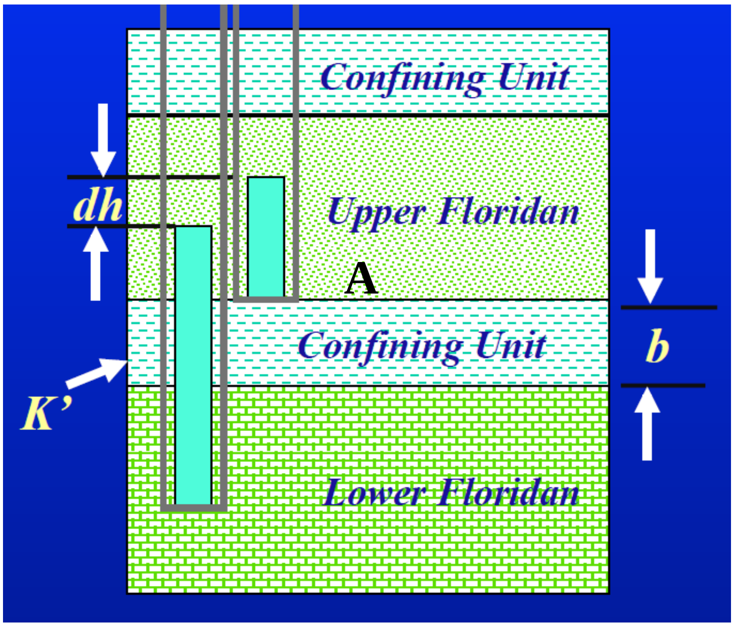

Figure 35: The signification of each parameter for Darcy’s Law (*Q* = discharge (m^3/s), *K′* = hydraulic conductivity (m/s), *A*=cross section area (m^2), dh/b = total potential gradient (hydraulic gradient) (m/m))

2. Parameters setting and interaquifer flows in Baoding area

The hydrogeological setting in the vicinity of Baoding city reveals that silt clay or clay dominates in this area, so the hydraulic conductivity K' range 1.2×10^{-8} ~ 6×10^{-7}m/s. But because an optimism scenario was considered in this research, the minimum value was selected. The area of Baoding city is used as the cross section area A. The potential difference dh between shallow and deep aquifer varies from 5 to 60 m along the transect line, so the results of interaquifer flows will be different with dh change in five classes, which are 5m, 15m, 30m, 45m and 60m. As to the thickness of the confining unit b, it was roughly estimated about 60m basing on hydrogeological setting information.

Estimated result of interaquifer flows in Baoding area was shown in Table 2. Basing on this result, the interaquifer flows from shallow aquifer to deep aquifer of one year will vary from 0.1 to maximum 1.19 with unit of 10^8m^3/year due to the difference of confining unit. Cao (2013) reported an interaquifer flows estimation by using numerical simulation, and this value reached up to about 3.5×10^8m^3/year around 2005. Comparing to this, the estimated result in this research is considered to distribute in a reasonable range. Furthermore, basing on interaquifer flows in Baoding area using Darcy's Law and the EMMA results, the absolute interaquifer flows recharging from shallow to deep aquifer also can be figured out, and the parameter setting and results is shown in Table 3 and Figure 36, respectively.

Table 2: The parameter setting of Darcy's Law for estimating interaquifer flows of all Baoding area

Items	Parameter Setting				
K' (m/s)			1.20E-07		
dh (m)	5	15	30	45	60
b (m)			60		
Q/A (m/s)	1.00E-09	3.00E-09	6.00E-09	9.00E-09	1.20E-08
Q/A (m/year)	0.03	0.09	0.19	0.28	0.38
Baoding city area (km^2)			315		
Q ($10^8 m^3$/year)	0.10	0.30	0.60	0.89	1.19

Table 3: The parameter setting and results of Darcy's Law for estimating interaquifer flows of small part area in the vicinity of Baoding city

Parameter	K' (m/s)	dh (m)	b (m)	Area(km^2)
	1.20E-07	30	60	10×10
Total interaquifer flows($10^8 m^3$/year)	0.19			

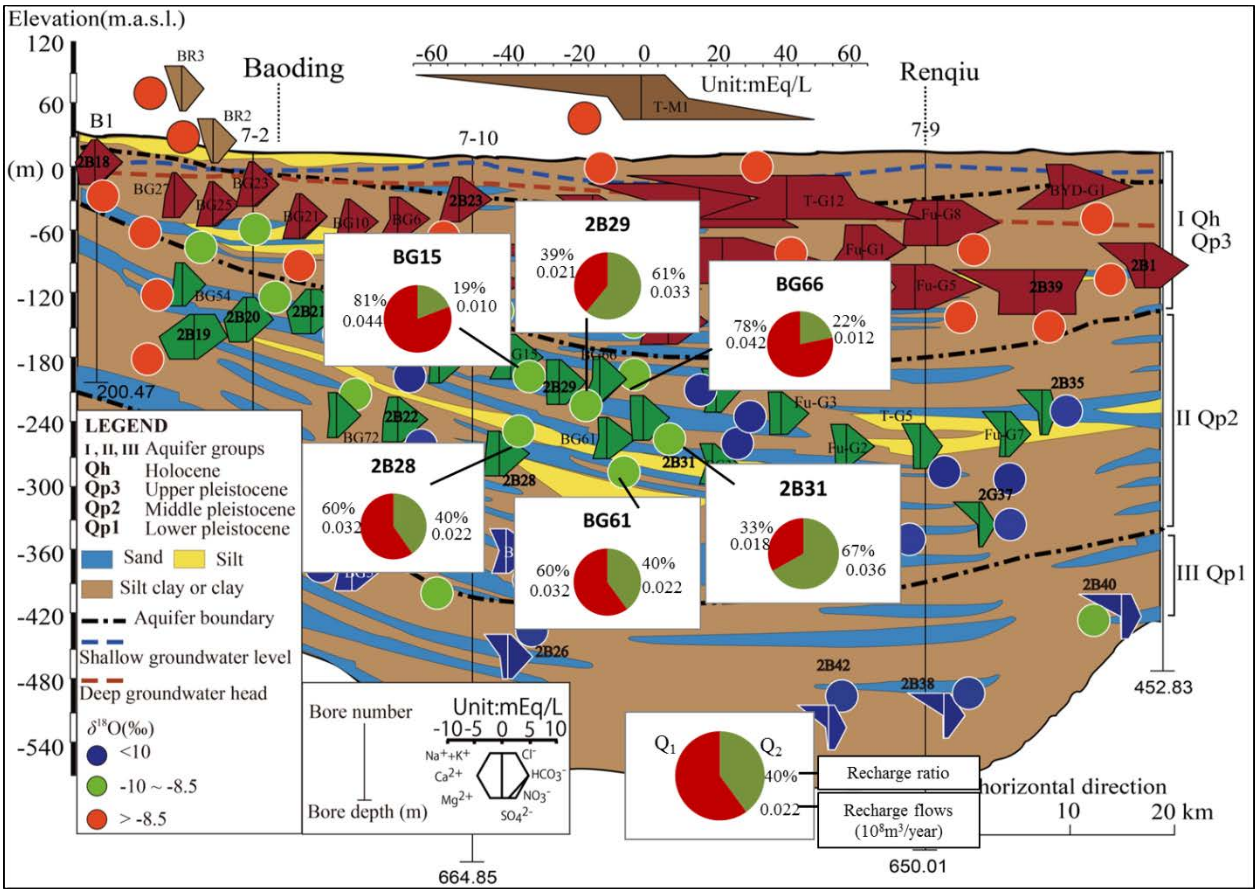

Figure 36: The recharge rate of interaquifer flow and lateral flow in the vicinity of Baoding city

There are not too many studies which report the interaction relationship between shallow and deep groundwater, especially those which figured out the mixing ratio of different recharge sources. However, two similar studies (Chen *et al.*, 2003; Carucci *et al.*, 2012) have still been found which make us can compare the results in this study with other cases. Table 4 shows the summary of these two studies and the main results in this research.

Though the study methods and main results is different each other, for example the contribution ratio is quite different with Study 1, and Study 2 reported a contrary recharge direction, but it is not difficult to reach some conclusions. First, it can be confirmed again that interaquifer flow can be dominant sometimes in certain flow system. Second, such kind of interaquifer flow is controlled by some factors, but the most triggering factor is the over-extraction of groundwater which might imply the big hydraulic head difference existing between shallow and deep groundwater.

Table 4: Comparison of the results with other similar studies

	This study	**Study 1**	**Study 2**
Reporter	-	Chen *et al*., 2003	Carucci *et al*., 2012
Sampling year	2011-2013	1999	Before 2011
Area	Baiyangdian Lake Watershed (North China Plain)	Littoral area of North China Plain	Tivoli Plain (Rome, Central Italy)
Main methods	Major ions and stable isotopes	^{14}C	Major ions, environmental isotopes ($\delta^{18}O$, $\delta^{2}H$, $^{87}Sr/^{86}Sr$, $\delta^{34}S$ and $\delta^{13}C$), and modeling PHREEQC
Description of the main results	Shallow →Deep Contribution ratio: about 60%	Shallow →Deep Contribution ratio about 10-20%	Deep →Shallow Contribution ratio: about 48%~62%
Incentive	The large depression cones caused by groundwater overexploitation	The large depression cones caused by groundwater overexploitation	groundwater extraction
Remarks		Saline water in shallow aquifer is mixed with fresh water	Modeling results confirm the hypothesis of a contribution by groundwater seepage through the aquitard from the deep carbonate aquifers to the travertine aquifer

III. District water budget based on the results of EMMA

It has been discussed in previous section that the interaquifer flows from shallow aquifer to deep aquifer contributes larger parts of deep groundwater recharge than lateral flows in Baoding area. The percentage of interaquifer flow accounts for about 60% (average value of 6 estimated locations) based on the results of End Member Mixing analysis. If assuming that this percentage value is suitable for all Baoding City, and then we can tentatively calculate the water budget in shallow and deep aquifer of Baoding city.

The groundwater recharge data (1991-2003), groundwater consumption situation (1996-2000) and groundwater outflow in shallow and deep aquifer were obtained from previous reports (Wang *et al*., 2009, Shi *et al*., 2011; Song, 2011). The parameters setting for calculating interaquifer flow is shown in Table 5. The results of water budget in shallow and deep aquifers of Baoding area are shown in Figure 37 and Table 6.

The results indicate that about 190mm/y shallow groundwater will recharge to deep groundwater through interaquifer flows every year. Comparing to the human exploitation amount in shallow groundwater, this part should be a considerable loss which imply a high risk of deep groundwater pollution due to such kind of interaquifer flows. Furthermore, a loss of about 546mm/y groundwater in deep aquifer has been evaluated in this area based on the water budget results. Therefore, we believe that although the government has set out to change the improper groundwater exploitation pattern since many years ago, the alarming water situation could not alter in a short time.

Table 5: Parameters setting for interaquifer flows calculation of Baoding area

Parameters	K' (m/s)	dh (m)	b (m)	Area(km^2)	Interaquifer flows contribution ratio
	1.20E-7	30	60	315	
Total interaquifer flows (mm/y)	190				60% (average of EMMA)

(Parameter explanation is shown in Figure 35)

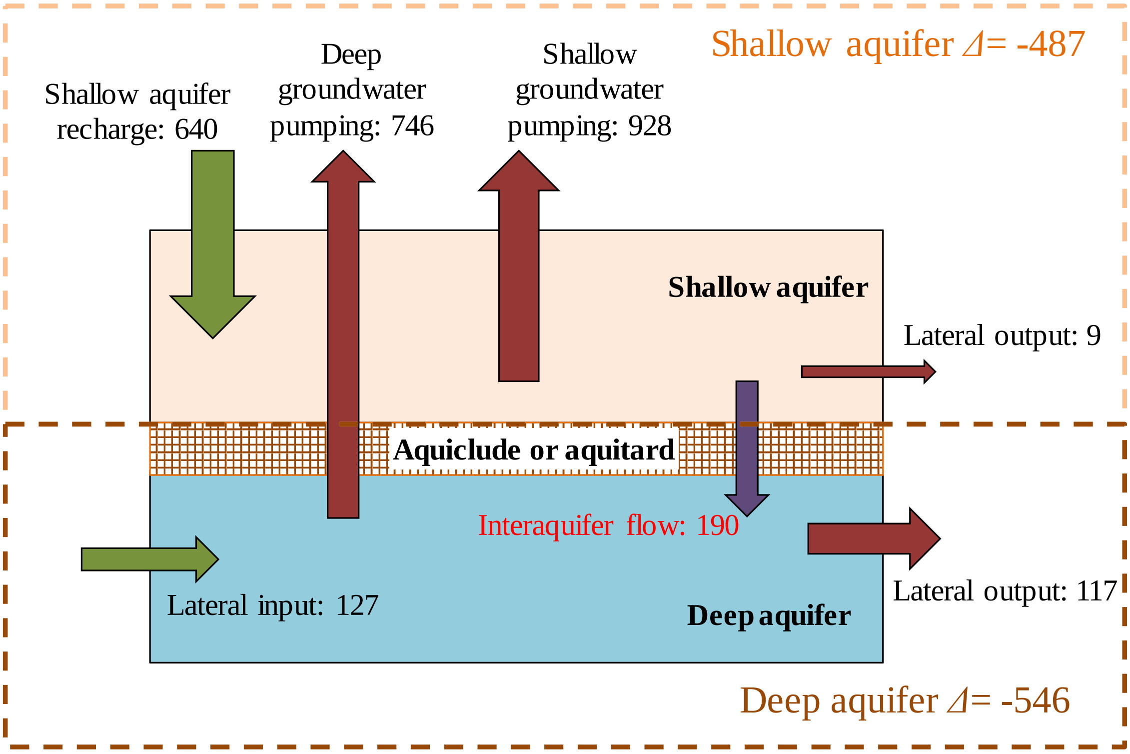

Figure 37: Water budget in shallow and deep aquifers of Baoding area (mm/y)

Table 6: The results of water budget in shallow and deep aquifers of Baoding area

(mm/y)

	Shallow aquifer	**Deep aquifer**	
		Lateral input	**Interaquifer flows**
Recharge	640	127	190
Human exploitation	-928	-746	
Interaquifer flows	-190	0	
Lateral output	-9	-117	
⊿S	-487	-546	
⊿S(total)	-1033		

One more thing we have to emphasis here is that the water budget results in this chapter can be figured out is because we assumed the percentage (60% in this chapter) of interaquifer flows contribution is suitable for all Baoding city. However, the fact is that this value is of course different depending on many other factors like the hydrogeology condition, or the degree of groundwater exploitation. So the interaquifer recharge may over-estimated or under-estimated here because the value of 60%. In fact, if comparing with previous report, it can be found that estimated deep groundwater recharge rate in this research (546mm/y) is smaller than that in other report (approximately 700~800mm/y) (Shi *et al.*, 2011). This indicates that the deep groundwater recharge rate is under-estimated based on the parameter setting in Table 5. Therefore, the hydraulic difference existing between shallow and deep aquifer might be bigger than current setting, which means the risk of deep groundwater polluted by shallow groundwater recharge through interaquifer flow processes would be bigger than current estimation. This is exactly the reason why calculated the water budget in shallow and deep groundwater, rather than supply an accurate water budget model. Because, after all this is not the main objective of this research, and also the data sources using in calculation is from different researches in different periods, so maybe it is not proper to combine them directly.

Chapter 6:　Conclusions and perspectives

As crucially important water resource in the North China Plain, deep groundwater is now widely used but in improper way in research area. For sustainable groundwater resource management, this research attempted to make clear the interaction relationship between shallow and deep groundwater by using major ions and stable isotopes. For this purpose, water sampling campaigns were carried out since June 2011 to March 2013 in research area, and the sampling locations were mainly located in plain area around Baoding city and Dingzhou city. The results indicate that it is feasible and useful by using stable isotopes and major ions to make clear the characteristic of the groundwater flow regime including the interaction between shallow and deep groundwater.

Hydrogeochemistry and hydrochemical processes

Throughout the Baiyangdian Lake Watershed, the dominated groundwater type can be represented by $Ca \cdot Mg\text{-}HCO_3$, which widely exists in mountain area, Dingzhou area and north of Baoding area, whereas $Na\text{-}HCO_3$ water type represents the deep groundwater type in downstream area of the watershed, which evolved from Ca·Mg-Na exchange reaction. Much more complicated situation is found in Baoding area, because the water type becomes quite diversiform due to the influences of surface water there.

Surface water and shallow groundwater represents the water with relatively high stable isotopic compositions in the watershed, because of the evaporation enrichment and the recharge relationship between surface water and shallow aquifer. The groundwater in mountain area and shallow groundwater in plain are mainly recharged by precipitation infiltration recharge, except the shallow groundwater taken in surface water region which mainly get the recharge from surface water. On the other hand, deep groundwater usually shows light isotopic compositions, and they are recharge in mountain area in different elevation.

Interaction relationship existed in study area

In the study, combination of the results of multi-tracers and previous studies confirm that interaquifer flows recharge processes exactly exist and have dominated in the southeast of Baoding city (Table 7), where a considerable deep groundwater depression cone exist due to over-exploitation. The interaquifer flow with direction from shallow to deep aquifer is the result of potential difference between shallow groundwater and deep groundwater. However, the interaction relationship existing between different aquifers were not found or at least not confirmed in other regions with study area, this is because the hydraulic difference is not big enough to make interaquifer flow dominate, or because of thicker confining bed restricting the interaquifer flow process.

Table 7: The interaction relationship between different aquifers in study area

	Baoding area		Dingzhou area
	city region	other regions	
Aquifer 1			
	existent	non-existent	non-existent
Aquifer 2			
	non-existent	non-existent	non-existent
Aquifer 3			

Distinct hydraulic connections are also found between surface water and shallow groundwater, as well as mountain groundwater and deep groundwater in plain area. There is no doubt that artificial river in surface water region of Baoding area are recharging and has brought great influences to the shallow groundwater in this region. The isotopic composition results also show that deep groundwater in Dingzhou area is recharge by the groundwater in south mountain area with altitude from 252m to more than 1000m, and the possibly existed concealed fault gives no or little influence to the groundwater flow system here.

Quantification of the interaction between shallow and deep groundwater

By using end member mixing analysis, it is clear that for the deep groundwater of Aquifer 2 in the vicinity of Baoding city where a deep groundwater depression cone existed, the interaquifer flows recharge has become dominated comparing to the lateral flows, and the former one contributed about 31% to maximum 81% of total deep groundwater recharge. An estimation of interaquifer flows by using Darcy’s Law reveals that interaquifer flows existed in Baoding area will range from $0.1\sim1.19\times10^8 m^3$/year depending on hydraulic difference between different aquifers and thickness of confining unit.

Furthermore, based on the estimation results of end member mixing analysis and groundwater utilization situation, a water budget in shallow and deep aquifer in Baoding area has been calculated tentatively. The results show that about 190mm/y shallow groundwater will recharge deep groundwater through interaquifer flow processes every year. Comparing with human exploitation amount from shallow aquifer, this part would be a non-negligible loss, which implies a high risk of deep groundwater pollution due to interaquifer flows from shallow groundwater. Besides, a loss of about 546 mm/y deep groundwater has been estimated in this area based on water budget results. Therefore, we believe that although the government has set out to change the improper groundwater exploitation pattern since many years ago, the situation of water budget could not alter in a short time.

Perspectives

Baiyangdian Lake Watershed is thought to be a mid-large scale catchment with an area of about 36 000 km^2. For this reason, water sampling activity in wider area will be helpful to grasp the characteristics of the groundwater flow regime further in study area. For example, new field surveys should cover more mountain areas, especially the north part of the study area. Besides, because it has been clear that the interaquifer flow processes exist in the vicinity of Baoding city, it is necessary to collect more groundwater samples around this region for defining the area where interaquifer flow dominates.

Stable isotopes and major ions were proved to be very effective tracers in hydrogeological investigation. However, some other tracers, such as Tritium and Carbon 14, are still suggested to be used in future study in this area, if some more information, such as groundwater ages, are expected to be obtained.

Interaquifer flows rate has been estimated in this study, but the parameter setting was thought to be very roughly due to lack of detailed hydrogeological information of the study area. Therefore, a more accurate estimation of the interaquifer flows is expected in the future work if more useful information can be obtained.

Acknowledgements

As the saying goes, there are so many ways to fail but only one way to succeed: Never give up. On the way of completing this thesis, I must thank these people who give me so great help and encouragement that I can keep going forward.

First of all, I must express my cordial and deepest gratitude to my supervisor Professor Dr. Maki Tsujimura, who treat us students just like his own children. Professor Tsujimura not only gives me strict but so effective guidance on my research work, but also makes so many opportunities which lead me grow. Without his earnest and patient help, I could never make it this far.

I would like to express my deep appreciation to my PhD thesis evaluation committee: Professor Dr. Jun ASANUMA, Professor Dr. Takehiko FUKUSHIMA and Professor Dr. Kuniaki MIYAMOTO for their warm guidance and helpful comments.

Grateful thanks to Professors of the Watershed Research group: Honorary Professor Dr. Norio TASE, Professor Dr. Michiaki SUGITA and Professor Dr. Atsushi KAWACHI, who always give helpful comments to help me conduct my research.

My special thanks must give to Professor Dr. Xianfang SONG and his group member Dr. Ruiqiang YUAN and Dr. Shiqin WANG from Institute of Geographical Sciences and Natural Resource Research, Chinese Academy of Sciences. Without their energetic supports, the field surveys in China cannot be successfully completed.

I also would like to thanks professors in Environmental Diplomatic Leadership Program, like Professor Dr. Takahiro ENDO, Professor Dr. Naomi WAKASUGI and Professor Dr. Xiaogang SUN, as well as other staff members. Thanks them to give me so many opportunities to broaden my knowledge vision and to make so many good friends.

A life without friends is a life without a sun. I must say thank you to my good friends, who talks with me, encourage me and grow with me. Especially, thanks Dr. Xizheng LIU, who let me know what a qualified researcher should be like. To be appreciative of all Tsujimura-Lab group members, who treat me like their brothers and grow with me, especially to Abe san, Ikeda san, Yamada kun, Sakakibara kun and Horiuchi kun.

I also cannot forget to express my deep appreciation to Mrs. Reiko FUKUOKA, who is my first Japanese teacher and taught me Japanese before I came to Japan.

I have to be obliged to my family who gives me great power and strong supports. Thanks my grandmother who took care of me since when I was born; thanks my parents for your understanding and encouragement. Finally, warm appreciation is expressed to LI, who gives me infinite energy and does like my buttress in these brilliant years. I wish I could hold your hand to the end of the time.

References

Ahmed MA, Samie AS, El-Maghrabi HM. 2011. Recharge and contamination sources of shallow and deep groundwater of Pleistocene aquifer in El-Sadat industrial city: isotope and hydrochemical approaches. *Environmental Earth Sciences* **62**: 751-768.

Ali AG, Roy GA, Turmel MC, Courchesne F. 2010. Source-to-stream connectivity assessment through end-member mixing analysis. *Journal of Hydrology* **392**: 119-135.

Barthold FK, Tyralla C, Schneider K, Vache KB, Frede HG, Breuer L. 2011. How many tracers do we need for end member mixing analysis (EMMA)? A sensitivity analysis. *Water Resources Research* **47**: W08519.

Berndtsson R. Larson M. 1987. Spatial variability of infiltration in a semi-arid environment. *Journal of hydrology* **90**: 117-133.

Cao GL. 2013. Evaluation of groundwater system in the North China Plain using groundwater modelling. Doctoral Dissertation, China University of Geosciences; 113 (in Chinese with English abstract).

Carucci V, Petitta M, Aravena R. 2012. Interaction between shallow and deep aquifers in the Tivoli Plain (Central Italy) enhanced by groundwater extraction: A multi-isotope approach and geochemical modeling. *Applied Geochemistry* **27**: 266-280.

Chen WH. 1987. Quaternary geology of Hebei, Geological Publishing House, Beijing, China; 179 (in Chinese).

Chen ZY, Fei YH, Miao JX, Song HB, Yang M, Zhang ZJ. 2009. Analysis on evolution of groundwater depression cones and its leading factors in North China Plain. *Resources Science* **31**: 394-399 (in Chinese with English abstract).

Chen ZY, Nie ZL, Zhang ZJ, Qi JX, Nan YJ. 2005. Isotopes and sustainability of ground water resources, North China Plain. *Groundwater* **43**: 485–493.

Chen ZY. 2003. Paleoclimatic interpretation of the past 30 ka from isotopic studies of the deep confined aquifer of the North China plain. *Applied Geochemistry* **23**: 997-1009.

Cheng TP, Shao JL, Cui YL, Mo ZY, Han Z, Li L. 2014. Parallel simulation of groundwater flow in the North China Plain. *Journal of Earth Science* **25**: 1059-1066.

Chkirbene A, Tsujimura M, Charef A, Tanaka T. 2009. Hydro-geochemical evolution of groundwater in an alluvial aquifer: Case of Kurokawa aquifer, Tochigi prefecture, Japan. *Desalination* **246**: 485-495.

Clark DI, Fritz P. 1997. Environmental Isotopes in Hydrogeology, CRC Press, Boca Raton, USA; 352.

Craig H, Gordon LI, Horibe Y. 1963. Isotopic exchange effects in the evaporation of water: 1. Low-temperature experimental results. *Journal of Geophysical Research* **68**: 5079–5087.

Craig H. 1961. Isotopic variations in meteoric waters. Science **133**:1702–1703.

Dai GH, Liu XH, Liang G, Han X, Shi L, Cheng DM, Gong WW. 2011. Distribution of organochlorine pesticides (OCPs) and polychlorinated biphenyls (PCBs) in surface water and sediments from Baiyangdian Lake in North China. *Journal of Environmental Sciences* **23**: 1640-1649.

Dansgaard W. 1964. Stable isotopes in precipitation. *Tellus* **16**:436-468.

Darcy H. 1856. Les Fontaines Publiques de la Ville de Dijon. Dalmont, Paris.

Dettinger MD. 1989. Reconnaissance Estimates of Natural Recharge to Desert Basins in Nevada, USA, by Using Chloride-Balance Calculations. *Journal of Hydrology* **106**: 55-78.

Dhar RK, Zheng Y, Stute M. 2008. Temporal variability of groundwater chemistry in shallow and deep aquifers of Araihazar, Bangladesh. *Journal of Contaminant Hydrology* **99**: 97-111.

Diaw M, Faye S, Stichler W, Maloszewski P. 2012. Isotopic and geochemical characteristics of groundwater in the Senegal River delta aquifer: implication of recharge and flow regime. *Environmental Earth Sciences* **66**: 1011-1020.

Esquivel MJ, Morales PG, Esteller VM. 2015. Groundwater monitoring network design using GIS and multicriteria analysis. *Water Resource Management* **29**: 3175-3194.

Fang QX, Mab L, Green TR, Yu Q, Wang TD, Ahujab LR. 2010. Water resources and water use efficiency in the North China Plain: Current status and agronomic management options. *Agricultural Water Management* **97**: 1102–1116.

Foster S, Chilton P. 2003. Groundwater: the processes and global significance of aquifer degradation. *Philosophical Transactions of the Royal Society Biological Sciences* **358**: 1957-1972.

Foster S, Garduno H, Evans R, Olson D, Tian Y, Zhang WZ, Han ZS. 2004. Quaternary aquifer of the North China Plain-assessing and achieving groundwater resource sustainability. *Hydrogeology Journal* **12**: 81-93.

Gat JR. 1980. Handbook of Environmental Isotope Geochemistry. In *The Isotopes of Hydrogen and Oxygen in Precipitation*, Fritz P, Fontes JC (eds). Elsevier, Amsterdam, the Netherlands; 21–47.

Gat JR. 1996. Oxygen and hydrogen isotopes in the hydrologic cycle. *Annual Review of Earth and Planetary Sciences* **24**:225–262.

Guba S, Somogyi V, Bardos ES. 2015. Groundwater remediation using biological and photocatalytic methods. *Hungarian Journal of Industry and Chemistry* **43**: 39-43.

Guo YH, Shen ZL. 1995. Relationship between saline water downgoing and desalination of shallow saline water, Hebei Plain. *Hydrogeology and Engineering Geology* **2**: 8–12 (in Chinese with English abstract).

Hamed KH, Rao AR. 1998. A modified Mann-Kendall trend test for autocorrelated data. *Journal of Hydrology* **204**: 182-196.

Harker L, Hutcheon I, Mayer B. 2015. Use of major ion and stable isotope geochemistry to delineate natural and anthropogenic sources of nitrate and sulfate in the Kettle River Basin, British Columbia, Canada. *Comptes Rendus Geoscience* **347**: 338-347.

Hem JD. 1985. Study and interpretation of the chemical characteristics of natural water. Water chemistry. U.S. Geological Survey, Water Supply Paper 2254.

Hooper RP, Christophersen N, Peters NE. 1990. Modeling streamwater chemistry as a mixture of soilwater end member: an application to the Panola Mountain catchment, Geogia, U.S.A. *Journal of Hydrology* **116**: 321-343.

Hu C, Delgado JA, Zhang X, Ma L. 2005. Assessment of groundwater use by wheat (Triticum aestivum L.) in the Luancheng Xian Region and potential implications for water conservation in the northwestern North China Plain. *Journal of Soil and Water Conservation* **93**: 271-280.

Hu KL, Huang YF, Li H, Li BG, Chen DL, White RE. 2005. Spatial variability of shallow groundwater level, electrical conductivity and nitrate concentration, and risk assessment of nitrate contamination in North China Plain. *Environment International* **31**: 896–903.

Juana PM, Yang YH, Li HL. 2010. Impact of water resource exploitation on the hydrology and water storage in Baiyangdian Lake. *Hydrological Processes* **24**: 3026–3039.

Kendall C, McDonnell JJ. 1998. Isotope Tracers in Catchment Hydrology. Elsevier Science, Amsterdam, the Netherlands;839.

Kohfahl C, Rodriguez M, Fenk C, Menz C, Benavente J, Hubberten H, Meyer H, Paul L, Knappe A, Lopez-Geta JA, Pekdeger A. 2008. Characterising flow regime and interrelation between surface-water and ground-water in the Fuente de Piedra salt lake basin by means of stable isotopes, hydrogeochemical and hydraulic data. *Journal of Hydrology* **351**: 170-187.

Lalehzari R, Tabatabaei SH, Kholghi M. 2013. Simulation of nitrate transport and wastewater seepage in groundwater flow system. *Environmental Science and Technology* **10**: 1367-1376.

Lernaer DN. 1990. Groundwater recharge in urban areas. *Atmospheric Environment* **248**: 29-33.

Li FC, Liu CQ, Guan YQ, Liu WW. 2006. Multivariate analysis method is applied to water quality of Baiyangdian Lake. *Journal of Hebei University* **26**: 405-410 (in Chinese with English abstract).

Li L, Zheng H. 2001. Environmental and ecological water requirements of a river system: a case study of the Haihe-Luanhe River System. *Journal of Geographical Sciences* **11**: 224–230.

Li W, Wang MY, Liu LY, Wang HF, Yu S. 2015. Groundwater heavy metal levels and associated human health risk in the North China Plain. *Arabian Journal of Geosciences* **8**: 10389-10398.

Li YS, Zhang FW, Han ZT, Wang P, Chen HH, Zhang ZJ. 2014. Evolution characteristics and influence factors of deep groundwater depression cone in North China Plain, China-A case study in Cangzhou region. *Journal of Earth Science* **25**: 1051-1058.

Liu CL, Xie GD, Xiao Y. 2007. The influence of climate change on the Baiyangdian wetland. *Chinese Journal of Mechanical Engineering* **16**: 245-250.

Liu JR, Song XF, Yuan GF, Sun XM, Yang LH. 2014. Stable isotopic compositions of precipitation in China. *Tellus B* **66**: 22567.

Liu KY, Zhang L, Zhang GH, Liu J, Yan MJ. 2007. The impact of human activities on north China Baiyangdian watershed runoff recognition research. *Journal of China Hydrology* **27**: 6-10 (in Chinese with no English abstract, original title: 人类活动对华北白洋淀流域径流影响的识别研究).

Long D, Gao YC, Vijay PS. 2010. Estimation of daily average net radiation from MODIS data and DEM over the Baiyangdian Watershed in north China for clear sky days. *Journal of Hydrology* **388**: 217–233.

Ma M, Wang ZJ, Zhu XR. 1995. Baiyangdian area pollution condition of biological toxicity assessment. *China Environmental Science* **15**: 166-170 (in Chinese with no English abstract, original title: 白洋淀地区污染状况的生物毒性评价).

Ma R, Wang YX, Sun ZY, Zheng CM, Ma T, Prommer H. 2011. Geochemical evolution of groundwater in carbonate aquifers in Taiyuan, northern China. *Applied Geochemistry* **26**: 884-897.

Mays LW. 2013. Groundwater resources sustainability: past, present, and future. *Water Resource Management* **27**: 4409-4424.

Mazor E. 2003. Chemical and Isotopic Groundwater Hydrology, CRC Press, Boca Raton, USA; 352.

McCarthy KA, McFarland WD, Wilkinson JM, White LD. 1992. The dynamic relationship between ground water and the Columbia River: using deuterium and oxygen-18 as tracers. *Journal of Hydrology* **135**: 1–12.

Misra AK, Mishra A. 2006. Groundwater quality monitoring in shallow and deep aquifers in Saidabad Tahsil Area, Mathura District, India. *Environmental Monitoring and Assessment* **117**: 345-355.

Mook WG. 2005. Introduction to Isotope Hydrology: Stable and Radioactive Isotopes of Hydrogen, Carbon, and Oxygen, CRC Press, Boca Raton, USA; 256.

Nakayama T. 2011. Simulation of complication and diverse water system accompanied by human intervention in the North China Plain. *Hydrological Processes* **25**: 2679-2639.

Owens L, Edwards W, Van Keuren R. 1992. Nitrate levels in shallow groundwater under pastures receiving ammonium nitrate or slow-release nitrogen fertilizer. *Journal of Environmental Quality* **21**: 607–613.

Onodera S, Saito M, Sawano M, Hosono T, Taniguchi M, Shimada J, Umezawa Y, Lubis RF, Buapeng S, Delino R. 2009. Effects of intensive urbanization on the intrusion of shallow groundwater into deep groundwater: Examples from Bangkok and Jakarta. *Science of the Total Environment* **404**: 401–410.

Ozawa K, Nagahara H. 2001. Chemical and isotopic fractionations by evaporation and their cosmochemical implications. *Geochimica et Cosmochimica Acta* **65**:2171-2199.

Piper AM. 1994. A graphic procedure in the geochemical interpretation of water-analyses. *USGS Groundwater Note* **12**.

Plummer JL. 1994. Water resources problems in west of America. *Water Resource Bulletin* **30**: 146-157.

Qian YP, Qin DJ, Pang ZH. 2006. A discussion of recharge sources of deep groundwater in the Ejin Basin in the lower reaches of Heihe River. *Hydrogeology and Engineering Geology* **3**: 25-29 (in Chinese with English abstract).

Ryu JH, Koh YK, Park SW, Kim GY, Choi JW. 2012. Geochemical characterization of deep groundwater in Kurt using geochemical modeling. *Journal of Environmental Engineering* **138**: 351-359.

Saether OM, Caritat P. 1996. Geochemical Process, Weathering and Groundwater Recharge in Catchments, CRC Press, Boca Raton, USA; 400.

Saha D, Sinha UK, Dwivedi SN. 2011. Characterization of recharge processes in shallow and deeper aquifers using isotopic signatures and geochemical behavior of groundwater in an arsenic-enriched part of the Ganga Plain. *Applied Geochemistry* **26**: 432–443.

Scanlon BR, Cook PG. 2002. Theme issue on groundwater recharge. *Hydrogeology Journal* **10**: 3–4.

Seiler KP, Lindner W. 1995. Near-surface and deep groundwaters. *Journal of Hydrology* **165**: 33–44.

Shi JS, Zhao W, Zhang ZJ, Fei YH, Li YS, Zhang FE, Chen JS, Qian Y. 2011. Assessment of deep groundwater over-exploitation in the North China Plain. *Geoscience Frontiers* **2**: 593–598.

Shikazono N. 2001. Compositional variation of major elements in groundwater caused by water-rock interaction (II) –influence of reaction kinetics and fluid flow. *Journal of Groundwater Hydrology* **43**: 161-170 (in Japanese with English abstract).

Shu YQ, Villholth KG, Jensen KH, Stisen S, Lei YP. 2012. Integrated hydrological modeling of the North China Plain: Options for sustainable groundwater use in the alluvial plain of Mt. Taihang. *Journal of Hydrology* **464-465**: 79-93.

Song ZH. 2011. Analysis on groundwater dynamic characteristics and forming causes in the Plain of Baoding. *Groundwater* **33**: 63-64 (in Chinese with English abstract).

Stewart KM. 1975. Stable isotope fractionation due to evaporation and isotopic exchange of falling waterdrops: Applications to atmospheric processes and evaporation of lakes. *Journal of Geophysical Research* **80**: 1133-1146.

Su CL, Wang YX, Pan YL. 2013. Hydrogeochemical and isotopic evidences of the groundwater regime in Datong Basin, Northern China. *Environmental Earth Sciences* **70**: 877-885.

Sun H, Shen Y, Yu Q, Flerchinger GN, Zhang Y, Liu C, Zhang X. 2010. Effect of precipitation change on water balance and WUE of the winter wheat-summer maize rotation in the North China Plain. *Agricultural Water Management* **97**: 1139–1145.

Taylor AC, Stefan GH. 2009. Shallow groundwater temperature response to climate change and urbanization. *Journal of Hydrology* **375**: 601-612.

Tsujimura M, Abe Y, Tanaka T, Shimada J, Higuchi S, Yamanaka T, Davaa G, Oyunbaatar D. 2007. Stable isotopic and geochemical characteristics of groundwater in Kherlen River basin, a semi-arid region in eastern Mongolia. *Journal of Hydrology* **333**: 47-57.

UNESCO. 2009. Water in a Changing World: The United Nations World Development Report 3. UNESCO and Berghahn Books, Paris and London; 318.

UNESCO. 2012. Managing Water under Uncertainty and Risk: The United Nations World Development Report 4. UNESCO and Berghahn Books, Paris and London; 866.

WMO/IAEA. 2003. Global Network of Isotopes in Precipitation database (GNIP database). http://www-naweb.iaea.org/napc/ih/IHS_resources_gnip.html. Last access June 7, 2015.

Wada Y, Beek PL, Kempen MC, Reckman WJ, Vasak S, Bierkens FM. 2010. Global depletion of groundwater resources. *Geophysical Research Letters* **37**: L20402.

Wang BG, SQ, Tang CY, Song XF, Wang QX, Zhang YH, Yuan RQ. 2014. The impacts of a linear wastewater reservoir on groundwater recharge and geochemical evolution in a semi-arid area of the Lake Baiyangdian watershed, North China Plain. *Science of the Total Environment* **482-483**: 325-335.

Wang DC. 1995. An Introduction to Hydrogeology. Geology Press, Beijing, China; 164 (in Chinese).

Wang F, Wang X, Zhao Y, Yang ZF. 2014. Temporal variations of NDVI and correlations between NDVI and hydro-climatological variables at Lake Baiyangdian, China. *International Journal of Biometeorology* **58**: 1531-1543.

Wang R, Liu ZF, Yao ZJ, Lei YP. 2014. Modeling the risk of nitrate leaching and nitrate runoff loss from intensive farmland in the Baiyangdian Basin of the North China Plain. *Environmental Earth Sciences* **72**: 3143-3157.

Wang SQ, Shao JL, Song XF, Zhang YB, Huo ZB, Zhou XY. 2008. Application of MODFLOW and geographic information system to groundwater flow simulation in North China Plain, China. *Environmental Geology* **55**: 1449-1462.

Wang SQ, Song XF, Wang QX, Xiao GQ, Liu CM, Liu JR. 2009. Shallow groundwater dynamics in North China Plain. *Journal of Geographical Sciences* **19**: 175-188.

Wang SQ, Tang CY, Song XF, Wang QX, Zhang YH, Yuan RQ. 2014. The impacts of a linear wastewater reservoir on groundwater recharge and geochemical evolution in a semi-arid area of the Lake Baiyangdian watershed, North China Plain. *Science of the Total Environment* **482–483**: 325–335.

Wang SQ, Tang CY, Song XF, Yuan RQ, Wang QX, Zhang YH. 2013. Using major ions and δ^{15}N-NO_3^- to identify nitrate sources and fate in an alluvial aquifer of the Baiyangdian lake watershed, North China Plain. *Environmental Science: Processes & Impacts* **15**: 1430-1443.

Yang LY, Hur J. 2014. Critical evaluation of spectroscopic indices for organic matter source tracing via end member mixing analysis based on two contrasting sources. *Water Research* **59**: 80-89.

Yang W, Yang ZF. 2014. Effects of long-term environmental flow releases on the restoration and preservation of Baiyangdian Lake, a regulated Chinese freshwater lake. *Hydrobiologia* **730**: 79-91.

Yang Y, Tian F. 2009. Abrupt change of runoff and its major driving factors in Haihe River Catchment, China. *Journal of Hydrology* **374**: 373–383.

Yuan RQ, Song XF, Zhang YH, Han DM, Wang SQ, Tang CY. 2011. Using major ions and stable isotopes to characterize recharge regime of a fault-influenced aquifer in Beiyishui River Watershed, North China Plain. *Journal of Hydrology* **405**: 512–521.

Zhang GH, Wang JZ. 2002. Mechanism of confined groundwater recharge and release in the Middle-East Plain of Haihe River Basin. *Hydrology* **22**: 5-9 (in Chinese with English abstract).

Zhang SZ, Tian JW, Li GB. 2007. Ecological problems and restoration measures of Baiyangdian wetland. *Bulletin of Soil and Water Conservation* **3**: 146-150 (in Chinese with English abstract).

Zhang XM, Tang YJ, Zhang S. 1997.Study on the content and distribution of contamination in soil plant system in Baiyangdian region. *Progress in Geography* **16**: 62-69 (in Chinese with English abstract).

Zhang Y, Li GM. 2014. Influence of south-to-north water diversion on major cones of depression in North China Plain. *Environmental Earth Sciences* **71**: 3845-3853.

Zhang Y, Wang JC, Jing JH, Sun JC. 2014. Response of groundwater to climate change under extreme climate conditions in North China Plain. *Journal of Earth Science* **25**: 612-618.

Zhang Y, Wang XL, Li B. 1999. Research on pollution mechanism and prevention in Baiyangdian Lake. *Water resources protection* **4**: 29-32 (in Chinese with no English abstract, original title: 白洋淀污染机理及防治探讨).

Zhang ZH, Li LR. 2005. Groundwater resources in China: Hebei volume, Sino Maps Press, Beijing, China; 117 (in Chinese).

Zhang ZH, Zhang GH, Ren FH, Fei J. 2006. Regional groundwater evolution process and its interaction with neighboring sphere layers, Geological Publishing House, Beijing, China; 248 (in Chinese).

Zhang ZJ, Fei YH, Chen ZY. 2009. Investigation and evaluation on groundwater sustained development in North China Plain, Geological Publishing House, Beijing, China; 471(in Chinese).

Zhang ZJ, Fei YH. 2009. Atlas of Groundwater Sustainable Utilizations in North China Plain. Sino Maps Press, Beijing, China; 185 (in Chinese).

Zhao X, Cui BS, Yang ZF. 2005. A study of the lowest ecological water level of Baiyangdian Lake. *Acta Ecologica Sinica* **25**: 1033-1040 (in Chinese with English abstract).

Zhao Y, Xia XH, Yang ZF, Wang F. 2012. Assessment of water quality in Baiyangdian Lake using multivariate statistical techniques. *Procedia Environmental Sciences* **13**: 1213-1226.

Zhuang CW, Ouyang ZY, Xu WH, Bai Y, Zhou WQ, Zheng H, Wang XK. 2011. Impacts of human activities on the hydrology of Baiyangdian Lake, China. *Environmental Earth Sciences* **62**: 1343-1350.

Appendix

Table S1 Water samples information: Mountain area (1)

Sampling Location information						
Sample ID	sampling date	sampling time	water type	Longitude	Latitude	Elevation
	y/m/d	h:m		°E	°N	m
W-M1	2011/06/13	11:00	rw	113.92	39.12	771
W-M2	2011/06/13	12:18	rw	113.97	39.13	728
W-M3	2011/06/13	14:18	rw	113.94	39.11	747
W-M4	2011/06/13	15:16	rw	113.97	39.07	570
W-M5	2011/06/13	16:32	rw	114.03	39.02	447
W-M6	2011/06/13	17:46	rw	114.05	38.97	425
W-M7	2011/06/13	18:40	rw	114.08	38.94	377
W-M8	2011/06/14	9:35	rw	114.11	38.91	320
W-M9	2011/06/14	11:50	rw	114.15	38.88	295
W-M10	2011/06/14	12:18	rw	114.14	38.86	280
W-M11	2011/06/14	14:41	rw	114.29	38.82	219
W-M12	2011/06/14	18:35	rw	114.42	38.77	204
W-D1	2011/06/04	16:26	dw	114.20	38.84	193
W-G1	2011/06/13	11:17	gw	113.93	39.12	761
W-G2	2011/06/13	12:32	gw	113.97	39.13	723
W-G3	2011/06/13	14:04	gw	113.94	39.11	758
W-G4	2011/06/13	16:17	gw	114.03	39.03	478
W-G5	2011/06/13	17:21	gw	114.06	38.97	436
W-G6	2011/06/13	18:27	gw	114.08	38.94	361
W-G7	2011/06/13	19:25	gw	114.07	38.94	391
W-G8	2011/06/14	11:02	gw	114.15	38.88	296
W-G9	2011/06/14	11:31	gw	114.15	38.88	293
W-G10	2011/06/14	13:38	gw	114.23	38.84	262
W-G12	2011/06/14	14:12	gw	114.38	38.82	216
W-G13	2011/06/14	15:22	gw	114.42	38.77	210

“rw”: river water; “gw”: groundwater; “dw”: dam water

Table S2 Water samples information: Mountain area (2)

Water samples quality													
Sample ID	water temperature	EC	pH	anion concentration (mg/L)				cation concentration (mg/L)				stable isotope (‰)	
	°C	μS/cm		Cl^-	NO_3^-	SO_4^{2-}	HCO_3^-	Na	Mg	K	Ca	$\delta^{18}O$	δD
W-M1	18.7	508	8.77	9.75	10.18	67.17	211.75	9.64	7.31	16.41	72.66	-9.75	-70.17
W-M2	24.3	478	8.69	9.07	6.49	49.87	208.26	12.90	4.42	16.39	64.36	-8.67	-64.41
W-M3	23.3	525	8.63	9.13	9.95	72.63	218.72	11.85	7.25	17.95	73.66	-9.47	-68.79
W-M4	23.3	471	8.49	11.07	5.80	63.03	189.96	13.02	5.70	18.14	59.89	-8.60	-64.45
W-M5	25.2	489	8.66	10.40	6.33	65.68	199.55	16.09	5.70	17.98	63.22	-8.32	-62.21
W-M6	23.6	530	8.42	10.25	8.60	63.18	228.30	14.35	4.94	20.13	68.61	-8.38	-62.48
W-M7	22.5	520	8.51	10.76	8.44	66.23	225.69	14.56	5.46	19.68	70.08	-8.16	-61.44
W-M8	20.2	485	8.22	9.95	5.04	67.40	191.70	14.17	4.66	17.12	65.59	-7.97	-59.33
W-M9	23.6	481	8.25	11.08	6.09	67.06	192.58	13.10	4.85	17.37	64.00	-7.89	-58.96
W-M10	23.2	493	8.15	9.50	5.07	65.77	204.34	12.95	4.59	17.20	68.45	-7.95	-59.53
W-M11	23.8	561	8.15	14.08	10.90	82.01	226.56	14.53	3.59	17.87	84.02	-8.15	-59.73
W-M12	21.4	575	8.00	16.70	12.17	79.08	233.53	14.41	3.47	17.49	85.98	-8.06	-59.44
W-D1	23.6	409	8.48	9.88	4.16	67.28	137.68	12.63	3.43	15.25	53.43	-6.65	-51.37
W-G1	12.3	603	8.30	10.96	12.21	89.75	264.03	13.89	6.13	22.93	85.74	-9.52	-68.76
W-G2	16.8	651	7.57	21.07	0.29	61.41	328.51	21.32	6.84	20.43	93.42	-8.95	-65.58
W-G3	13.4	574	8.04	9.57	13.97	77.80	223.07	13.40	6.13	18.40	85.15	-9.68	-70.35

Table S2 Water samples information: Mountain area (2) (Continued)

Sample ID	water temperature	EC	pH	anion concentration (mg/L)				cation concentration (mg/L)				stable isotope (‰)	
	°C	µS/cm		Cl^-	NO_3^-	SO_4^{2-}	HCO_3^-	Na	Mg	K	Ca	$\delta^{18}O$	δD
W-G4	17.1	1162	7.81	75.30	136.69	95.09	301.50	45.61	7.28	45.94	136.88	-8.62	-62.49
W-G5	13.3	571	7.95	10.18	12.03	44.31	312.83	12.89	2.67	26.47	78.22	-8.77	-62.31
W-G6	13.9	627	8.22	18.55	31.81	72.39	241.37	18.61	4.66	20.85	89.48	-8.62	-62.43
W-G7	16.0	521	8.05	8.19	11.86	59.38	211.75	18.74	5.19	18.91	70.00	-8.62	-62.55
W-G8	19.3	689	7.31	29.85	33.68	0.10	250.96	22.63	7.68	27.42	92.64	-8.51	-61.66
W-G9	13.3	623	7.31	18.07	18.11	87.68	238.76	16.56	4.10	21.39	92.84	-8.53	-60.83
W-G10	13.7	809	7.69	21.23	30.07	96.71	338.10	22.70	4.18	26.68	125.67	-8.57	-62.55
W-G12	16.5	499	8.03	10.19	12.04	69.68	198.68	12.18	1.68	13.22	81.56	-7.83	-57.39
W-G13	13.7	507	7.79	9.42	18.13	47.78	241.37	12.52	1.82	13.83	81.57	-7.88	-58.03

Table S3 Water samples information: Plain area (1)

Sampling Location information									
Sample ID	**sampling date**	**sampling time**	**water type**	**Region**	**longitude**	**latitude**	**elevation**	**well depth**	**Aquifer**
	y/m/d	**h:m**			**°E**	**°N**	**m**	**m**	
R1	2013/03/21	10:15	gw	NBD	116.07	39.05	16	50	1
R3	2013/03/21	11:05	gw	NBD	116.03	39.08	18	60	1
R4	2013/03/21	12:59	gw	NBD	115.97	39.08	17	40	1
R6	2013/03/21	14:17	gw	NBD	115.86	39.07	18	65	1
R8	2013/03/22	9:57	gw	NBD	115.81	39.07	15	70	1
R10	2013/03/22	11:12	gw	NBD	115.75	39.12	21	75	1
R12	2013/03/22	12:43	gw	NBD	115.71	39.15	24	30	1
R13	2013/03/22	13:19	gw	NBD	115.64	39.18	33	42	1
R14	2013/03/22	13:49	gw	NBD	115.62	39.22	37	74	1
R15	2013/03/22	14:48	gw	NBD	115.73	39.16	25	30	1
R17	2013/03/22	15:32	gw	NBD	115.68	39.09	25	40	1
R2	2013/03/21	10:20	gw	NBD	116.03	39.09	16	200	2
R11	2013/03/22	11:22	gw	NBD	115.76	39.13	20	300	2
R16	2013/03/22	15:11	gw	NBD	115.69	39.11	22	300	2
R5	2013/03/21	13:50	gw	NBD	115.92	39.09	17	400	3
R7	2013/03/21	14:46	gw	NBD	115.86	39.11	19	400	3
R9	2013/03/22	10:31	gw	NBD	115.80	39.09	19	400	3
BG2	2012/03/02	10:11	gw	BD	115.58	38.94	22	80	1
BG6	2012/03/02	11:40	gw	BD	115.64	39.00	21	60	1
BG10	2012/03/02	14:21	gw	BD	115.56	39.05	36	80	1
BG21	2012/03/03	13:00	gw	BD	115.32	39.00	50	320	1
BG22	2012/03/03	13:45	gw	BD	115.29	39.01	40	150	1
BG23	2012/03/03	13:50	gw	BD	115.29	39.01	55	50	1
BG25	2012/03/03	14:50	gw	BD	115.31	39.06	62	75	1
BG27	2012/03/03	16:50	gw	BD	115.30	39.09	113	130	1
BG42	2012/03/04	16:00	gw	BD	115.18	39.00	139	80	1
BG43	2012/03/04	16:30	gw	BD	115.18	38.99	93	60	1

"gw": groundwater; "NBD": North of Baoding; "BD": Baoding

Table S3 Water samples information: Plain area (1) (Continued)

Sample ID	sampling date	sampling time	water type	Region	longitude	latitude	elevation	well depth	Aquifer
	y/m/d	h:m			°E	°N	m	m	
BG44	2012/03/04	16:50	gw	BD	115.18	38.99	132	78	1
BG48	2012/03/05	10:10	gw	BD	115.32	38.80	40	65	1
BG60	2012/03/06	8:51	gw	BD	115.50	38.80	90	40	1
BG62	2012/03/06	9:25	gw	BD	115.48	38.73	31	120	1
BG63	2012/03/06	9:35	gw	BD	115.48	38.73	28	80	1
BG64	2012/03/06	10:10	gw	BD	115.48	38.68	27	75	1
BG69	2012/03/06	12:50	gw	BD	115.36	38.68	40	30	1
BG73	2012/03/06	13:40	gw	BD	115.30	38.69	30	40	1
BYD-G1	2011/06/11	13:29	gw	BD	115.93	38.90	14	4.8	1
Fu-G1	2011/06/10	14:37	gw	BD	115.67	38.83	9	100	1
Fu-G4	2011/06/10	15:49	gw	BD	115.66	38.83	13	55	1
Fu-G5	2011/06/10	17:04	gw	BD	115.73	38.86	8	80	1
Fu-G6	2011/06/10	18:34	gw	BD	115.75	38.88	9	5.23	1
Fu-G8	2011/06/11	11:06	gw	BD	115.83	38.88	11	55	1
T-G1	2011/06/11	18:15	gw	BD	115.84	38.82	10	30	1
T-G10	2011/06/12	13:14	gw	BD	115.76	38.84	8	65	1
T-G12	2011/06/12	14:44	gw	BD	115.79	38.82	9	90	1
T-G13	2011/06/12	15:55	gw	BD	115.66	38.80	13	80	1
T-G3	2011/06/11	19:42	gw	BD	115.84	38.82	8	90	1
T-G6	2011/06/12	10:11	gw	BD	115.69	38.81	10	42	1
T-G8	2011/06/12	11:12	gw	BD	115.71	38.80	12	80	1
2B18	2013/03/23	9:15	gw	BD	115.30	38.99	69	40	1
2B23	2013/03/23	14:07	gw	BD	115.50	38.95	22	50	1
2B25	2013/03/23	15:00	gw	BD	115.56	38.94	19	85	1
2B27	2013/03/24	10:13	gw	BD	115.61	38.89	14	70	1
2B30	2013/03/24	16:19	gw	BD	115.65	38.85	12	110	1
2B32	2013/03/24	17:30	gw	BD	115.71	38.79	7	120	1
2B36	2013/03/25	11:28	gw	BD	115.92	38.74	11	40	1
2B39	2013/03/25	15:11	gw	BD	116.04	38.65	7	50	1

“gw”: groundwater; “BD”: Baoding

Table S3 Water samples information: Plain area (1) (Continued 2)

Sample ID	**sampling date**	**sampling time**	**water type**	**Region**	**longitude**	**latitude**	**elevation**	**well depth**	**Aquifer**
	y/m/d	**h:m**			**°E**	**°N**	**m**	**m**	
2B41	2013/03/25	15:52	gw	BD	116.09	38.65	11	7	1
2B43	2013/03/25	17:35	gw	BD	116.02	38.68	12	7	1
BG1	2012/03/02	9:42	gw	BD	115.56	38.94	125	260	2
BG3	2012/03/02	10:40	gw	BD	115.59	38.97	52	325	2
BG15	2012/03/02	16:18	gw	BD	115.44	38.97	37	120	2
BG49	2012/03/05	10:30	gw	BD	115.32	38.80	31	148	2
BG53	2012/03/05	13:20	gw	BD	115.16	38.70	50	100	2
BG54	2012/03/05	13:40	gw	BD	115.10	38.72	62	110	2
BG61	2012/03/06	8:55	gw	BD	115.50	38.80	13	200	2
BG66	2012/03/06	10:42	gw	BD	115.46	38.64	36	180	2
BG72	2012/03/06	13:30	gw	BD	115.30	38.69	42	260	2
Fu-G2	2011/06/10	15:07	gw	BD	115.67	38.82	20	260	2
Fu-G3	2011/06/10	15:28	gw	BD	115.67	38.82	23	170	2
Fu-G7	2011/06/11	10:35	gw	BD	115.82	38.88	7	210	2
T-G5	2011/06/12	9:59	gw	BD	115.69	38.81	12	300	2
2B19	2013/03/23	9:56	gw	BD	115.34	38.98	36	140	2
2B20	2013/03/23	10:30	gw	BD	115.38	38.96	29	125	2
2B21	2013/03/23	11:20	gw	BD	115.43	38.97	32	140	2
2B22	2013/03/23	13:33	gw	BD	115.50	38.95	23	200	2
2B24	2013/03/23	14:36	gw	BD	115.56	38.94	20	260	2
2B28	2013/03/24	10:25	gw	BD	115.61	38.89	11	300	2
2B29	2013/03/24	16:09	gw	BD	115.65	38.85	13	183	2
2B31	2013/03/24	16:50	gw	BD	115.67	38.82	14	180	2
2B33	2013/03/24	17:56	gw	BD	115.72	38.76	12	270	2
2B34	2013/03/25	10:19	gw	BD	115.84	38.78	10	220	2
2B35	2013/03/25	10:45	gw	BD	115.84	38.75	11	200	2
2B37	2013/03/25	12:20	gw	BD	115.97	38.72	11	300	2
BG5	2012/03/02	11:10	gw	BD	115.62	38.99	25	325	3
BG8	2012/03/02	13:47	gw	BD	115.61	39.03	30	320	3

“gw”: groundwater; “BD”: Baoding

Table S3 Water samples information: Plain area (1) (Continued 3)

Sample ID	sampling date	sampling time	water type	Region	longitude	latitude	elevation	well depth	Aquifer
	y/m/d	h:m			°E	°N	m	m	
BG9	2012/03/02	14:11	gw	BD	115.56	39.05	38	320	3
2B26	2013/03/23	15:17	gw	BD	115.59	38.96	18	400	3
2B38	2013/03/25	14:55	gw	BD	116.04	38.65	7	600	3
2B40	2013/03/25	15:52	gw	BD	116.10	38.63	12	500	3
2B42	2013/03/25	17:27	gw	BD	116.02	38.68	14	500	3
DG1	2012/08/28	9:40	gw	DZ	114.87	38.56	81	50	1
DG2	2012/08/28	10:25	gw	DZ	114.83	38.57	83	30	1
DG3	2012/08/28	11:00	gw	DZ	114.80	38.60	84	30	1
DG4	2012/08/28	11:20	gw	DZ	114.79	38.61	88	125	1
DG5	2012/08/28	12:00	gw	DZ	114.78	38.57	85	43	1
DG6	2012/08/28	13:00	gw	DZ	114.74	38.61	88	25	1
DG8	2012/08/28	14:45	gw	DZ	114.65	38.59	131	10	1
DG9	2012/08/28	15:00	gw	DZ	114.65	38.59	131	25	1
DG10	2012/08/28	16:15	gw	DZ	114.58	38.51	107	20	1
DG11	2012/08/28	16:50	gw	DZ	114.58	38.49	109	45	1
DG12	2012/08/28	17:20	gw	DZ	114.61	38.48	99	50	1
DG13	2012/08/28	18:05	gw	DZ	114.62	38.48	97	28	1
DG14	2012/08/28	18:40	gw	DZ	114.62	38.42	89	45	1
DG15	2012/08/28	19:10	gw	DZ	114.61	38.41	89	32	1
DG16	2012/08/29	8:55	gw	DZ	114.89	38.48	66	60	1
DG18	2012/08/29	9:45	gw	DZ	114.94	38.47	55	30	1
DG20	2012/08/29	10:15	gw	DZ	114.94	38.47	54	52	1
DG21	2012/08/29	11:05	gw	DZ	114.83	38.42	62	50	1
DG23	2012/08/29	11:55	gw	DZ	114.78	38.41	71	60	1
DG24	2012/08/29	12:20	gw	DZ	114.74	38.46	81	60	1
DG25	2012/08/29	14:50	gw	DZ	114.82	38.32	61	78	1
DG26	2012/08/29	15:00	gw	DZ	114.83	38.32	62	45	1
DG27	2012/08/29	15:25	gw	DZ	114.87	38.27	54	50	1

“gw”: groundwater; “BD”: Baoding; “DZ”: Dingzhou

Table S3 Water samples information: Plain area (1) (Continued 4)

Sample ID	sampling date	sampling time	water type	Region	longitude	latitude	elevation	well depth	Aquifer
	y/m/d	h:m			°E	°N	m	m	
DG29	2012/08/29	16:25	gw	DZ	115.01	38.31	48	25	1
DG32	2012/08/29	17:40	gw	DZ	115.04	38.35	48	40	1
DG33	2012/08/30	18:30	gw	DZ	114.97	38.39	52	25	1
DG35	2012/08/30	9:25	gw	DZ	115.07	38.48	58	115	1
DG36	2012/08/30	9:35	gw	DZ	115.06	38.47	55	33	1
DG38	2012/08/30	10:40	gw	DZ	115.11	38.41	43	34	1
DG40	2012/08/30	12:00	gw	DZ	115.24	38.45	40	70	1
DG42	2012/08/30	14:10	gw	DZ	115.35	38.29	33	80	1
DG44	2012/08/30	15:10	gw	DZ	115.16	38.30	41	100	1
2D44	2013/03/26	8:53	gw	DZ	115.09	38.49	49	60	1
2D45	2013/03/26	9:10	gw	DZ	115.17	38.47	41	60	1
2D46	2013/03/26	9:55	gw	DZ	115.36	38.36	29	70	1
2D47	2013/03/26	10:34	gw	DZ	115.43	38.31	28	50	1
2D50	2013/03/26	12:08	gw	DZ	115.39	38.34	29	75	1
2D52	2013/03/26	14:39	gw	DZ	115.32	38.47	30	70	1
2D54	2013/03/26	15:52	gw	DZ	115.22	38.46	39	100	1
2D57	2013/03/27	9:04	gw	DZ	115.10	38.51	47	50	1
DG7	2012/08/28	13:25	gw	DZ	114.74	38.61	89	150	2
DG19	2012/08/29	10:05	gw	DZ	114.94	38.46	54	230	2
DG28	2012/08/29	16:00	gw	DZ	114.94	38.24	46	180	2
DG30	2012/08/29	16:35	gw	DZ	115.01	38.31	47	225	2
DG37	2012/08/30	10:00	gw	DZ	115.06	38.47	53	300	2
DG39	2012/08/30	10:55	gw	DZ	115.13	38.41	43	200	2
DG41	2012/08/30	13:25	gw	DZ	115.31	38.37	35	200	2
DG43	2012/08/30	15:00	gw	DZ	115.17	38.30	38	200	2
2D49	2013/03/26	11:40	gw	DZ	115.38	38.34	33	250	2
2D51	2013/03/26	12:31	gw	DZ	115.36	38.37	31	300	2
2D53	2013/03/26	15:15	gw	DZ	115.36	38.47	31	300	2
2D55	2013/03/26	16:18	gw	DZ	115.23	38.47	40	300	2

“gw”: groundwater; “DZ”: Dingzhou

Table S3 Water samples information: Plain area (1) (Continued 5)

Sample ID	**sampling date**	**sampling time**	**water type**	**Region**	**longitude**	**latitude**	**elevation**	**well depth**	**Aquifer**
	y/m/d	**h:m**			**°E**	**°N**	**m**	**m**	
2D56	2013/03/26	17:11	gw	DZ	115.16	38.49	45	120	2
2D58	2013/03/27	9:16	gw	DZ	115.09	38.51	50	200	2
2D59	2013/03/27	9:49	gw	DZ	115.06	38.50	49	230	2
DG17	2012/08/29	9:20	gw	DZ	114.90	38.48	64	300	3
DG22	2012/08/29	11:30	gw	DZ	114.84	38.43	65	300	3
DG31	2012/08/29	17:15	gw	DZ	115.03	38.35	48	300	3
DG34	2012/08/30	19:00	gw	DZ	114.96	38.39	47	250	3
2D48	2013/03/26	11:05	gw	DZ	115.46	38.30	26	400	3
RM1	2013/03/21	11:24	rw	SWR	116.03	39.08	15	-	-
BR3	2012/03/03	15:45	rw	BD	115.30	39.08	69	-	-
BR2	2012/03/03	14:10	rw	BD	115.29	39.04	39	-	-
Fu-M4	2011/06/11	10:12	rw	SWR	115.82	38.88	12	-	-
BYD-L1	2011/06/11	14:05	rw	SWR	115.94	38.90	11	-	-
BYD-L2	2011/06/11	15:35	rw	SWR	115.99	38.91	7	-	-
BYD-L3	2011/06/11	17:04	rw	SWR	115.94	38.84	6	-	-
T-M1	2011/06/12	11:45	rw	SWR	115.71	38.80	9	-	-
DM1	2012/08/28	12:35	rw	DZ	114.88	38.59	85	-	-
DM2	2012/08/28	15:35	rw	DZ	114.59	38.56	111	-	-

“rw”: river water; “DZ”: Dingzhou; “SWR”: surface water region

Table S4 Water samples information: Plain area (2)

Water samples quality													
Sample ID	**water temperature**	**EC**	**pH**	**anion concentration (mg/L)**				**cation concentration (mg/L)**				**stable isotope (‰)**	
	°C	**μS/cm**		**Cl^-**	**NO_3^-**	**SO_4^{2-}**	**HCO_3^-**	**Na**	**Mg**	**K**	**Ca**	**$\delta^{18}O$**	**δD**
R1	13.5	730	7.37	22.13	0.00	40.56	438.37	73.44	39.87	1.30	58.20	-9.90	-73.62
R3	14.1	720	7.22	41.75	0.00	50.28	348.14	30.79	43.48	1.11	71.60	-8.61	-64.29
R4	13.9	610	7.69	16.29	0.00	10.00	382.89	34.16	37.44	1.21	53.36	-9.22	-68.19
R6	14.9	560	7.64	17.38	0.00	5.62	354.85	22.16	37.46	1.61	58.64	-8.63	-63.91
R8	14.2	430	7.70	8.49	2.63	6.29	271.32	30.56	22.42	1.99	43.38	-9.01	-65.19
R10	10.5	560	7.61	40.10	10.26	5.21	270.10	24.72	28.72	1.98	60.00	-8.92	-65.01
R12	14.2	410	7.50	8.54	4.80	3.88	253.64	16.06	22.22	1.54	50.12	-8.81	-64.35
R13	15.7	830	7.35	149.79	22.45	14.41	185.96	20.44	26.91	1.22	112.04	-8.26	-62.36
R14	12.6	590	7.60	38.16	44.90	10.71	257.90	19.67	29.18	1.18	72.18	-8.96	-66.20
R15	9.6	430	7.64	8.65	4.16	7.92	264.00	15.78	22.50	1.64	54.64	-8.80	-63.57
R17	14	590	7.42	16.65	30.32	25.01	307.29	18.57	33.56	1.92	72.18	-8.69	-63.64
R2	4.8	310	8.16	4.29	1.49	16.20	200.59	55.70	8.73	1.35	17.51	-11.22	-83.91
R11	7.5	370	7.58	4.99	6.11	3.38	240.83	15.66	20.20	1.90	45.54	-8.81	-64.85
R16	9	530	7.54	10.02	2.73	27.00	314.61	54.58	24.04	2.47	43.34	-10.55	-77.33
R5	7.4	340	8.21	4.93	0.00	15.85	199.98	69.76	5.17	1.81	11.81	-10.98	-81.28
R7	10.9	390	7.82	9.48	2.42	21.13	220.10	66.90	8.35	2.23	20.86	-10.79	-80.76
R9	13.7	410	7.84	5.10	2.59	8.21	261.56	34.40	19.23	2.05	38.26	-9.44	-68.78

Table S4 Water samples information: Plain area (2) (Continued)

Sample ID	water temperature	EC	pH	anion concentration (mg/L)				cation concentration (mg/L)				stable isotope (‰)	
	°C	μS/cm		Cl^-	NO_3^-	SO_4^{2-}	HCO_3^-	Na	Mg	K	Ca	$\delta^{18}O$	δD
BG2	13	888	7.89	35.50	25.69	90.05	480.05	147.88	60.40	0.69	45.96	-8.55	-63.07
BG6	4.6	369	8.36	12.13	4.12	20.02	346.46	30.44	40.88	1.72	54.22	-8.54	-61.80
BG10	15.1	416	8.23	5.21	7.68	5.92	315.96	11.25	29.64	1.40	64.84	-9.19	-64.68
BG21	6.4	396	8.92	15.83	24.64	20.98	294.62	12.20	34.36	1.01	70.92	-8.14	-59.21
BG22	8	345	8.66	7.54	16.75	8.77	269.00	7.56	28.68	0.39	57.78	-8.92	-63.51
BG23	12.1	467	8.37	13.21	27.37	15.40	294.62	10.29	33.28	0.51	72.20	-8.70	-61.53
BG25	5.1	401	7.99	11.81	18.39	19.22	266.56	10.36	27.76	0.56	67.34	-8.07	-58.19
BG27	6.5	314	8.77	8.25	12.49	33.54	230.57	8.32	24.94	0.62	65.54	-7.40	-54.07
BG42	8.9	363	8.51	9.32	24.89	18.23	273.88	7.24	31.94	5.06	64.44	-9.69	-64.50
BG43	6.9	464	8.65	18.64	65.65	65.13	277.54	10.25	45.30	2.02	79.72	-9.53	-63.26
BG44	13.8	588	8.36	16.53	55.52	43.21	345.85	10.64	43.90	1.37	98.60	-9.70	-64.10
BG48	9.5	396	8.65	5.18	5.56	6.31	350.12	14.38	33.32	0.70	71.40	-10.09	-68.29
BG60	13.1	715	8.41	68.08	7.78	40.36	398.92	58.92	60.88	1.66	63.84	-8.57	-62.22
BG62	11.8	328	8.41	3.51	2.99	7.30	266.56	35.94	19.71	2.16	44.98	-9.33	-67.65
BG63	8.4	652	8.43	61.05	11.46	32.10	442.23	55.28	60.28	0.98	85.56	-8.62	-61.29
BG64	14.5	430	8.49	7.91	16.52	15.66	295.84	39.44	27.44	1.93	44.82	-9.32	-67.07
BG69	16.2	358	8.39	6.36	5.86	7.04	239.11	13.45	22.18	3.55	49.36	-9.04	-66.20
BG73	8.3	377	8.48	12.07	7.44	14.93	298.28	16.67	31.56	1.05	59.48	-8.84	-65.11
BYD-G1	15.2	1001	7.83	54.74	0.42	47.61	751.13	65.75	93.63	0.36	43.78	-6.95	-54.03

Table S4 Water samples information: Plain area (2) (Continued 2)

Sample ID	water temperature	EC	pH	anion concentration (mg/L)				cation concentration (mg/L)				stable isotope (‰)	
	°C	μS/cm		Cl^-	NO_3^-	SO_4^{2-}	HCO_3^-	Na	Mg	K	Ca	$\delta^{18}O$	δD
Fu-G1	7.93	1143	23.4	88.94	25.04	65.02	486.23	67.39	72.62	0.85	66.49	-8.07	-60.38
Fu-G4	7.5	1583	18.7	157.00	31.30	159.73	643.08	151.54	73.93	0.48	100.98	-7.54	-57.24
Fu-G5	7.69	1183	13.1	116.37	0.72	105.71	720.64	149.38	81.92	0.27	67.97	-7.95	-59.93
Fu-G6	7.55	1342	12.5	172.33	0.39	143.27	713.66	141.50	81.67	0.54	116.27	-7.53	-56.64
Fu-G8	7.51	1202	13.5	155.35	0.30	84.73	669.22	97.07	72.77	0.30	114.11	-7.27	-56.88
T-G1	8.13	925	14.9	48.75	1.86	111.68	542.00	205.78	31.79	0.06	18.82	-4.42	-40.94
T-G10	7.67	2650	13.8	245.15	0.68	847.58	623.91	450.59	149.44	0.60	120.82	-7.16	-57.22
T-G12	7.77	3520	14	347.78	1.18	1145.28	770.30	654.44	195.16	0.37	99.30	-6.51	-53.60
T-G13	7.69	2410	15.7	119.99	1.25	594.28	1079.65	288.01	197.40	0.27	101.59	-7.87	-59.56
T-G3	7.92	1322	14.7	153.34	0.78	256.74	409.55	226.78	51.46	0.25	60.96	-9.13	-72.63
T-G6	8.25	1498	16.3	182.26	4.15	152.23	386.11	392.88	147.38	0.00	120.73	-8.92	-67.29
T-G8	7.75	2870	15	188.16	0.61	913.50	742.42	530.86	138.38	0.14	100.66	-7.40	-57.44
2B18	12.1	570	7.69	17.66	27.90	23.78	299.36	15.12	34.10	1.47	71.26	-8.17	-56.73
2B23	14.6	540	7.52	13.95	1.32	4.92	358.50	24.90	43.58	0.69	48.54	-8.23	-60.46
2B25	14.4	1030	7.73	45.85	15.34	44.57	560.92	165.56	47.00	1.24	33.60	-8.69	-60.46
2B27	14	1090	7.55	77.57	28.18	68.60	480.44	88.92	76.32	1.32	61.96	-8.85	-62.70
2B30	14.2	960	7.44	61.63	19.94	62.95	432.89	62.84	62.76	1.27	79.80	-8.85	-63.22
2B32	13.3	2800	7.96	182.91	0.00	1249.29	302.41	423.40	157.90	3.00	124.30	-9.78	-72.68
2B36	15.2	6000	7.48	1083.67	0.00	1739.65	645.06	1171.40	266.80	4.08	163.72	-8.90	-63.99

Table S4 Water samples information: Plain area (2) (Continued 3)

Sample ID	water temperature	EC	pH	anion concentration (mg/L)				cation concentration (mg/L)				stable isotope (‰)	
	°C	μS/cm		Cl^-	NO_3^-	SO_4^{2-}	HCO_3^-	Na	Mg	K	Ca	$\delta^{18}O$	δD
2B39	15.6	2300	7.40	334.05	0.00	357.37	446.91	330.00	76.12	1.92	122.30	-8.46	-64.74
2B41	11.9	1140	7.53	56.84	4.32	135.37	485.32	190.96	20.12	1.25	65.84	-8.35	-58.24
2B43	14.8	4500	7.24	466.96	301.03	1134.64	713.35	593.80	233.60	100.48	216.00	-8.48	-60.62
BG1	5.8	379	7.56	16.58	11.05	31.92	257.41	59.70	24.76	0.87	35.94	-10.91	-80.00
BG3	6.1	402	8.37	14.07	7.21	26.48	312.30	56.06	29.60	0.84	46.26	-10.30	-75.04
BG15	9.1	473	8.32	32.80	4.70	10.95	348.90	18.11	42.68	0.36	72.50	-8.72	-62.56
BG49	1.8	288	8.43	3.05	3.05	10.92	284.25	33.82	20.30	1.19	58.74	-10.77	-73.22
BG53	11.5	342	8.95	9.51	9.47	15.04	231.18	12.36	15.24	0.92	82.28	-8.70	-65.87
BG54	6.5	338	8.84	12.67	10.53	19.07	259.24	25.96	27.88	1.99	130.16	-8.44	-63.67
BG61	6.5	387	8.39	7.32	7.91	15.48	333.65	36.08	29.94	1.46	60.46	-9.25	-66.81
BG66	15.2	469	8.66	16.38	11.73	17.53	287.91	24.24	33.94	1.51	55.88	-8.79	-64.45
BG72	14.9	330	8.50	3.57	3.09	7.65	236.06	24.84	15.81	1.53	40.98	-9.50	-68.50
Fu-G2	17.4	540	8.53	9.77	2.85	0.97	306.73	56.77	20.57	3.38	37.48	-10.41	-76.34
Fu-G3	16.7	529	8.37	7.38	0.16	58.98	323.28	51.82	24.06	1.41	42.71	-10.26	-74.83
Fu-G7	17.5	505	8.54	31.67	2.97	29.81	269.26	92.07	12.33	0.71	18.42	-10.79	-81.20
T-G5	-	594	8.57	30.03	5.65	49.34	235.27	72.89	13.93	1.75	25.07	-10.60	-81.64
2B19	14.8	950	7.32	131.14	23.03	14.05	362.16	17.17	52.20	1.24	123.60	-8.21	-57.61
2B20	8.9	630	8.08	57.15	12.02	7.08	303.63	10.77	37.94	1.19	82.12	-8.62	-59.45
2B21	7.1	710	7.51	58.96	17.29	17.18	332.29	20.83	41.00	1.30	86.84	-8.72	-61.07

Table S4 Water samples information: Plain area (2) (Continued 4)

Sample ID	water temperature	EC	pH	anion concentration (mg/L)				cation concentration (mg/L)				stable isotope (‰)	
	°C	μS/cm		Cl^-	NO_3^-	SO_4^{2-}	HCO_3^-	Na	Mg	K	Ca	$\delta^{18}O$	δD
2B22	6.9	530	7.62	9.47	6.84	32.54	328.02	37.90	33.96	0.93	51.92	-10.25	-73.09
2B24	13.6	640	7.76	17.33	8.09	81.20	290.83	70.46	31.22	1.24	41.80	-10.72	-78.62
2B28	11.4	560	7.58	4.77	0.00	43.64	330.46	44.72	33.14	1.39	48.38	-9.26	-65.91
2B29	12	560	7.78	8.22	0.00	54.95	289.61	52.56	27.50	1.74	47.48	-9.78	-69.42
2B31	8.5	520	8.14	4.54	0.00	54.71	290.22	52.30	23.64	1.66	45.22	-9.93	-70.71
2B33	8.6	490	8.28	26.04	8.27	57.86	171.33	81.60	10.38	1.97	20.44	-10.69	-79.72
2B34	11.8	510	8.39	46.24	7.72	42.62	160.96	99.72	4.31	1.01	13.12	-11.08	-82.12
2B35	14.9	550	8.78	50.56	11.51	47.81	151.21	101.88	4.77	1.61	15.40	-11.07	-81.44
2B37	12	460	8.86	19.84	0.00	32.77	200.59	110.10	0.41	0.69	4.95	-10.84	-78.96
BG5	10.2	397	8.24	11.48	6.77	30.64	331.21	21.70	37.46	1.87	87.94	-10.59	-77.40
BG8	8.8	422	8.47	3.95	2.61	17.94	373.30	22.94	36.94	2.08	69.48	-9.68	-68.74
BG9	10.2	454	8.16	9.88	5.34	23.29	353.78	62.04	29.24	2.06	47.92	-10.35	-74.80
2B26	12.3	560	7.91	20.90	7.64	34.50	273.76	95.74	11.03	1.68	27.48	-10.57	-77.30
2B38	16.7	610	9.03	39.82	0.00	42.74	235.34	147.24	0.00	0.74	2.25	-10.21	-74.00
2B40	6.4	720	9.02	65.48	0.00	66.60	223.15	176.48	0.00	1.27	2.69	-9.99	-73.43
2B42	19.1	630	8.79	41.85	0.00	60.86	210.35	133.66	1.14	0.69	10.57	-10.57	-77.93
DG1	17	570	7.50	26.18	31.01	44.77	250.59	13.91	21.90	0.98	85.78	-8.56	-63.15
DG2	17	420	7.40	7.42	5.55	10.41	260.34	11.22	15.36	0.74	69.20	-8.27	-60.35
DG3	16.3	590	7.50	28.70	12.32	45.55	293.88	27.78	31.64	0.69	67.36	-7.60	-56.67

Table S4 Water samples information: Plain area (2) (Continued 5)

Sample ID	**water temperature**	**EC**	**pH**	**anion concentration (mg/L)**				**cation concentration (mg/L)**				**stable isotope (‰)**	
	°C	**μS/cm**		**Cl^-**	**NO_3^-**	**SO_4^{2-}**	**HCO_3^-**	**Na**	**Mg**	**K**	**Ca**	**$\delta^{18}O$**	**δD**
DG4	14.8	720	7.40	22.38	1.67	116.97	321.92	47.32	27.50	0.92	83.44	-7.82	-57.87
DG5	14.6	890	7.00	25.95	87.28	84.83	378.01	24.71	35.01	1.80	122.28	-7.31	-54.15
DG6	15.4	1580	7.00	168.79	40.12	255.23	484.10	116.15	45.51	0.93	184.20	-7.78	-56.96
DG8	17.2	1360	7.00	66.25	152.39	238.64	426.79	38.33	24.76	1.55	225.65	-7.62	-55.51
DG9	20.4	1450	7.00	107.15	298.70	205.93	257.29	26.66	41.75	2.20	217.60	-7.50	-56.49
DG10	16.6	580	7.40	13.22	46.35	59.22	276.19	14.19	22.42	1.05	84.14	-7.81	-58.55
DG11	15	570	7.40	13.79	53.29	51.93	281.07	17.50	17.45	1.26	90.20	-7.76	-58.04
DG12	16.3	720	7.40	19.42	74.38	94.78	264.00	21.03	21.92	4.23	107.16	-7.37	-54.95
DG13	15.9	750	7.40	22.45	83.11	99.05	275.58	20.10	23.81	1.46	116.92	-7.41	-55.51
DG14	15.8	610	7.60	48.75	89.72	32.15	186.57	15.04	14.33	1.20	93.94	-8.21	-60.51
DG15	15.7	720	7.20	37.45	90.48	48.76	271.93	18.67	19.08	1.39	116.32	-8.14	-59.53
DG16	15.6	600	7.50	22.41	66.04	49.53	265.83	15.90	20.28	1.69	93.22	-8.06	-59.59
DG18	15.7	680	7.80	32.82	57.80	58.49	287.17	22.76	20.24	1.53	89.26	-8.23	-60.74
DG20	16.1	390	7.80	10.16	11.19	16.96	198.76	10.15	11.77	1.36	55.94	-8.32	-62.08
DG21	16.3	490	7.70	12.36	42.50	33.25	206.69	12.40	16.08	2.05	68.52	-7.72	-57.64
DG23	15	360	7.70	6.03	14.95	22.42	178.64	9.75	11.48	2.03	49.00	-7.88	-58.43
DG24	15.2	540	7.70	12.39	53.81	67.28	184.13	11.09	16.49	2.47	76.48	-7.35	-55.74
DG25	16.1	690	7.90	20.62	88.62	58.40	235.34	20.90	21.04	1.61	85.90	-8.49	-62.53
DG26	15.6	570	7.50	18.99	29.00	44.23	245.10	19.91	19.51	1.45	72.16	-8.50	-63.06

Table S4 Water samples information: Plain area (2) (Continued 6)

Sample ID	**water temperature**	**EC**	**pH**	**anion concentration (mg/L)**				**cation concentration (mg/L)**				**stable isotope (‰)**	
	°C	**µS/cm**		**Cl^-**	**NO_3^-**	**SO_4^{2-}**	**HCO_3^-**	**Na**	**Mg**	**K**	**Ca**	**$\delta^{18}O$**	**δD**
DG27	15.2	680	7.50	35.32	69.36	60.88	232.91	22.40	23.74	1.34	87.54	-8.34	-62.01
DG29	14.8	630	7.80	46.94	29.26	54.99	235.34	15.81	21.68	1.82	88.30	-8.42	-62.84
DG32	15.2	400	7.70	3.88	3.34	24.48	231.69	11.76	10.87	1.98	61.62	-8.36	-61.73
DG33	14.2	960	7.70	104.77	85.98	67.16	258.51	32.60	25.64	2.00	134.96	-8.54	-63.25
DG35	15	650	7.50	40.28	53.14	45.06	260.95	22.66	21.92	1.35	84.12	-8.65	-63.26
DG36	14.8	890	7.30	45.45	55.49	110.88	360.33	34.86	27.21	2.14	130.60	-7.37	-55.34
DG38	16.1	510	7.80	18.40	6.53	33.21	243.88	13.13	20.10	2.73	63.74	-8.12	-60.59
DG40	15.2	680	7.30	35.37	7.91	68.16	351.19	28.10	33.52	2.60	73.32	-6.59	-57.26
DG42	16.2	270	8.20	4.15	0.25	10.38	198.76	29.42	10.90	2.38	28.72	-9.35	-67.09
DG44	24	280	7.90	3.00	0.60	12.85	195.10	29.25	9.32	2.25	21.40	-9.31	-66.78
2D44	14.6	590	7.45	23.43	18.65	33.41	282.29	24.44	18.88	1.50	85.50	-8.33	-65.42
2D45	13.9	600	7.42	18.34	6.06	47.45	306.68	17.87	28.72	2.64	81.34	-8.00	-61.41
2D46	15.5	480	7.60	9.67	3.90	14.10	287.17	33.40	21.24	2.95	51.76	-8.90	-66.76
2D47	15.1	1060	7.60	126.55	0.00	89.33	337.77	86.76	50.68	2.68	84.92	-8.63	-64.78
2D50	15.3	520	7.69	21.55	0.00	15.02	285.34	38.86	29.12	2.14	43.54	-8.70	-65.09
2D52	15.4	510	7.45	12.22	2.27	12.44	298.75	20.54	25.66	1.88	65.96	-8.57	-63.58
2D54	15	670	7.43	31.00	25.83	45.40	310.34	21.80	30.66	2.31	94.84	-7.96	-59.48
2D57	14	710	7.38	25.31	14.36	43.76	379.23	32.36	28.36	2.15	103.60	-8.46	-62.08
DG7	15.2	850	7.20	89.41	1.51	76.35	307.90	28.87	41.36	1.46	96.64	-8.15	-61.35

Table S4 Water samples information: Plain area (2) (Continued 7)

Sample ID	**water temperature**	**EC**	**pH**	**anion concentration (mg/L)**				**cation concentration (mg/L)**				**stable isotope (‰)**	
	°C	**μS/cm**		**Cl^-**	**NO_3^-**	**SO_4^{2-}**	**HCO_3^-**	**Na**	**Mg**	**K**	**Ca**	**$\delta^{18}O$**	**δD**
DG19	18.1	290	7.90	3.12	3.56	7.62	174.37	8.45	10.72	2.18	38.30	-8.57	-63.93
DG28	17.9	290	8.00	3.63	3.43	6.23	173.76	13.35	8.77	1.41	38.51	-8.57	-63.41
DG30	-	300	8.00	3.51	0.90	7.14	176.81	13.20	10.44	1.47	33.90	-8.30	-62.76
DG37	22.4	450	7.60	14.82	9.29	20.00	216.44	12.75	14.23	1.89	59.78	-8.50	-62.99
DG39	28.6	290	7.80	3.68	3.45	6.71	181.08	10.17	12.06	2.64	34.84	-8.72	-63.11
DG41	-	280	8.00	2.95	2.27	6.95	195.10	40.40	7.67	2.60	23.72	-8.59	-66.16
DG43	-	280	8.00	4.23	0.67	20.59	181.69	34.35	8.82	2.38	30.87	-9.40	-67.61
2D49	15.7	420	7.72	6.95	0.00	8.21	265.83	35.84	19.97	2.61	39.08	-8.79	-64.96
2D51	7.6	320	7.90	2.82	2.54	4.21	220.10	44.37	9.39	2.99	25.90	-9.45	-69.13
2D53	8.5	390	7.78	5.70	7.50	5.20	235.34	42.56	10.57	3.45	39.24	-9.30	-67.55
2D55	11.1	470	7.53	12.33	0.00	17.21	270.10	15.14	25.34	1.87	61.44	-8.58	-63.31
2D56	10.4	370	7.61	6.48	2.45	8.41	224.37	13.63	15.99	2.21	51.80	-8.82	-63.88
2D58	8.4	360	7.75	5.84	4.82	9.05	218.88	13.77	14.86	2.48	51.32	-8.86	-66.24
2D59	12.4	470	7.52	8.60	8.59	7.59	251.81	17.60	18.45	2.55	58.18	-8.76	-65.56
DG17	21.6	270	8.20	2.23	0.86	9.05	205.47	27.78	9.01	2.36	33.72	-9.89	-71.15
DG22	20.5	420	8.00	6.32	0.67	23.95	229.25	38.12	11.87	2.60	38.00	-10.18	-74.99
DG31	27.4	320	7.80	3.68	0.37	11.23	177.42	21.20	9.80	2.15	33.73	-8.72	-64.79
DG34	25.6	510	7.70	10.37	1.04	52.89	245.71	49.84	12.36	2.29	46.64	-10.30	-76.34
2D48	21.6	500	8.48	38.22	6.74	81.08	99.99	96.56	2.79	2.46	12.56	-10.67	-77.79

Table S4 Water samples information: Plain area (2) (Continued 8)

Sample ID	water temperature	EC	pH	anion concentration (mg/L)				cation concentration (mg/L)				stable isotope (‰)	
	°C	μS/cm		Cl^-	NO_3^-	SO_4^{2-}	HCO_3^-	Na	Mg	K	Ca	$\delta^{18}O$	δD
RM1	7.4	980	8.56	91.21	49.05	135.00	242.05	85.24	31.66	6.88	100.48	-7.69	-57.71
BR3	7.2	322	8.90	9.08	8.44	33.34	253.75	8.41	27.94	1.68	61.06	-7.61	-56.35
BR2	7.6	344	8.61	12.99	9.32	33.99	244.60	9.31	28.40	1.56	57.02	-7.50	-54.88
Fu-M4	25.8	1461	7.59	170.58	16.91	71.52	537.64	132.79	20.82	41.78	87.36	-7.22	-55.81
BYD-L1	26.9	1467	7.67	175.15	35.19	66.98	510.63	128.51	21.22	41.64	88.59	-6.98	-56.31
BYD-L2	27.2	1269	7.80	182.21	0.32	93.83	370.34	144.21	16.50	44.13	62.46	-4.14	-40.11
BYD-L3	25.7	1172	7.82	124.56	0.44	148.89	338.97	127.21	9.30	47.66	62.34	-3.57	-38.17
T-M1	29.9	6250	8.60	247.08	2.13	2393.73	831.30	1460.19	20.30	54.86	185.89	-6.30	-52.32
DM1	27.1	620	8.00	42.01	9.14	124.59	173.15	32.80	30.28	1.29	61.92	-6.54	-50.72
DM2	23.8	520	8.10	13.32	13.30	98.71	184.13	14.71	17.58	3.32	74.46	-7.08	-53.05